UNIVERSITY OF CALIFORNIA
RIVERSIDE

Gut-Brain Endocannabinoid Control of Obesity and Anxiety

A Dissertation submitted in partial satisfaction
of the requirements for the degree of

Doctor of Philosophy

in

Neuroscience

by

Courtney Page Wood

June 2023

Dissertation Committee:
Dr. Nicholas V. DiPatrizio, Chairperson
Dr. Khaleel A. Razak
Dr. Margarita Curras-Collazo

The Dissertation of Courtney Page Wood is approved:

_____

_____

_____

Committee Chairperson

University of California, Riverside

ABSTRACT OF THE DISSERTATION

Gut-Brain Endocannabinoid Control of Obesity and Anxiety

by

Courtney Page Wood

Doctor of Philosophy, Graduate Program in Neuroscience
University of California, Riverside, June 2023
Dr. Nicholas V. DiPatrizio, Chairperson

The endocannabinoid system (ECS) exerts control over energy homeostasis via interactions between lipid messengers called endocannabinoids (eCBs) and cannabinoid receptors. ECS components are abundant in the CNS and the gastrointestinal (GI) tract. Bi-directional communication between the CNS and GI tract occurs via the vagus nerve. Dysregulation of vagal signaling is associated with adverse physiological and psychological outcomes, such as obesity and anxiety disorders, respectively. We previously showed that eCBs in the GI tract of obese rodents are elevated and drive feeding through peripheral cannabinoid receptor activation. Here, we examined the effects of diet-induced obesity (DIO) on efferent vagus nerve signaling and intestinal eCB formation. We tested the hypothesis that elevated parasympathetic signaling by the efferent vagus is the source of the elevated eCB content and hyperphagia observed in obese mice. We first measured cFos immunoreactivity in the dorsal motor nucleus (DMV) of the efferent vagus in DIO

mice. Next, we tested the effects of treatment with muscarinic acetylcholine receptor (mAChR) antagonists on intestinal eCB formation, eCB synthetic enzyme activity, and food intake. Finally, we utilized our conditional intestinal epithelium-specific cannabinoid receptor subtype-1 (CB_1R) knockout model ($IntCB_1$-/-) to elucidate the role of intestinal CB_1Rs in this process. DMV neuronal activation was significantly elevated in DIO mice compared to lean controls. Treatment with mAChR antagonists reduced intestinal eCB levels, eCB synthetic enzyme activity, and caloric intake in DIO animals. Furthermore, we showed that intestinal CB_1Rs are required for mAChR antagonist-induced attenuation of food intake. To evaluate the contribution of intestinal ECS components to the expression of anxious behaviors, we subjected $IntCB_1$-/- male and female mice to a battery of behavioral tests. We quantified circulating corticosterone (CORT) levels at baseline and immediately following behavioral testing. $IntCB_1$-/- male mice exhibited an anxiolytic phenotype that was absent in females. These sex differences were associated with a significant increase in plasma CORT levels for female mice at both time points, regardless of genotype. This body of work reveals a previously unidentified role for the vagus nerve in the context of DIO and behavioral anxiety and highlights critical contributions of the ECS to gut-brain signaling.

Table of Contents

List of Tables

Chapter 1

List of Figures

Chapter 1

Chapter 2

Introduction

The Endocannabinoid System

The endocannabinoid system (ECS) contributes to the homeostatic regulation of several organ systems and physiological mechanisms (Harkany et al., 2008; Marsicano and Lafenêtre, 2009; Bermudez-Silva et al., 2010; DiPatrizio and Piomelli, 2012; Ruehle et al., 2012; Maldonado et al., 2013; Crowe et al., 2014; Lutz et al., 2015). It is comprised of cannabinoid receptors (CB_1R and CB_2R) (Matsuda et al., 1990; Munro et al., 1993), lipid-derived signaling molecules called endocannabinoids (eCBS) – N-arachidonoyl ethanolamide (anandamide, AEA) (Devane et al., 1992) and 2-arachidonoyl-*sn*-glycerol (2-AG) (Mechoulam et al., 1995; Sugiura et al., 1995), and their corresponding biosynthetic and degradative enzymes.

In recent decades, research investigating CB_1R has grown exponentially due to the discovery that Δ^9-tetrahydrocannabinol (Δ^9-THC), the primary psychoactive component of cannabis, exerts its effects via activation of CB_1Rs in the CNS (Howlett, 1995; Howlett et al., 2002; Howlett, 2005; Mechoulam and Parker, 2013). CB_1R is one of the most abundant GPCRs in the CNS (Herkenham et al., 1991; Mackie, 2008; Marsicano and Kuner, 2008), though it is also found in metabolically active tissues throughout the periphery (Croci et al., 1998; Izzo et al., 1998; Wang and Ueda, 2008). CB_1Rs are typically coupled to the $G_{i/o}$ inhibitory g-protein, leading to the activation of A-type and inwardly rectifying potassium channels, inhibition of P/Q-type calcium channels, and ultimately a reduction

in intracellular cAMP (Glass and JK, 1999; Howlett, 2005). Under certain conditions, CB_1R has been shown to couple to the G_s stimulatory g-protein or the $G_{q/11}$ modulatory g-protein (Varga et al., 2008; Bosier et al., 2010).

Originally, CB_2R was thought to be expressed only on immune tissues (Howlett et al., 2002), but recent studies indicate its existence in brain tissue (Van Sickle et al., 2005; Ashton et al., 2006; Gong et al., 2006; Onaivi et al., 2008), particularly on microglia (Núñez et al., 2004; Stella, 2004). It is classically accepted that CB_2R couples to the $G_{i/o}$ inhibitory g-protein, but CB_2R activation has also been shown to lead to a sustained increase in intracellular cAMP levels which ultimately suppresses T cell receptor signaling through the cAMP/PKA/Csk/Lck pathway (Börner et al., 2009). Roles for CB_2R activation in energy homeostasis and metabolism are less defined, but it has been speculated that cannabinoid signaling via CB_2R is "part of a protective machinery" and serves to protect against inflicted damage (Pacher and Mechoulam, 2011). That said, the mechanisms investigated in the following body of work would benefit by follow-up experiments to elucidate the function of CB_2R in gut-brain signaling that controls obesity and anxiety.

2-AG is a monoacylglycerol, its primary synthetic pathway requires the phospholipase-C (PLC)-dependent generation of the diacylglycerol 1-stearoyl-2-arachidonoyl-*sn*-glycerol (SAG) (Prescott and Majerus, 1983). SAG is subsequently hydrolyzed by diacylglycerol lipase alpha and beta (DAGLα/β) (Bisogno et al., 2003) to generate 2-AG, which can be further degraded by monoacylglycerol lipase (MAGL) into

arachidonic acid and glycerol (Blankman et al., 2007; Gao et al., 2010). Hydrolysis of 2-AG may also occur via a minor pathway involving the enzyme α/β hydrolyzing domain 6 (ABHD6) (Thomas et al., 2013) in a tissue-dependent manner (Wiley et al., 2021). 2-AG is a full agonist at both cannabinoid receptors (McAllister and Glass, 2002; Sugiura et al., 2002; Sugiura et al., 2006).

The fatty acid amide, AEA, is typically synthesized via the two-step 'transacylation-phosphodiesterase pathway' (Schmid et al., 1990; Di Marzo et al., 1994; Hansen et al., 2000; Schmid, 2000), which first requires the transfer of an acyl group from the *sn*-1 position of a glycerophospholipid to a phosphatidylethanolamine by the enzyme *N*-acyltransferase to generate *N*-acyl phosphatidylethanolamine (NAPE). NAPE is converted to AEA via the enzyme NAPE phospholipase-D (NAPE-PLD) (Okamoto et al., 2004; Leung et al., 2006), and AEA can be further hydrolyzed into arachidonic acid and ethanolamine by fatty acid amide hydrolase (FAAH) (McKinney and Cravatt, 2005; Ahn et al., 2008). AEA is a partial agonist for CB_1R and a weak agonist at CB_2R (Sugiura et al., 2002; Smita et al., 2007).

The ECS and Food Intake

The ECS is a key regulator of food seeking and feeding behaviors both by central and peripheral mechanisms (Kirkham et al., 2002; Di Marzo et al., 2009; Argueta and DiPatrizio, 2017; Argueta et al., 2019; Gianessi et al., 2019; Avalos et al., 2020). Increased eCB tone is associated with the development of metabolic diseases such as obesity, type

II diabetes, and fatty liver disease (Tam et al., 2018), leading many investigators to pursue ECS inhibition as a therapeutic target for such diseases. Indeed, treatment with the synthetic CB_1R inverse agonist rimonabant (SR141716A) leads to decreased food intake and weight gain in obese and lean animal models (Colombo et al., 1998; Ravinet Trillou et al., 2003; Wiley et al., 2005). In obese and overweight humans with metabolic syndrome, rimonabant treatment also improves glucose homeostasis, leptin and insulin resistance, and hepatic steatosis (Van Gaal et al.; Després et al., 2005; Hollander et al., 2010). Rimonabant was approved for use as an anti-obesity drug in 2006. Unfortunately, a proportion of individuals being treated with rimonabant experienced suicidal thoughts and enhanced anxiety problems as an unforeseen side effect (Christensen et al., 2007), causing rimonabant to be withdrawn from the market in 2009. As a result, some investigators have shifted to the exploration of peripherally restricted CB_1R antagonists for obesity treatment. Exhibiting minimal or no brain penetrance, many of these treatments show promise in treating obesity and its associated metabolic outcomes in rodents, with limited CNS-mediated side effects (LoVerme et al., 2009; Cluny et al., 2010; Tam et al., 2010).

Studies in our lab indicate that the endogenous ligands for CB_1R, or CB_1R itself may be dysregulated in one or more peripheral tissues in animal models of obesity. For example, diet-induced obese (DIO) mice exhibit significantly increased levels of 2-AG in the upper intestinal epithelium compared to lean littermates (Argueta and DiPatrizio, 2017). Moreover, blockade of peripheral CB_1R led to decreased food intake in the DIO

animals but had no effect in lean controls. We further demonstrated that this effect is mediated by a CCK-dependent mechanism which may also involve the afferent fibers of the vagus nerve (Argueta et al., 2019). These studies provide substantial evidence for gastrointestinal CB_1R-mediated control of food intake, which lends support to my focus on the role of eCB activity in the upper small intestine of our DIO rodent model.

The ECS and Anxiety

The patients who experienced negative psychological outcomes in the rimonabant study (Christensen et al., 2007) provide substantial evidence for the role of CB_1R in anxiety. It has been suggested that certain variants of the gene that encodes CB_1R (Cnr1) contribute to the development of anxiety and depression more strongly than others (Lazary et al., 2011). Given that the effects of cannabis consumption in humans range from a perceived sense of well-being and relaxation to increased anxiety and dysphoria (Wade et al., 2003; D'Souza et al., 2004), this hypothesis is highly probable. In any case, the ECS appears to contribute heavily to the expression of affective behaviors both in animals and humans.

Generally, ECS activation is anxiolytic. For example, an injection of a stable analog of AEA, methanandamide, into the prefrontal cortex reduced anxiety-like behaviors in rats (Rubino et al., 2008). Systemic inhibition of FAAH in rat is also anxiolytic, an effect that can be prevented by CB_1R antagonism (Kathuria et al., 2003). Enhancement of 2-AG levels is also anxiolytic; rats under highly aversive environmental conditions exhibited

anxiolysis following treatment with the MGL inhibitor JZL184 (Sciolino et al., 2011). Tonic ECS activity attenuates HPA axis activation and restores homeostasis via glucocorticoid recruitment of eCB signaling (Hill et al., 2011). Moreover, downregulation of ECS activity following chronic stress can lead to anxiety and depression in humans (Riebe and Wotjak, 2011).

Recent evidence indicates a role for CB_2R in behavioral anxiety as well. Mice overexpressing CB_2R exhibited reduced anxiety behaviors on the elevated plus maze (EPM), open field test, and light dark box (García-Gutiérrez and Manzanares, 2011). In another study, the anxiolytic effects of JZL184 were absent in mice that were pre-treated with CB_2R antagonists and in CB_2R-knockout mice (Busquets-Garcia et al., 2011). Even though CB_2R activation is not associated with any adverse psychotropic effects and therefore should be considered a valuable target for anxiety-reducing pharmacological therapies, the focus of the work that follows is specifically meant to address the role of intestinal CB_1Rs in the expression of behavioral anxiety.

Gut-Brain Signaling

Gut-brain communication occurs primarily by two mechanisms: 1) afferent fibers receive sensory input from the gastrointestinal (GI) tract and transmit directly to the brain via the vagus nerve and 2) secreted hormones, neurotransmitters, and other signaling molecules enter the brain from circulation via fenestrated capillaries that surround the area postrema (AP), a structure within the medulla (Price et al., 2008). The vagus nerve is

the tenth and longest cranial nerve and enables bi-directional communication between the CNS and many peripheral organs such as the esophagus, stomach, small intestine, liver, pancreas, heart, and lungs (Berthoud and Neuhuber, 2000). Vagal afferent fibers facilitate visceral control over CNS-mediated behaviors, while motor efferents exert extrinsic neural control over GI activities such as mucosal secretion and blood flow (Browning and Travagli, 2014).

The efferent vagus provides dense parasympathetic innervation to the stomach and GI tract, which becomes sparser with progression distally along the intestines (Berthoud et al., 1991; Altschuler et al., 1993). The cell bodies of the efferent vagus that project to the GI tract reside in the dorsal motor nucleus (DMV) of the brainstem (Kalia and Sullivan, 1982; Altschuler et al., 1989; Berthoud et al., 1990; Berthoud et al., 1991; Altschuler et al., 1993). GI innervating motor neurons within the DMV exhibit a "columnar" organization that is based on the five subdiaphragmatic branches: anterior gastric, posterior gastric, hepatic, celiac, and accessory celiac (Fox and Powley, 1985; Norgren and Smith, 1988). One study indicates that most DMV neurons that project to the duodenum originate from the accessory celiac branch (Hayakawa et al., 2013), while others show that the small intestine is innervated by all five branches (Berthoud et al., 1990; Altschuler et al., 1993). Efferent vagus fibers release acetylcholine onto their peripheral targets, which consist largely of enteric neurons in the GI tract (Schemann and Grundy, 1992; Walter et al., 2009). Postganglionic neurons in the upper small intestine express muscarinic acetylcholine receptors, and their activation enables smooth muscle

contraction (Travagli et al., 2006). Though the properties of vagal efferents have been studied thoroughly in regard to gastric acid secretion (White et al., 1991; Konturek et al., 2004), much less is known about CNS control over other gastric secretions via the efferent vagus.

The afferent vagus is composed of primarily unmyelinated c fibers or Aδ fibers which can be activated by mechanical stimulation (stretch), changes in osmotic pressure, or chemical activation (Brookes et al., 2013). Signaling by vagal afferents may also participate in nociception or affective behaviors (Berthoud and Neuhuber, 2000). The cell bodies of the afferent vagus are found in the nodose ganglia and enter the brainstem via the nucleus of the solitary tract (NTS) (Maggi, 1991; Williams et al., 2016; Kupari et al., 2019) and signal using glutamate as their primary neurotransmitter (Andresen and Yang, 1990). Notably, CB_1Rs are present in the nodose ganglia on vagal afferent fibers that originate in the stomach and the duodenum, and their expression increases following food deprivation and is immediately restored to baseline levels following feeding (Burdyga et al., 2004). This further suggests that increased CB_1R signaling may serve to initiate food-seeking behaviors. While some vagal afferents terminate in the NTS, other have been shown to make monosynaptic connections with the DMV (Rinaman et al., 1989) or AP (Leslie and Gwyn, 1984). Together, the NTS, DMV, and AP make up the dorsal vagal complex (DVC). The DVC both independently and in communication with other feeding-associated brain structures, such as the hypothalamus, is a key player in autonomic regulation of food intake and energy balance (Grijalva and Novin, 1990).

It has been shown by several groups that obesity severely dysregulates the ability of vagal afferents to communicate with the CNS. Specifically, intestine projecting vagal afferents in DIO mice displayed impaired responses to the satiety-signaling peptide, cholecystokinin (CCK), as measured by ratiofluorometric calcium imaging (Daly et al., 2011). A different study demonstrated that mice maintained on a high-fat diet for 12-weeks displayed reduced sensitivity of gastric tension in vagal afferent responses to mechanical stimulation (Kentish et al., 2012). Efferent vagal signaling may also be impaired in DIO. As demonstrated by Browning et al., vagal efferents of DIO rats exhibited decreased membrane input resistance, decreased action potential firing frequency, and decreased responsiveness to the satiety peptides CCK and GLP-1 (Browning et al., 2013). These findings lend evidence to the hypothesis that vagal nerve signaling is dysregulated in DIO and may also contribute to the development of DIO.

References

Ahn K, McKinney MK, Cravatt BF (2008) Enzymatic pathways that regulate endocannabinoid signaling in the nervous system. Chem Rev 108:1687-1707.

Altschuler S, Escardo J, Lynn R, Miselis R (1993) The Central Organization of the Vagus Nerve Innervating the Colon of the Rat. In, pp 502-509. Gastroenterology.

Altschuler SM, Bao XM, Bieger D, Hopkins DA, Miselis RR (1989) Viscerotopic representation of the upper alimentary tract in the rat: sensory ganglia and nuclei of the solitary and spinal trigeminal tracts. J Comp Neurol 283:248-268.

Andresen MC, Yang MY (1990) Non-NMDA receptors mediate sensory afferent synaptic transmission in medial nucleus tractus solitarius. Am J Physiol 259:H1307-1311.

Argueta D, DiPatrizio N (2017) Peripheral endocannabinoid signaling controls hyperphagia in western diet-induced obesity. Physiology & Behavior 171:32-39.

Argueta D, Perez P, Makriyannis A, DiPatrizio N (2019) Cannabinoid CB1 Receptors Inhibit Gut-Brain Satiation Signaling in Diet-Induced Obesity. Frontiers in Physiology 10.

Ashton JC, Friberg D, Darlington CL, Smith PF (2006) Expression of the cannabinoid CB2 receptor in the rat cerebellum: an immunohistochemical study. Neurosci Lett 396:113-116.

Avalos B, Argueta D, Perez P, Wiley M, Wood C, DiPatrizio N (2020) Cannabinoid CB1 Receptors in the Intestinal Epithelium Are Required for Acute Western-Diet Preferences in Mice. Nutrients 12.

Bermudez-Silva FJ, Viveros MP, McPartland JM, Rodriguez de Fonseca F (2010) The endocannabinoid system, eating behavior and energy homeostasis: the end or a new beginning? Pharmacol Biochem Behav 95:375-382.

Berthoud H, Carlson N, Powley T (1991) Topography of Efferent Vagal Innervation of the Rat Gastrointestinal-Tract. American Journal of Physiology 260:R200-R207.

Berthoud HR, Neuhuber WL (2000) Functional and chemical anatomy of the afferent vagal system. Auton Neurosci 85:1-17.

Berthoud HR, Jedrzejewska A, Powley TL (1990) Simultaneous labeling of vagal innervation of the gut and afferent projections from the visceral forebrain with dil injected into the dorsal vagal complex in the rat. J Comp Neurol 301:65-79.

Bisogno T, Howell F, Williams G, Minassi A, Cascio MG, Ligresti A, Matias I, Schiano-Moriello A, Paul P, Williams EJ, Gangadharan U, Hobbs C, Di Marzo V, Doherty P (2003) Cloning of the first sn1-DAG lipases points to the spatial and temporal regulation of endocannabinoid signaling in the brain. J Cell Biol 163:463-468.

Blankman JL, Simon GM, Cravatt BF (2007) A comprehensive profile of brain enzymes that hydrolyze the endocannabinoid 2-arachidonoylglycerol. Chem Biol 14:1347-1356.

Bosier B, Muccioli GG, Hermans E, Lambert DM (2010) Functionally selective cannabinoid receptor signalling: therapeutic implications and opportunities. Biochem Pharmacol 80:1-12.

Brookes SJ, Spencer NJ, Costa M, Zagorodnyuk VP (2013) Extrinsic primary afferent signalling in the gut. Nat Rev Gastroenterol Hepatol 10:286-296.

Browning K, Fortna S, Hajnal A (2013) Roux-en-Y gastric bypass reverses the effects of diet-induced obesity to inhibit the responsiveness of central vagal motoneurones. Journal of Physiology-London 591:2357-2372.

Browning KN, Travagli RA (2014) Central nervous system control of gastrointestinal motility and secretion and modulation of gastrointestinal functions. Compr Physiol 4:1339-1368.

Burdyga G, Lal S, Varro A, Dimaline R, Thompson DG, Dockray GJ (2004) Expression of cannabinoid CB1 receptors by vagal afferent neurons is inhibited by cholecystokinin. J Neurosci 24:2708-2715.

Busquets-Garcia A, Puighermanal E, Pastor A, de la Torre R, Maldonado R, Ozaita A (2011) Differential role of anandamide and 2-arachidonoylglycerol in memory and anxiety-like responses. Biol Psychiatry 70:479-486.

Börner C, Smida M, Höllt V, Schraven B, Kraus J (2009) Cannabinoid receptor type 1- and 2-mediated increase in cyclic AMP inhibits T cell receptor-triggered signaling. J Biol Chem 284:35450-35460.

Christensen R, Kristensen PK, Bartels EM, Bliddal H, Astrup A (2007) Efficacy and safety of the weight-loss drug rimonabant: a meta-analysis of randomised trials. Lancet 370:1706-1713.

Cluny NL, Vemuri VK, Chambers AP, Limebeer CL, Bedard H, Wood JT, Lutz B, Zimmer A, Parker LA, Makriyannis A, Sharkey KA (2010) A novel peripherally restricted

cannabinoid receptor antagonist, AM6545, reduces food intake and body weight, but does not cause malaise, in rodents. Br J Pharmacol 161:629-642.

Colombo G, Agabio R, Diaz G, Lobina C, Reali R, Gessa GL (1998) Appetite suppression and weight loss after the cannabinoid antagonist SR 141716. Life Sci 63:PL113-117.

Croci T, Manara L, Aureggi G, Guagnini F, Rinaldi-Carmona M, Maffrand JP, Le Fur G, Mukenge S, Ferla G (1998) In vitro functional evidence of neuronal cannabinoid CB1 receptors in human ileum. Br J Pharmacol 125:1393-1395.

Crowe MS, Nass SR, Gabella KM, Kinsey SG (2014) The endocannabinoid system modulates stress, emotionality, and inflammation. Brain Behav Immun 42:1-5.

D'Souza DC, Perry E, MacDougall L, Ammerman Y, Cooper T, Wu YT, Braley G, Gueorguieva R, Krystal JH (2004) The psychotomimetic effects of intravenous delta-9-tetrahydrocannabinol in healthy individuals: implications for psychosis. Neuropsychopharmacology 29:1558-1572.

Daly DM, Park SJ, Valinsky WC, Beyak MJ (2011) Impaired intestinal afferent nerve satiety signalling and vagal afferent excitability in diet induced obesity in the mouse. J Physiol 589:2857-2870.

Després J-P, Golay A, Sjöström L (2005) Effects of Rimonabant on Metabolic Risk Factors in Overweight Patients with Dyslipidemia. The New England Journal of Medicine 353:2121-2134.

Devane WA, Hanus L, Breuer A, Pertwee RG, Stevenson LA, Griffin G, Gibson D, Mandelbaum A, Etinger A, Mechoulam R (1992) Isolation and structure of a brain constituent that binds to the cannabinoid receptor. Science 258:1946-1949.

Di Marzo V, Ligresti A, Cristino L (2009) The endocannabinoid system as a link between homoeostatic and hedonic pathways involved in energy balance regulation. Int J Obes (Lond) 33 Suppl 2:S18-24.

Di Marzo V, Fontana A, Cadas H, Schinelli S, Cimino G, Schwartz JC, Piomelli D (1994) Formation and inactivation of endogenous cannabinoid anandamide in central neurons. Nature 372:686-691.

DiPatrizio NV, Piomelli D (2012) The thrifty lipids: endocannabinoids and the neural control of energy conservation. Trends Neurosci 35:403-411.

Fox EA, Powley TL (1985) Longitudinal columnar organization within the dorsal motor nucleus represents separate branches of the abdominal vagus. Brain Res 341:269-282.

Gao Y et al. (2010) Loss of retrograde endocannabinoid signaling and reduced adult neurogenesis in diacylglycerol lipase knock-out mice. J Neurosci 30:2017-2024.

García-Gutiérrez MS, Manzanares J (2011) Overexpression of CB2 cannabinoid receptors decreased vulnerability to anxiety and impaired anxiolytic action of alprazolam in mice. J Psychopharmacol 25:111-120.

Gianessi CA, Groman SM, Taylor JR (2019) Bi-directional modulation of food habit expression by the endocannabinoid system. Eur J Neurosci 49:1610-1622.

Glass M, JK N (1999) Agonist selective regulation of G proteins by cannabinoid CB1 and CB2 receptors. Molecular Pharmacology 56:1362-1369.

Gong JP, Onaivi ES, Ishiguro H, Liu QR, Tagliaferro PA, Brusco A, Uhl GR (2006) Cannabinoid CB2 receptors: immunohistochemical localization in rat brain. Brain Res 1071:10-23.

Grijalva CV, Novin D (1990) The role of the hypothalamus and dorsal vagal complex in gastrointestinal function and pathophysiology. Ann N Y Acad Sci 597:207-222.

Hansen HS, Moesgaard B, Hansen HH, Petersen G (2000) N-Acylethanolamines and precursor phospholipids - relation to cell injury. Chem Phys Lipids 108:135-150.

Harkany T, Mackie K, Doherty P (2008) Wiring and firing neuronal networks: endocannabinoids take center stage. Curr Opin Neurobiol 18:338-345.

Hayakawa T, Kuwahara-Otani S, Maeda S, Tanaka K, Seki M (2013) Collateral projections of the dorsal motor nucleus of the vagus nerve to the stomach and the intestines in the rat. Okajimas Folia Anatomica Japonica 90:7-15.

Herkenham M, Lynn AB, Johnson MR, Melvin LS, de Costa BR, Rice KC (1991) Characterization and localization of cannabinoid receptors in rat brain: a quantitative in vitro autoradiographic study. J Neurosci 11:563-583.

Hill MN, McLaughlin RJ, Pan B, Fitzgerald ML, Roberts CJ, Lee TT, Karatsoreos IN, Mackie K, Viau V, Pickel VM, McEwen BS, Liu QS, Gorzalka BB, Hillard CJ (2011) Recruitment of prefrontal cortical endocannabinoid signaling by glucocorticoids contributes to termination of the stress response. J Neurosci 31:10506-10515.

Hollander PA, Amod A, Litwak LE, Chaudhari U (2010) Effect of Rimonabant on Glycemic Control in Insulin-Treated Type 2 Diabetes: The ARPEGGIO Trial. Diabetes care 33:605-607.

Howlett AC (1995) Pharmacology of cannabinoid receptors. Annu Rev Pharmacol Toxicol 35:607-634.

Howlett AC (2005) Cannabinoid receptor signaling. Handb Exp Pharmacol:53-79.

Howlett AC, Barth F, Bonner TI, Cabral G, Casellas P, Devane WA, Felder CC, Herkenham M, Mackie K, Martin BR, Mechoulam R, Pertwee RG (2002) International Union of Pharmacology. XXVII. Classification of cannabinoid receptors. Pharmacol Rev 54:161-202.

Izzo AA, Mascolo N, Borrelli F, Capasso F (1998) Excitatory transmission to the circular muscle of the guinea-pig ileum: evidence for the involvement of cannabinoid CB1 receptors. Br J Pharmacol 124:1363-1368.

Kalia M, Sullivan JM (1982) Brainstem projections of sensory and motor components of the vagus nerve in the rat. J Comp Neurol 211:248-265.

Kathuria S, Gaetani S, Fegley D, Valiño F, Duranti A, Tontini A, Mor M, Tarzia G, La Rana G, Calignano A, Giustino A, Tattoli M, Palmery M, Cuomo V, Piomelli D (2003) Modulation of anxiety through blockade of anandamide hydrolysis. Nat Med 9:76-81.

Kentish S, Li H, Philp LK, O'Donnell TA, Isaacs NJ, Young RL, Wittert GA, Blackshaw LA, Page AJ (2012) Diet-induced adaptation of vagal afferent function. J Physiol 590:209-221.

Kirkham TC, Williams CM, Fezza F, Di Marzo V (2002) Endocannabinoid levels in rat limbic forebrain and hypothalamus in relation to fasting, feeding and satiation: stimulation of eating by 2-arachidonoyl glycerol. Br J Pharmacol 136:550-557.

Konturek PC, Konturek SJ, Ochmański W (2004) Neuroendocrinology of gastric H+ and duodenal HCO3- secretion: the role of brain-gut axis. Eur J Pharmacol 499:15-27.

Kupari J, Häring M, Agirre E, Castelo-Branco G, Ernfors P (2019) An Atlas of Vagal Sensory Neurons and Their Molecular Specialization. Cell Rep 27:2508-2523.e2504.

Lazary J, Juhasz G, Hunyady L, Bagdy G (2011) Personalized medicine can pave the way for the safe use of CB_1 receptor antagonists. Trends Pharmacol Sci 32:270-280.

Leslie RA, Gwyn DG (1984) Neuronal connections of the area postrema. Fed Proc 43:2941-2943.

Leung D, Saghatelian A, Simon GM, Cravatt BF (2006) Inactivation of N-acyl phosphatidylethanolamine phospholipase D reveals multiple mechanisms for the biosynthesis of endocannabinoids. Biochemistry 45:4720-4726.

LoVerme J, Duranti A, Tontini A, Spadoni G, Mor M, Rivara S, Stella N, Xu C, Tarzia G, Piomelli D (2009) Synthesis and characterization of a peripherally restricted CB1 cannabinoid antagonist, URB447, that reduces feeding and body-weight gain in mice. Bioorg Med Chem Lett 19:639-643.

Lutz B, Marsicano G, Maldonado R, Hillard CJ (2015) The endocannabinoid system in guarding against fear, anxiety and stress. Nat Rev Neurosci 16:705-718.

Mackie K (2008) Cannabinoid receptors: where they are and what they do. J Neuroendocrinol 20 Suppl 1:10-14.

Maggi CA (1991) The pharmacology of the efferent function of sensory nerves. J Auton Pharmacol 11:173-208.

Maldonado R, Robledo P, Berrendero F (2013) Endocannabinoid system and drug addiction: new insights from mutant mice approaches. Curr Opin Neurobiol 23:480-486.

Marsicano G, Kuner R (2008) Anatomical distribution of receptors, ligands and enzymes in the brain and in the spinal cord: Circuitries and neurochemistry. In: Cannabinoids and the brain, pp (2008), p 2161-2743.

Marsicano G, Lafenêtre P (2009) Roles of the endocannabinoid system in learning and memory. Curr Top Behav Neurosci 1:201-230.

Matsuda LA, Lolait SJ, Brownstein MJ, Young AC, Bonner TI (1990) Structure of a cannabinoid receptor and functional expression of the cloned cDNA. Nature 346:561-564.

McAllister SD, Glass M (2002) CB(1) and CB(2) receptor-mediated signalling: a focus on endocannabinoids. Prostaglandins Leukot Essent Fatty Acids 66:161-171.

McKinney MK, Cravatt BF (2005) Structure and function of fatty acid amide hydrolase. Annu Rev Biochem 74:411-432.

Mechoulam R, Parker LA (2013) The endocannabinoid system and the brain. Annu Rev Psychol 64:21-47.

Mechoulam R, Ben-Shabat S, Hanus L, Ligumsky M, Kaminski NE, Schatz AR, Gopher A, Almog S, Martin BR, Compton DR (1995) Identification of an endogenous 2-monoglyceride, present in canine gut, that binds to cannabinoid receptors. Biochem Pharmacol 50:83-90.

Munro S, Thomas KL, Abu-Shaar M (1993) Molecular characterization of a peripheral receptor for cannabinoids. Nature 365:61-65.

Norgren R, Smith GP (1988) Central distribution of subdiaphragmatic vagal branches in the rat. J Comp Neurol 273:207-223.

Núñez E, Benito C, Pazos MR, Barbachano A, Fajardo O, González S, Tolón RM, Romero J (2004) Cannabinoid CB2 receptors are expressed by perivascular microglial cells in the human brain: an immunohistochemical study. Synapse 53:208-213.

Okamoto Y, Morishita J, Tsuboi K, Tonai T, Ueda N (2004) Molecular characterization of a phospholipase D generating anandamide and its congeners. J Biol Chem 279:5298-5305.

Onaivi ES et al. (2008) Functional expression of brain neuronal CB2 cannabinoid receptors are involved in the effects of drugs of abuse and in depression. Ann N Y Acad Sci 1139:434-449.

Pacher P, Mechoulam R (2011) Is lipid signaling through cannabinoid 2 receptors part of a protective system? Prog Lipid Res 50:193-211.

Prescott SM, Majerus PW (1983) Characterization of 1,2-diacylglycerol hydrolysis in human platelets. Demonstration of an arachidonoyl-monoacylglycerol intermediate. J Biol Chem 258:764-769.

Price CJ, Hoyda TD, Ferguson AV (2008) The area postrema: a brain monitor and integrator of systemic autonomic state. Neuroscientist 14:182-194.

Ravinet Trillou C, Arnone M, Delgorge C, Gonalons N, Keane P, Maffrand JP, Soubrie P (2003) Anti-obesity effect of SR141716, a CB1 receptor antagonist, in diet-induced obese mice. Am J Physiol Regul Integr Comp Physiol 284:R345-353.

Riebe CJ, Wotjak CT (2011) Endocannabinoids and stress. Stress 14:384-397.

Rinaman L, Card JP, Schwaber JS, Miselis RR (1989) Ultrastructural demonstration of a gastric monosynaptic vagal circuit in the nucleus of the solitary tract in rat. J Neurosci 9:1985-1996.

Rubino T, Realini N, Castiglioni C, Guidali C, Viganó D, Marras E, Petrosino S, Perletti G, Maccarrone M, Di Marzo V, Parolaro D (2008) Role in anxiety behavior of the endocannabinoid system in the prefrontal cortex. Cereb Cortex 18:1292-1301.

Ruehle S, Rey AA, Remmers F, Lutz B (2012) The endocannabinoid system in anxiety, fear memory and habituation. J Psychopharmacol 26:23-39.

Schemann M, Grundy D (1992) Electrophysiological identification of vagally innervated enteric neurons in guinea pig stomach. Am J Physiol 263:G709-718.

Schmid HH (2000) Pathways and mechanisms of N-acylethanolamine biosynthesis: can anandamide be generated selectively? Chem Phys Lipids 108:71-87.

Schmid HH, Schmid PC, Natarajan V (1990) N-acylated glycerophospholipids and their derivatives. Prog Lipid Res 29:1-43.

Sciolino NR, Zhou W, Hohmann AG (2011) Enhancement of endocannabinoid signaling with JZL184, an inhibitor of the 2-arachidonoylglycerol hydrolyzing enzyme monoacylglycerol lipase, produces anxiolytic effects under conditions of high environmental aversiveness in rats. Pharmacol Res 64:226-234.

Smita K, Sushil Kumar V, Premendran JS (2007) Anandamide: an update. Fundam Clin Pharmacol 21:1-8.

Stella N (2004) Cannabinoid signaling in glial cells. Glia 48:267-277.

Sugiura T, Kobayashi Y, Oka S, Waku K (2002) Biosynthesis and degradation of anandamide and 2-arachidonoylglycerol and their possible physiological significance. Prostaglandins Leukot Essent Fatty Acids 66:173-192.

Sugiura T, Kishimoto S, Oka S, Gokoh M (2006) Biochemistry, pharmacology and physiology of 2-arachidonoylglycerol, an endogenous cannabinoid receptor ligand. Prog Lipid Res 45:405-446.

Sugiura T, Kondo S, Sukagawa A, Nakane S, Shinoda A, Itoh K, Yamashita A, Waku K (1995) 2-Arachidonoylglycerol: a possible endogenous cannabinoid receptor ligand in brain. Biochem Biophys Res Commun 215:89-97.

Tam J, Hinden L, Drori A, Udi S, Azar S, Baraghithy S (2018) The therapeutic potential of targeting the peripheral endocannabinoid/CB. Eur J Intern Med 49:23-29.

Tam J, Vemuri VK, Liu J, Bátkai S, Mukhopadhyay B, Godlewski G, Osei-Hyiaman D, Ohnuma S, Ambudkar SV, Pickel J, Makriyannis A, Kunos G (2010) Peripheral CB1 cannabinoid receptor blockade improves cardiometabolic risk in mouse models of obesity. J Clin Invest 120:2953-2966.

Thomas G et al. (2013) The serine hydrolase ABHD6 Is a critical regulator of the metabolic syndrome. Cell Rep 5:508-520.

Travagli RA, Hermann GE, Browning KN, Rogers RC (2006) Brainstem circuits regulating gastric function. Annu Rev Physiol 68:279-305.

Van Gaal L, Pi-Sunyer X, Després J-P, McCarthy C, Scheen A Efficacy and Safety of Rimonabant for Improvement of Multiple Cardiometabolic Risk Factors in Overweight/Obese Patients: Pooled 1-year data from the Rimonabant in Obesity (RIO) program. Diabetes care.

Van Sickle MD, Duncan M, Kingsley PJ, Mouihate A, Urbani P, Mackie K, Stella N, Makriyannis A, Piomelli D, Davison JS, Marnett LJ, Di Marzo V, Pittman QJ, Patel KD, Sharkey KA (2005) Identification and functional characterization of brainstem cannabinoid CB2 receptors. Science 310:329-332.

Varga EV, Georgieva T, Tumati S, Alves I, Salamon Z, Tollin G, Yamamura HI, Roeske WR (2008) Functional selectivity in cannabinoid signaling. Curr Mol Pharmacol 1:273-284.

Wade DT, Robson P, House H, Makela P, Aram J (2003) A preliminary controlled study to determine whether whole-plant cannabis extracts can improve intractable neurogenic symptoms. Clin Rehabil 17:21-29.

Walter GC, Phillips RJ, Baronowsky EA, Powley TL (2009) Versatile, high-resolution anterograde labeling of vagal efferent projections with dextran amines. J Neurosci Methods 178:1-9.

Wang J, Ueda N (2008) Role of the endocannabinoid system in metabolic control. Curr Opin Nephrol Hypertens 17:1-10.

White RL, Rossiter CD, Hornby PJ, Harmon JW, Kasbekar DK, Gillis RA (1991) Excitation of neurons in the medullary raphe increases gastric acid and pepsin production in cats. Am J Physiol 260:G91-96.

Wiley JL, Burston JJ, Leggett DC, Alekseeva OO, Razdan RK, Mahadevan A, Martin BR (2005) CB1 cannabinoid receptor-mediated modulation of food intake in mice. Br J Pharmacol 145:293-300.

Wiley M, Perez P, Argueta D, Avalos B, Wood C, DiPatrizio N (2021) UPLC-MS/MS Method for Analysis of Endocannabinoid and Related Lipid Metabolism in Mouse Mucosal Tissue. Frontiers in Physiology 12.

Williams EK, Chang RB, Strochlic DE, Umans BD, Lowell BB, Liberles SD (2016) Sensory Neurons that Detect Stretch and Nutrients in the Digestive System. Cell 166:209-221.

Chapter 1: Cholinergic Neurotransmission Controls Orexigenic Endocannabinoid Signaling in the Gut in Diet-Induced Obesity

Authors: Courtney P. Wood[1] and Nicholas V. DiPatrizio[1]

[1]Division of Biomedical Sciences, School of Medicine, University of California, Riverside, Riverside, CA, 92521, USA; University of California Riverside Center for Cannabinoid Research, Riverside, CA, 92521, USA

Acknowledgements: Research is funded by the National Institutes of Health (R01 DK119498 and L30 DK1149978) and the Tobacco-Related Disease Research Program (T29KT0232). The authors thank Samantha Sutley and Dr. Iryna Ethell's laboratory for their guidance in developing the cFos IHC assay, as well as Jeffrey Koury and Dr. Marcus Kaul's laboratory for training and use of the fluorescence microscope, and Will Cruz for assistance with chemical analyses.

Abstract

The brain bidirectionally communicates with the gut to control food intake and energy balance, which becomes dysregulated in obesity. For example, endocannabinoid (eCB) signaling in the small-intestinal epithelium (SI) is upregulated in diet-induced obese mice (DIO) and promotes overeating by a mechanism that includes inhibiting gut-brain satiation signaling. Upstream neural and molecular mechanism(s) involved in overproduction of orexigenic gut eCBs in DIO, however, are unknown. We tested the hypothesis that overactive parasympathetic signaling at muscarinic acetylcholine receptors (mAChRs) in the SI increases biosynthesis of the eCB, 2-arachidonoyl-*sn*-glycerol (2-AG), which drives hyperphagia via local CB_1Rs in DIO. Male mice were maintained on a high-fat/high-sucrose western-style diet for 60 days, then administered several mAChR antagonists 30 min prior tissue harvest or a food intake test. Levels of 2-AG and activity of its metabolic enzymes in the SI were quantitated. DIO mice, when compared to those fed a low-fat/no-sucrose diet, displayed increased expression of cFos protein in the dorsal motor nucleus of the vagus, which suggests increased activity of efferent cholinergic neurotransmission. These mice exhibited elevated levels of 2-AG biosynthesis in the SI, which was reduced to control levels by mAChR antagonists. Moreover, the peripherally-restricted mAChR antagonist, methylhomatropine bromide, and the peripherally-restricted CB_1R antagonist, AM6545, reduced food intake in DIO mice for up to 24 h but had no effect in mice conditionally deficient in SI CB_1Rs. These results suggest that

hyperactivity at mAChRs in the periphery increases formation of 2-AG in the SI and activates local CB_1Rs, which drives hyperphagia in DIO.

Significance Statement

Gut-brain signaling controls food intake and energy homeostasis; however, it is poorly understood how gut-brain signaling becomes dysregulated in obesity. In this study, we demonstrated that brain to gut communication is altered in obesity, leading to an increase in endocannabinoid signaling in the GI tract, which drives overeating. Acutely blocking activity at muscarinic acetylcholine receptors in the periphery attenuates intestinal endocannabinoid production and calorie intake in obese animals across a 24-hour period. This effect was absent in mice conditionally lacking CB_1Rs in the intestinal epithelium. These findings expand our understanding of the complex pathophysiology associated with obesity and mechanisms of brain-gut-brain signaling.

Introduction

Food intake and energy balance are controlled by gut-brain neurotransmission, and this communication becomes dysregulated in obesity (Berthoud, 2008; de Lartigue et al., 2011; de Lartigue et al., 2014; Argueta et al., 2019; McDougle et al., 2021). For example, vagal afferent neurons in diet-induced obese (DIO) mice displayed impaired responses to the satiation peptide, cholecystokinin (CCK) (Daly et al., 2011), as well as reduced sensitivity to mechanical stimulation (Kentish et al., 2012) and leptin signaling

(de Lartigue et al., 2011). Mounting evidence also suggests that overactive endocannabinoid (eCB) signaling in the upper small-intestinal lining in DIO mice (Artmann et al., 2008; Izzo et al., 2009; Argueta and DiPatrizio, 2017) contributes to overeating and dysregulated gut brain-mediated satiation by a mechanism that includes inhibiting nutrient-induced CCK release (Argueta et al., 2019; DiPatrizio, 2021). Furthermore, recent studies highlight an important function for gut-brain communication in the control of food preferences and reward (Han et al., 2018; Sclafani, 2018; Li et al., 2022), and the contribution of gut-brain eCB signaling in these processes (DiPatrizio et al., 2013; Avalos et al., 2020; Berland et al., 2022). Indeed, acute preferences for western-style high-fat/sucrose diets versus low-fat/no-sucrose diets are absent in mice conditionally lacking cannabinoid subtype-1 receptors (CB_1Rs) in intestinal epithelial cells, which underscores an essential role for CB_1Rs in the intestinal lining in gut-brain control of preferences for palatable foods (Avalos et al., 2020).

Less is known about how obesity affects activity of vagal efferent neurons, which provide dense cholinergic innervation to the gastrointestinal tract from the caudal brainstem (Berthoud et al., 1991; Altschuler et al., 1993). Nonetheless, early studies suggest that this parasympathetic neurotransmission may play an important role in brain-gut signaling that controls feeding behavior. The peripherally-restricted muscarinic acetylcholine receptor (mAChR) antagonist, atropine methyl nitrate, inhibited intake of a liquid diet in sham-feeding rats (Lorenz et al., 1978) and prevented refeeding after a fast (Pradhan and Roth, 1968). In addition, activity of cholinergic efferent vagal neurons that

project from the dorsal motor nucleus of the vagus (DMV) to the gut is controlled by central melanocortin-4 receptors (MC4Rs) (Sohn et al., 2013), which play a key role in energy homeostasis and attenuation of food intake (Williams and Elmquist, 2012). Specific roles for the eCB system in brain-gut cholinergic control of food intake and its dysregulation in obesity, however, are unclear.

Several reports suggest that mAChR signaling controls eCB production in the central nervous system (Kim et al., 2002; Straiker and Mackie, 2007; Zhao and Tzounopoulos, 2011; Rinaldo and Hansel, 2013). Similarly, cholinergic signaling in the periphery stimulates biosynthesis of orexigenic eCBs in the upper small-intestinal epithelium of fasted rats, an effect that was blunted by surgical resection of the vagus nerve below the diaphragm or after administration of several mAChR antagonists (DiPatrizio et al., 2015). Moreover, tasting dietary fats increased biosynthesis of eCBs in this organ and promoted further intake of fat through activating local CB_1Rs (DiPatrizio et al., 2011; DiPatrizio et al., 2013). This increased eCB activity was also blocked in vagotomized animals. Together, these studies suggest an important role for the efferent vagus nerve in the biosynthesis of appetite-promoting eCBs in cells lining the upper intestine.

A primary biosynthetic pathway for the abundant eCB, 2-arachidonoyl-*sn*-glycerol (2-AG), requires a two-step enzymatic process that includes phospholipase C (PLC) and diacylglycerol lipase (DGL) activity (Stella et al., 1997; Piomelli et al., 2007; Aaltonen et al., 2014). This pathway can be activated by metabotropic receptors coupled to G_q-type g-

proteins such as group I metabotropic glutamate receptors or muscarinic acetylcholine receptor sub-types 1 and 3 (m_1 and m_3 mAChR, respectively) (Hulme et al., 1990; Caulfield and Birdsall, 1998; Jung et al., 2007; Aaltonen et al., 2014). Here, we tested the hypothesis that overactive parasympathetic signaling at mAChRs increases biosynthesis of 2-AG in the upper small-intestinal epithelium in DIO, which drives overeating via local CB_1Rs.

Materials & Methods

Animals

C57BL/6 male mice (Taconic, Oxnard, CA, USA) or transgenic mice (described below in *Transgenic Mouse Generation*) 8-10 weeks of age were group-housed with *ad-libitum* access to standard rodent laboratory diet (SD; Teklad 2020x, Envigo, Huntingdon, UK; 16% kcal from fat, 24% kcal from protein, 60% kcal from carbohydrates) or Western Diet (WD; Research Diets D12709B, New Brunswick, NJ, USA; 40% kcal from fat, 17% kcal from protein, 43% kcal from carbohydrates as mostly sucrose) and water throughout all experiments unless otherwise stated. Mice were maintained on a 12-h dark/light cycle beginning at 1800 h. All procedures met the U.S. National Institute of Health guidelines for care and use of laboratory animals and were approved by the Institutional Animal Care and Use Committee (IACUC) of the University of California, Riverside.

Transgenic Mouse Generation

Conditional intestinal epithelium-specific CB_1R-deficient mice (IntCB_1-/-, Cnr1$^{tm1.1\ mrl}$/vil-cre ERT2) were generated by crossing Cnr1-floxed mice (IntCB_1+/+, Cnr1$^{tm1.1\ mrl}$;

Taconic, Oxnard, CA, USA; Model #7599) with Vil-CRE ERT2 mice donated by Dr. Randy Seeley (University of Michigan, Ann Arbor, MI, USA) with permission from Dr. Sylvie Robin (Curie Institute, Paris, France). Cre recombinase expression in the intestinal epithelium is driven by the villin promotor, which allows for conditional tamoxifen-dependent Cre recombinase action to remove the *Cnr1* gene from these cells, as described by el Marjou et al. (el Marjou et al., 2004). $Cnr1^{tm1.1\ mrl}$/vil-cre ERT2 mice used in these experiments are referred to as $IntCB_1$-/-, and $Cnr1^{tm1.1\ mrl}$ control mice (lacking Cre recombinase) are referred to as $IntCB_1$+/+. Tail snips were collected from pups at weaning and DNA was extracted and analyzed by conventional PCR using the following primers (5'-3'): GCAGGGATTATGTCCCTAGC (CNR1-ALT), CTGTTACCAGGAGTCTTAGC (1415-35), GGCTCAAGGAATACACTTATACC (1415-37), GAACCTGATGGACATGTTCAGG (vilcre, AA), AGTGCGTTCGAACGCTAGAGCCTGT (vilcre, SS), TTACGTCCATCGTGG-ACAGC (vilcre, MYO F), TGGGCTGGGTGTTAGCCTTA (vilcre, MYO R). Knockdown of Cnr1 expression in the intestinal epithelium was verified by RT-qPCR immediately following feeding behavior experiments ($intCB_1$+/+ control mice, 1.000 ± 0.2869; $intCB_1$-/- mice, 0.1226 ± 0.0149; $t_{(13)} = 3.282$, $p = 0.0060$ via two-tailed t-test).

Drug Preparation and Administration

$IntCB_1$-/- and $intCB_1$+/+ mice were administered tamoxifen (IP, 40 mg per kg) daily for five consecutive days. Tamoxifen (Sigma-Aldrich, St. Louis, MO, USA) was dissolved in corn oil using bath sonication at a concentration of 10 mg per mL then stored at 37°C protected from light until administration. Mice were group housed in disposable cages

throughout the injection period and for a 3-day post-injection period. JZL-184 (Tocris, Bristol, UK) was incubated with intestinal epithelium tissue homogenate to inhibit MGL activity in the DGL enzyme activity assay. The peripherally-restricted non-selective muscarinic acetylcholine receptor antagonist methylhomatropine (bromide) (ATR; Cayman Chemicals, Ann Arbor, MI, USA) was dissolved in 0.9% sterile sodium chloride solution (LabChem, Zelienople, PA, USA) and administered (IP, 2 mg per kg per 2 mL) 30 minutes prior to tissue harvest and testing. The selective muscarinic M_3 receptor antagonist DAU 5884 hydrochloride (DAU; Tocris Bioscience, Minneapolis, MN, USA) was dissolved in 0.9% sterile sodium chloride solution (LabChem, Zelienople, PA, USA) and administered (IP, 2 mg per kg per 2 mL) 30 minutes prior to tissue harvest and testing. The selective muscarinic M_1 receptor antagonist Pirenzepine dihydrochloride (PIR; Sigma-Aldrich, St. Louis, MO, USA) was dissolved in 0.9% sterile sodium chloride solution (LabChem, Zelienople, PA, USA) and administered (IP, 2 mg per kg per 2 mL) 30 minutes prior to tissue harvest and testing. The peripherally-restricted CB_1R neutral antagonist AM6545 (Northeastern University Center for Drug Discovery, Boston, MA, USA) was administered (IP, 10 mg per kg per 2 mL) 30 minutes prior to testing. The vehicle for AM6545 consisted of 7.5% dimethyl sulfoxide (DMSO, Sigma-Aldrich, St. Louis, MO, USA), 7.5% Tween 80 (Chem Implex Intl Inc., Wood Dale, IL, USA), and 85% 0.9% sterile sodium chloride solution (LabChem, Zelienople, PA, USA).

Lipid Extraction

Animals were anesthetized with isoflurane at the time of tissue harvest (0900 h) following *ad libitum* food and water access. Jejunum was quickly removed and washed in ice cold phosphate-buffered saline (PBS), opened longitudinally on a stainless-steel tray on ice, and contents were removed. Jejunum mucosa was isolated using glass slides to scrape epithelial layer and was snap-frozen in liquid nitrogen (N_2). Samples were stored at -80°C until analysis. Frozen tissues were weighed and then homogenized in 1 mL methanol (MeOH) solution containing 500 pmol [$^2H_5$]-2-AG, 5 pmol [$^2H_4$]-AEA, and 5 pmol [$^2H_4$]-OEA or 500 pmol of dinonadecadienoin (19:2 diacylglycerol, 19:2 DAG; Nu-Check Prep, Waterville, MN, USA) as internal standards. Lipids were extracted as previously described (Argueta and DiPatrizio, 2017) and resuspended in 0.2 mL $CHCl_3$:MeOH (1:1). 1 µL of the resulting sample was analyzed via ultra-performance liquid chromatography/tandem mass spectrometry (UPLC-MS/MS).

LCMS Detection of 1-stearoyl, 2-arachidonoyl-sn-lycerol (SAG), MAGs, and FAEs

Data were acquired using an Acquity I Class UPLC with direct connection to a Xevo TQ-S Micro Mass Spectrometer (Waters Corporation, Milford, MA, USA) with electrospray ionization (ESI) sample delivery. 2-Arachidonoyl-*sn*-Glycerol (2-AG) and other analytes were detected as previously described (Argueta et al., 2019). SAG was separated using an Acquity UPLC BEH C_{18} column (2.1 mm x 50 mm i.d., 1.7 µm, Waters Corporation), and eluted by a gradient of water, isopropyl alcohol (IPA), and acetonitrile (ACN) containing 10 mM NH_4 formate at a flow rate of 0.4 mL per min and gradient: 80% ACN:water (60:40)

and 20% ACN:IPA (10:90) 0.5 min, 80% to 0% ACN:water 0.5 – 6.0 min, 0% ACN:water 6.0 – 6.25 min, 0% to 80% ACN:water 6.25 – 6.50 min. The column was maintained at 50°C, and samples were kept at 10°C in accompanying sample manager. MS/MS detection was in positive ion mode with capillary voltage maintained at 1.10 kV, and argon (99.998%) was used as collision gas. Cone voltages and collision energies for respective analytes: SAG (18:0, 20:4) = 38v, 14v; 2-AG (20:4) = 30v, 12v; 2-OG (18:1) = 42v, 10v; 2-DG (22:6) = 34v, 14v; 2-LG (18:2) = 30v, 10v; 19:2 DAG = 26v, 14v; [$^2H_5$]-2-AG = 25v, 44v. Lipids were quantitated using a stable isotope dilution method detecting H^+ or Na^+ adducts of the molecular ions $[M + H/Na]^+$ in multiple reaction monitoring mode (MRM). Extracted ion chromatograms for MRM transitions were used to quantitate analytes: SAG (*m/z* = 662.9> 341.3), 2-AG (*m/z* = 379.3 > 287.3), 2-OG (*m/z* = 357.4 > 265.2), 2-DG (*m/z* = 403.3 > 311.2), 2-LG (*m/z* = 355.3 > 263.3), with 19:2 DAG (*m/z* = 662.9 > 627.5) as internal standard for SAG, and [$^2H_5$]-2-AG (*m/z* = 384.3 > 93.4) as internal standard for all MAGs. One "blank" sample that did not include any experimental tissue was processed and analyzed in the same manner as all other samples. This control revealed no detectable eCBs and related lipids included in our analysis.

Enzyme Activity Assays

Intestinal epithelium was collected as described above (*Lipid Extracts*) and approximately 100 mg of frozen tissue was homogenized in 2 mL of ice-cold 50 mM Tris-HCl, 320 mM sucrose (pH 7.5) buffer, as previously described (Wiley et al., 2021). Homogenates were centrifuged at 800 g for 10 min at 4°C and supernatant was collected.

Protein supernatants were sonicated twice for 10 s and then freeze-thawed in liquid N_2 twice. Samples were spun again, and supernatant protein content was quantified using BCA assay and diluted to working concentration with Tris-HCl/sucrose buffer. For the DGL activity assay, small-intestinal epithelial tissue homogenates (25 µg, room temperature) were incubated with the MGL inhibitor, JZL-184 (0.3 µM; Tocris, Bristol, UK), and any other drugs tested for 10 minutes. Homogenates were then incubated in 0.2 mL Tris-HCl with 0.2% Triton X-100 (pH 7.0 at 37°C) containing 20 nmol 19:2 DAG (Nu-Check Prep, Waterville, MN, USA) at 37°C for 30 min. Reactions were stopped by adding 1 mL ice-cold methanol containing 25 pmol [$^2H_5$]-2-AG as internal standard. Lipids were extracted and the product of the reaction, monononadecadienoin (19:2 monoacylglycerol, 19:2 MAG), was analyzed via UPLC-MS/MS as previously described (Argueta et al., 2019). For the MGL activity assay, small-intestinal epithelial tissue (10 µg) was incubated with 0.4 mL Tris-HCl with 0.1% bovine serum albumin (BSA) (pH 8.0 at 37°C) containing 50 nmol 19:2 MAG (Nu-Check Prep, Waterville, MN, USA; final volume 0.5 mL per reaction) at 37°C for 10 min. Reactions were stopped by adding 1 mL MeOH containing 10 nmol heptadecanoic acid (17:1 free fatty acid, 17:1 FFA; Nu-Check Prep) as internal standard. Lipids were extracted and the product of the reaction (19:2 free fatty acid, 19:2 FFA) was analyzed via UPLC-MS/MS as previously described (Argueta et al., 2019). GraphPad Prism software generated the following error message for the enzyme inhibition curves in **Figures 4*B*, *C*,** and ***D***: *"For at least one parameter, Prism was able to find a best-fit value but was unable to calculate a complete confidence interval. This best-fit value should be interpreted with*

caution". Negative R^2 values are indicative of no correlation between the drug concentration and enzyme activity, so we included this information to further demonstrate that DAU, PIR, and ATR are not directly inhibiting DGL activity.

Feeding Behavior

Mice were single-housed in two-hopper feeding chambers (TSE Systems, Chesterfield, MO, USA) for five days to acclimate, and received *ad-libitum* access to food and water throughout behavioral testing. Total caloric intake of each diet (kcal), water intake (mL), and distance travelled (km) were calculated every minute across the testing period, beginning at the start of the dark cycle (1800 h) for 24 h. Data were processed using TSE Phenomaster software, as previously described (Avalos et al., 2020).

Gene Expression

Total RNA from intestinal epithelium tissue was extracted using an RNeasy kit (Qiagen, Valencia, CA, USA) and first-strand cDNA was generated using M-MLV reverse transcriptase (Invitrogen, Carlsbad, CA, USA). Areas used for tissue collection and processing were sanitized with 70% ethanol solution then treated with RNAse inhibitor (RNAse Out, G-Biosciences, St. Louis, MO, USA). Reverse transcription of total RNA was performed as previously described (Argueta et al., 2019). Quantitative RT-PCR was performed using preconfigured SYBR green PrimePCR assays (Biorad, Irvine, CA, USA) with the primer for the CB_1R (Cnr1) gene transcript. Hprt was used as a housekeeping gene. Reactions were run in duplicates and values expressed as relative mRNA expression.

cFos Immunohistochemistry

On the day of the experiment, mice were allowed *ad-libitum* access to food and water for the entire day, and then fasted 30 minutes prior to the onset of the dark cycle (1730h) to reduce gut-brain feedback resulting from food consumption. cFos protein can be detected 20-90 minutes following the stimulus (Bullitt, 1990), therefore mice were perfused between 1845h and 1915h (45-75 minutes following the onset of the dark period) to enable optimal cFos detection in the brainstem. Experiments occurred in the absence of any drug or other treatment to examine whether DMV neuronal activation differs between SD- and WD-fed mice in basal conditions. Animals were deeply anesthetized with isoflurane and transcardially perfused with 40 mL of ice-cold PBS immediately followed by 40 mL of ice-cold 4% paraformaldehyde (PFA). The brainstem was immediately collected and stored at 4°C overnight in 4% PFA. Brainstems were transferred to a solution containing 30% sucrose and 0.01% sodium azide in PBS and stored at 4°C until adequate cryopreservation was achieved (when tissue had completely sunk to the bottom of the solution). Brainstems were stored in OCT compound at -20°C until processing. On the day of the assay, 50 µM sections of the medulla were transferred to PBS and then sequentially incubated (including PBS and/or PBST wash steps between incubations) in: 1) 10 mM citrate buffer, pH 6.0; 2) 4% normal goat serum (NGS) (Millipore Sigma, Burlington, MA, USA) in PBST; 3) anti-cFos rabbit monoclonal antibody (1:500, Cell Signaling Technology, Danvers, MA, USA) in blocking buffer; 4) anti-rabbit IgG Alexa Fluor 488 conjugate (1:500, Cell Signaling Technology, Danvers, MA, USA) in blocking buffer.

Sections were mounted on glass slides, allowed to air-dry overnight, and coverslips were added with VECTASHIELD mounting medium with DAPI (Vector Laboratories, Newark, CA, USA) prior to imaging.

Microscopy & Image Analysis

Fluorescent images were taken on a Zeiss 200 M fluorescence deconvolution microscope equipped with a computer-controlled stage and the appropriate filters for DAPI and FITC (Carl Zeiss Microscopy GmbH, Jena, Germany). Slidebook software (version 6, Intelligent Imaging Innovations, Inc., Denver, CO) was used for all image acquisition. Quantitative analysis of $cFos^+$ cells in the DMV was performed as described previously (Igelstrom et al., 2010; Perrin-Terrin et al., 2016). Briefly, one section per animal was imaged at 10× so that local landmarks were visible to enable consistent analysis between samples. The exposure period was kept the same for all analyzed images. cFos immunoreactivity was quantified using Fiji open-source software (Schindelin et al., 2012). Images were subject to identical black/white thresholding to enable counting of positive nuclei. $cFos^+$ puncta were counted using the Particle Analysis function within bilateral fixed areas of each image.

Experimental Design & Statistical Analysis

Details regarding the experimental design of individual experiments are provided in the figure legends. Data were analyzed by GraphPad Prism version 9.5.0 (GraphPad Software, La Jolla, CA, USA) using unpaired Student's *t*-tests (two-tailed), one-way ANOVA, two-way ANOVA, or three-way ANOVA with Holm-Sidak's multiple comparisons

post-hoc test when appropriate. Inhibition curves in **Figure 4** were generated using a least squares fit of log[inhibitor] vs. normalized response. Results are expressed as means ± S.E.M. and significance was determined at $p<0.05$.

Results

Neuronal Activity is Increased in the DMV of DIO Animals

We tested the hypothesis that parasympathetic neurotransmission is overactive in DIO, which drives overproduction of gut eCBs and associated hyperphagia. $cFos^+$ cells in the dorsal motor nucleus of the vagus (DMV) of untreated lean control mice fed SD (**Fig. 1.1*A***) and DIO mice fed WD (**Fig. 1.1*B***) were quantified. WD-fed mice exhibited an increased number of $cFos^+$ cells in the DMV when compared to SD-fed controls, which suggests increased activity of DMV neurons in obesity (**Fig. 1.1*C***). These mice also gained significantly more body weight (**Supplemental Fig. 1.1*A***), demonstrated increased change in body weight (**Supplemental Fig. 1.1*B***), consumed more calories (**Supplemental Fig. 1.1*C***), and displayed increased epididymal fat mass (**Supplemental Fig. 1.1*D***), similar to previous studies (Argueta and DiPatrizio, 2017; Argueta et al., 2019).

MAChR Antagonism Normalizes ECB Levels in the Upper Intestinal Epithelium in DIO Mice

We next investigated if inhibiting activity of mAChRs blocks overactive eCB activity in the upper small-intestinal epithelium. Consistent with our previous findings (Argueta and DiPatrizio, 2017; Argueta et al., 2019), mice fed WD exhibited higher levels of 2-AG in

the upper small-intestinal epithelium (**Fig. 1.2*A***) when compared to SD control mice. WD mice treated with a single IP injection of the selective m_3 mAChR antagonist, DAU (2 mg per kg), had significantly reduced levels of 2-AG (**Fig. 1.2*A***) and other monoacylglycerols (**Fig. 1.2*B, C***) in the upper small-intestinal epithelium, when compared to vehicle-treated WD mice. Notably, levels were reduced to those found in SD mice. Treatment with the selective m_1 mAChR antagonist, PIR (2 mg per kg), did not significantly affect levels of 2-AG, but did reduce levels of 2-OG in WD mice (**Fig. 1.2*C***). Lastly, the peripherally-restricted non-selective mAChR antagonist, ATR (2 mg per kg), reduced levels of 2-AG (**Fig. 1.2*A***) and 2-DG (**Fig. 1.2*B***) in WD mice to levels found in SD mice.

SAG Formation and DGL Activity in Jejunum Mucosa are Inhibited by MAChR Antagonism

We next tested if changes in metabolism of monoacylglycerols (see **Fig. 1.3*D***) in the upper small-intestinal epithelium led to increased levels of 2-AG in WD mice and the ability for mAChR antagonists to normalize levels to those found in SD control mice. We first analyzed levels of the diacylglycerol precursor of 2-AG, 1-stearoyl,2-arachidonoyl-*sn*-glycerol (SAG). Similar to 2-AG, levels of SAG were significantly elevated in the intestinal epithelium of vehicle-treated WD mice when compared to vehicle-treated SD mice, and treatment with DAU (2 mg per kg), PIR (2 mg per kg), and ATR (2 mg per kg) reduced SAG levels in WD mice to those found in SD mice (**Fig. 1.3*A***). Furthermore, activity of diacylglycerol lipase (DGL) – an eCB biosynthetic enzyme responsible for the hydrolysis of SAG and its conversion to 2-AG – was similarly reduced by treatment with mAChR

antagonists (**Fig. 1.3*B***). Activity of monoacylglycerol lipase (MGL), a primary degradative enzyme responsible for 2-AG inactivation (Dinh et al., 2002) was not significantly affected by drug treatments (**Fig. 1.3*C***).

Anticholinergics Do Not Affect 2-AG Metabolic Enzyme Activity Ex Vivo

We utilized our UPLC/MS^2-based DGL activity assay (Wiley et al., 2021) to confirm that DGL activity was not directly disrupted *ex vivo* (see **Fig. 1.3*B***) by any of the drugs used *in vivo*. Activity of DGL in intestinal epithelium tissue from WD mice was inhibited in a concentration-dependent manner by an inhibitor of DGL, tetrahydrolipstatin (THL, 3nM to 1μM range) (**Fig. 1.4*A***). In contrast to THL, incubation of tissue with a wide range of concentrations of mAChR antagonists used in these studies including ATR (**Fig. 1.4*B,*** 10nM to 10μM range), DAU (**Fig. 1.4*C,*** 10nM to 100μM range), and PIR (**Fig. 1.4*C,*** 10nM to 10μM range) failed to affect enzymatic activity of DGL, which suggests that these drugs do not directly interfere with DGL activity.

MAChR Antagonism Reduces Caloric Intake in DIO Mice

Roles for peripheral mAChRs in overeating associated with DIO mice were evaluated next. A single dose of ATR (2mg per kg) reduced caloric intake for up to 24 h in WD mice (**Fig. 1.5*A***) but had no effect in SD mice (**Fig. 1.5*B***). Moreover, ATR treatment in WD mice reduced caloric intake to similar levels induced by the peripherally-restricted CB_1R antagonist, AM6545 (**Fig. 1.5*A*,** 10 mg/kg). When ATR and AM6545 were co-

administered in WD mice, caloric intake was comparable to intakes found after administration of each drug alone (**Fig. 1.5*A***). Treatment with AM6545 alone or in combination with ATR did not significantly affect intake in SD mice (**Fig. 1.5*B***). A single injection of DAU (2mg per kg) also caused a reduction in caloric intake in WD mice – but not SD mice – for up to 12 h (**Fig. 1.5*C*, 1.5*D***). In contrast to DAU and ATR, PIR (2mg per kg) had no effect on intake irrespective of diet (**Fig. 1.5*E*, 1.5*F***).

Inhibiting Peripheral CB_1Rs or MAChRs Failed to Affect Food Intake in Mice Conditionally Lacking CB_1Rs in the Intestinal Epithelium

We next utilized conditional intestinal epithelium-specific CB_1R-deficient mice [intCB_1-/- (Avalos et al., 2020; Wiley and DiPatrizio, 2022)] to determine if CB_1Rs in the intestinal epithelial cells were required for the appetite-suppressing effects of peripherally-restricted CB_1R and mAChR antagonists in obese WD mice. IntCB_1-/- mice and control mice with functional CB_1Rs in the intestinal epithelium (intCB_1+/+) were placed on WD for 60 days. AM6545 (10 mg/kg) or ATR (2 mg/kg) treatment reduced caloric intake for up to 24 hours in WD intCB_1+/+ control mice (**Fig. 1.6*A***). Notably, however, neither drug had an effect on intake in WD intCB_1-/- mice (**Fig. 1.6*B***). Both intCB_1+/+ and intCB_1-/- mice had largely similar body weights throughout diet exposure (**Fig. 1.6*C***); however, analysis of change in body weight from baseline by two-way ANOVA revealed a genotype effect that indicated intCB_1-/- mice had lower body weight gain when compared to intCB_1+/+ control mice (**Fig. 1.6*D***).

Discussion

We report that *(i)* neuronal activity in the DMV of DIO mice is increased when compared lean mice, *(ii)* cholinergic activity at peripheral mAChRs in DIO promotes biosynthesis of 2-AG in the upper-intestinal epithelium by a mechanism that includes increased production of local 2-AG precursors and their conversion to 2-AG, and *(iii)* CB_1Rs in the intestinal epithelium are required for hyperphagia associated with overstimulation of these pathways in DIO. These results suggest a novel brain-gut mechanism that drives overeating in DIO through interactions between cholinergic neurotransmission and orexigenic eCB signaling in the gut.

DIO mice, when compared to lean controls, displayed a significantly larger number of $cFos^+$ cells in the DMV, which suggests increased activity of efferent parasympathetic vagal fibers. The DMV is the primary source of parasympathetic input to the digestive system (Gibbons, 2019); therefore, it is likely that most – if not all – of the labeled cells are cholinergic. Moreover, motor neurons originating in the DMV have functionally and anatomically discrete outputs to distinct segments of the gastrointestinal tract and other organs (Rogers et al., 2006; Schubert and Peura, 2008; Mawe et al., 2018; Tao et al., 2021). Future experiments will be necessary to further confirm if the same DMV neurons that are activated in obese mice are the source of mAChR hyperactivity that leads to overproduction of 2-AG in the upper small-intestinal epithelium.

Although not quantified, an increase in the number of $cFos^+$ cells in other regions of the intermediate medulla, namely the nucleus of the solitary tract (NTS), was observed.

Thus, it is possible that a general dysregulation within the medulla of obese mice occurs. Accordingly, it was recently reported that the daily rhythms of oscillating cells within the NTS are disrupted by exposure to high-fat diet (Chrobok et al., 2022b). The same group also demonstrated that high-fat diet exposure amplified the daily variation of time-keeping cells within the DMV and blunted neuronal responsiveness to metabolic neuromodulators (Chrobok et al., 2022a). These studies and others (Kentish et al., 2012; Kentish et al., 2016; Clyburn et al., 2018; Zhang et al., 2020; Kovacs and Hajnal, 2022) support the notion that select brainstem nuclei, which are responsible for sensing nutritional status and maintaining metabolic homeostasis (i.e., DMV and NTS), become dysregulated in response to metabolic challenges.

Our data reveal the necessity for mAChRs in controlling eCB biosynthesis in the intestinal epithelium in DIO mice. These animals had elevated levels of the 2-AG precursor, SAG, activity of DGL, and 2-AG in the intestinal epithelium, which was attenuated by treatment with the m_3-specific antagonist, DAU, or the non-selective peripherally-restricted mAChR antagonist, ATR. While the m_1-specifc antagonist, PIR, was effective in reducing both SAG and DGL activity levels, it did not significantly reduce 2-AG formation, nor did it have a significant effect on caloric intake in DIO mice. Together, these results suggest a more prominent role for the m_3 mAChR subtype in driving eCB biosynthesis and overeating in DIO. Interestingly, m_3 mAChR activation in the central nervous system initiates a signaling cascade that rapidly upregulates expression of Cnr1 mRNA and potentiates responses to CB_1R agonists, such as 2-AG (Marini et al., 2023). In

further support of the role of m_3 versus m_1 AChRs in the current experiments, we reported that following 24 hr of food deprivation (another metabolic challenge that has been shown to elevate intestinal 2-AG), DAU, but not PIR, blocked biosynthesis of 2-AG in the upper small-intestinal epithelium of rats (DiPatrizio et al., 2015). Given that mRNA for both m_1 and m_3 subtypes is expressed in mouse duodenum, jejunum, and ileum epithelial cells (Muise et al., 2017), future studies should determine the expression patterns of these receptors in specific cell types and their co-localization with eCB metabolic enzymes and CB_1Rs throughout the gastrointestinal tract.

The effects of acute mAChR antagonism on caloric intake in DIO mice last for up to 24 h. Thus, it is possible that treatment with DAU or ATR would be beneficial for reducing caloric intake in obesity; however, there are several concerns using this strategy that include possible deleterious side effects. **Supplemental Figures 1.2*A*** and **1.3*A*** reveal a minor effect of ATR on ambulation in DIO mice. In combination with AM6545, ATR also yielded reductions in ambulation in both lean and DIO mice (**Supplemental Fig. 1.2*A, B*** and accompanying **Supplemental Table 1.1**). Though it was reported by Cluny *et al*. that daily injections of AM6545 did not cause malaise in rodents (Cluny et al., 2010), it is possible that AM6545 and ATR in combination may synergistically generate unfavorable side effects. Independently, AM6545 reduced ambulation in intCB_1+/+ mice, but had no effect on ambulation in intCB_1-/- animals (**Supplemental Fig. 1.*3A, B*** and accompanying **Supplemental Table 1.2**). AM6545 also reduced water intake in intCB_1-/- mice but did not affect intCB_1+/+ water intake (**Supplemental Fig. 1.3*C, D*** and accompanying

Supplemental Table 1.2). DAU did not impact ambulation but did have an overall effect on water intake in WD mice (**Supplemental Fig. 1.2*G*** and accompanying **Supplemental Table 1.1**), which may be a result of reduced food intake (**Figure 1.5*C***). An additional concern associated with the therapeutic use of ATR is the role for m_2 AChRs in the regulation of cardiac function (Peter et al., 2005). Cardiac function was not measured in the current study, but if ATR or related drugs are to be investigated for their potential as a treatment for obesity, possible cardiac side-effects must be considered.

The eCB system plays a critical role in the seeking and sensing of calorie-dense foods (DiPatrizio and Piomelli, 2012). Indeed, we reported a role for intestinal CB_1Rs in preferences for WD (Avalos et al., 2020). In these studies, mice treated with the CB_1R inverse agonist, AM251, displayed no preference for the highly-palatable WD for up to 3 h. In addition, preferences for WD were largely abolished for up to 6 hours in mice conditionally lacking CB_1Rs in the intestinal epithelium. Notably, preferences for the WD returned by 24 h after initiation of the preference test in these mice. These findings suggest that *(i)* CB_1Rs in the intestinal epithelium are essential for acute preferences for high-fat, high-sugar foods and (*ii*) other biochemical mechanisms may override eCB control of food preferences over time and should be evaluated in the future (Avalos et al., 2020).

The eCB system also directly and indirectly interacts with afferent vagal signaling to control food intake, which becomes dysregulated in DIO (Argueta et al., 2019; Christie et al., 2020c; Christie et al., 2020b, a; DiPatrizio, 2021). For example, CB_1Rs are expressed

in enteroendocrine I cells in the intestinal epithelium (Sykaras et al., 2012; Argueta et al., 2019). In response to nutrients entering the lumen, these cells produce and secrete the satiation peptide, CCK, which induces satiation via interactions with CCK_A receptors on afferent vagal fibers (Clemmensen et al., 2017). We reported that elevated levels of 2-AG in the small-intestinal epithelium of DIO mice inhibits gut-brain satiation signaling by a mechanism that includes blocking nutrient-induced release of CCK (Argueta et al., 2019). This effect was reversed by the peripheral CB_1R antagonist, AM6545, which restored the ability for nutrients to induce CCK release. Moreover, the hypophagic effects of AM6545 were completely reversed by a CCK_A antagonist in DIO mice. Together, these data suggest that in DIO, overactive eCB signaling at CB_1Rs on I cells in the upper-intestinal lining inhibits nutrient-induced CCK release, which may reduce activity of vagal afferent neurons and allow DIO mice to continue feeding past satiation. A direct test of this hypothesis, however, remains for future experiments. Future studies should also examine whether ATR treatment is reducing caloric intake in DIO mice via a similar CCK-mediated mechanism. While this work is yet to be completed, participation of the afferent vagus nerve in these processes is likely. Accordingly, multiple studies have revealed the necessity of intact vagal afferent signaling for preventing hyperphagia and weight gain, particularly in DIO (Covasa and Ritter, 1998; Daly et al., 2011; Kentish et al., 2012; de Lartigue et al., 2014; McDougle et al., 2021). In addition, recent studies identified a specialized subset of enteroendocrine cells lining the intestine that detect nutrients and communicate with vagal afferent fibers via functional synapses (Kaelberer et al., 2018;

Kaelberer et al., 2020). Studies examining whether CB_1Rs also control neuropod activity in these processes and may become dysregulated in DIO remain to be performed.

In summary, our results identify a previously undescribed brain-gut pathway that recruits cholinergic signaling to drive eCB-mediated overeating in DIO. Components of this pathway may be targets for anti-obesity therapeutics.

References

Aaltonen N, Riera Ribas C, Lehtonen M, Savinainen JR, Laitinen JT (2014) Brain regional cannabinoid CB(1) receptor signalling and alternative enzymatic pathways for 2-arachidonoylglycerol generation in brain sections of diacylglycerol lipase deficient mice. Eur J Pharm Sci 51:87-95.

Altschuler S, Escardo J, Lynn R, Miselis R (1993) The Central Organization of the Vagus Nerve Innervating the Colon of the Rat. In, pp 502-509. Gastroenterology.

Argueta D, DiPatrizio N (2017) Peripheral endocannabinoid signaling controls hyperphagia in western diet-induced obesity. Physiology & Behavior 171:32-39.

Argueta D, Perez P, Makriyannis A, DiPatrizio N (2019) Cannabinoid CB1 Receptors Inhibit Gut-Brain Satiation Signaling in Diet-Induced Obesity. Frontiers in Physiology 10.

Artmann A, Petersen G, Hellgren LI, Boberg J, Skonberg C, Nellemann C, Hansen SH, Hansen HS (2008) Influence of dietary fatty acids on endocannabinoid and N-acylethanolamine levels in rat brain, liver and small intestine. Biochim Biophys Acta 1781:200-212.

Avalos B, Argueta D, Perez P, Wiley M, Wood C, DiPatrizio N (2020) Cannabinoid CB1 Receptors in the Intestinal Epithelium Are Required for Acute Western-Diet Preferences in Mice. Nutrients 12.

Berland C, Castel J, Terrasi R, Montalban E, Foppen E, Martin C, Muccioli GG, Luquet S, Gangarossa G (2022) Identification of an endocannabinoid gut-brain vagal mechanism controlling food reward and energy homeostasis. Mol Psychiatry 27:2340-2354.

Berthoud H, Carlson N, Powley T (1991) Topography of Efferent Vagal Innervation of the Rat Gastrointestinal-Tract. American Journal of Physiology 260:R200-R207.

Berthoud HR (2008) The vagus nerve, food intake and obesity. Regul Pept 149:15-25.

Bullitt E (1990) Expression of C-Fos-Like Protein as a Marker for Neuronal-Activity Following Noxious-Stimulation in the Rat. Journal of Comparative Neurology 296:517-530.

Caulfield MP, Birdsall NJ (1998) International Union of Pharmacology. XVII. Classification of muscarinic acetylcholine receptors. Pharmacol Rev 50:279-290.

Christie S, O'Rielly R, Li H, Wittert GA, Page AJ (2020a) High fat diet induced obesity alters endocannabinoid and ghrelin mediated regulation of components of the endocannabinoid system in nodose ganglia. Peptides 131:170371.

Christie S, O'Rielly R, Li H, Wittert GA, Page AJ (2020b) Biphasic effects of methanandamide on murine gastric vagal afferent mechanosensitivity. J Physiol 598:139-150.

Christie S, O'Rielly R, Li H, Nunez-Salces M, Wittert GA, Page AJ (2020c) Modulatory effect of methanandamide on gastric vagal afferent satiety signals depends on nutritional status. J Physiol 598:2169-2182.

Chrobok L, Klich JD, Jeczmien-Lazur JS, Pradel K, Palus-Chramiec K, Sanetra AM, Piggins HD, Lewandowski MH (2022a) Daily changes in neuronal activities of the dorsal motor nucleus of the vagus under standard and high-fat diet. J Physiol 600:733-749.

Chrobok L, Klich JD, Sanetra AM, Jeczmien-Lazur JS, Pradel K, Palus-Chramiec K, Kepczynski M, Piggins HD, Lewandowski MH (2022b) Rhythmic neuronal activities of the rat nucleus of the solitary tract are impaired by high-fat diet - implications for daily control of satiety. J Physiol 600:751-767.

Clemmensen C, Müller TD, Woods SC, Berthoud HR, Seeley RJ, Tschöp MH (2017) Gut-Brain Cross-Talk in Metabolic Control. Cell 168:758-774.

Cluny NL, Vemuri VK, Chambers AP, Limebeer CL, Bedard H, Wood JT, Lutz B, Zimmer A, Parker LA, Makriyannis A, Sharkey KA (2010) A novel peripherally restricted cannabinoid receptor antagonist, AM6545, reduces food intake and body weight, but does not cause malaise, in rodents. Br J Pharmacol 161:629-642.

Clyburn C, Travagli R, Browning K (2018) Acute high-fat diet upregulates glutamatergic signaling in the dorsal motor nucleus of the vagus. American Journal of Physiology-Gastrointestinal and Liver Physiology 314:G623-G634.

Covasa M, Ritter RC (1998) Rats maintained on high-fat diets exhibit reduced satiety in response to CCK and bombesin. Peptides 19:1407-1415.

Daly DM, Park SJ, Valinsky WC, Beyak MJ (2011) Impaired intestinal afferent nerve satiety signalling and vagal afferent excitability in diet induced obesity in the mouse. J Physiol 589:2857-2870.

de Lartigue G, Ronveaux CC, Raybould HE (2014) Deletion of leptin signaling in vagal afferent neurons results in hyperphagia and obesity. Mol Metab 3:595-607.

de Lartigue G, de la Serre C, Espero E, Lee J, Raybould H (2011) Diet-induced obesity leads to the development of leptin resistance in vagal afferent neurons. American Journal of Physiology-Endocrinology and Metabolism 301:E187-E195.

Dinh TP, Carpenter D, Leslie FM, Freund TF, Katona I, Sensi SL, Kathuria S, Piomelli D (2002) Brain monoglyceride lipase participating in endocannabinoid inactivation. Proceedings of the National Academy of Sciences of the United States of America 99:10819-10824.

DiPatrizio NV (2021) Endocannabinoids and the Gut-Brain Control of Food Intake and Obesity. Nutrients 13.

DiPatrizio NV, Piomelli D (2012) The thrifty lipids: endocannabinoids and the neural control of energy conservation. Trends Neurosci 35:403-411.

DiPatrizio NV, Joslin A, Jung KM, Piomelli D (2013) Endocannabinoid signaling in the gut mediates preference for dietary unsaturated fats. FASEB J 27:2513-2520.

DiPatrizio NV, Astarita G, Schwartz G, Li X, Piomelli D (2011) Endocannabinoid signal in the gut controls dietary fat intake. Proceedings of the National Academy of Sciences of the United States of America 108:12904-12908.

DiPatrizio NV, Igarashi M, Narayanaswami V, Murray C, Gancayco J, Russell A, Jung KM, Piomelli D (2015) Fasting stimulates 2-AG biosynthesis in the small intestine: role of cholinergic pathways. Am J Physiol Regul Integr Comp Physiol 309:R805-813.

el Marjou F, Janssen KP, Chang BH, Li M, Hindie V, Chan L, Louvard D, Chambon P, Metzger D, Robine S (2004) Tissue-specific and inducible Cre-mediated recombination in the gut epithelium. Genesis 39:186-193.

Gibbons CH (2019) Chapter 27 - Basics of autonomic nervous system function. In: Handbook of Clinical Neurology (Aminoff MJ, Boller F, Swaab DF, eds), pp 407-418: Elsevier.

Han W, Tellez LA, Perkins MH, Perez IO, Qu T, Ferreira J, Ferreira TL, Quinn D, Liu ZW, Gao XB, Kaelberer MM, Bohórquez DV, Shammah-Lagnado SJ, de Lartigue G, de Araujo IE (2018) A Neural Circuit for Gut-Induced Reward. Cell 175:887-888.

Hulme EC, Birdsall NJ, Buckley NJ (1990) Muscarinic receptor subtypes. Annu Rev Pharmacol Toxicol 30:633-673.

Igelstrom K, Herbison A, Hyland B (2010) ENHANCED c-Fos EXPRESSION IN SUPERIOR COLLICULUS, PARAVENTRICULAR THALAMUS AND SEPTUM DURING LEARNING OF CUE-REWARD ASSOCIATION. Neuroscience 168:706-714.

Izzo A, Piscitelli F, Capasso R, Aviello G, Romano B, Borrelli F, Petrosino S, Di Marzo V (2009) Peripheral endocannabinoid dysregulation in obesity: relation to intestinal motility and energy processing induced by food deprivation and re-feeding. British Journal of Pharmacology 158:451-461.

Jung KM, Astarita G, Zhu C, Wallace M, Mackie K, Piomelli D (2007) A key role for diacylglycerol lipase-alpha in metabotropic glutamate receptor-dependent endocannabinoid mobilization. Mol Pharmacol 72:612-621.

Kaelberer MM, Rupprecht LE, Liu WW, Weng P, Bohórquez DV (2020) Neuropod Cells: The Emerging Biology of Gut-Brain Sensory Transduction. Annu Rev Neurosci 43:337-353.

Kaelberer MM, Buchanan KL, Klein ME, Barth BB, Montoya MM, Shen X, Bohórquez DV (2018) A gut-brain neural circuit for nutrient sensory transduction. Science 361.

Kentish S, Vincent A, Kennaway D, Wittert G, Page A (2016) High-Fat Diet-Induced Obesity Ablates Gastric Vagal Afferent Circadian Rhythms. Journal of Neuroscience 36:3199-3207.

Kentish S, Li H, Philp L, O'Donnell T, Isaacs N, Young R, Wittert G, Blackshaw L, Page A (2012) Diet-induced adaptation of vagal afferent function. Journal of Physiology-London 590:209-221.

Kim J, Isokawa M, Ledent C, Alger BE (2002) Activation of muscarinic acetylcholine receptors enhances the release of endogenous cannabinoids in the hippocampus. J Neurosci 22:10182-10191.

Kovacs P, Hajnal A (2022) Short-term high-fat diet consumption increases body weight and body adiposity and alters brain stem taste information processing in rats. Chemical Senses 47.

Li M, Tan HE, Lu Z, Tsang KS, Chung AJ, Zuker CS (2022) Gut-brain circuits for fat preference. Nature 610:722-730.

Lorenz D, Nardi P, Smith GP (1978) Atropine methyl nitrate inhibits sham feeding in the rat. Pharmacol Biochem Behav 8:405-407.

Marini P, Cowie P, Ayar A, Bewick GS, Barrow J, Pertwee RG, MacKenzie A, Tucci P (2023) M3 Receptor Pathway Stimulates Rapid Transcription of the CB1 Receptor Activation through Calcium Signalling and the CNR1 Gene Promoter. Int J Mol Sci 24.

Mawe G, Lavoie B, Nelson M, Pozo M (2018) Neuromuscular Function in the Biliary Tract. In: Physiology of the Gastrointestinal Tract (Said H, ed), pp 453-468: Elsevier/Academic Press.

McDougle M, Quinn D, Diepenbroek C, Singh A, de la Serre C, de Lartigue G (2021) Intact vagal gut-brain signalling prevents hyperphagia and excessive weight gain in response to high-fat high-sugar diet. Acta Physiol (Oxf) 231:e13530.

Muise ED, Gandotra N, Tackett JJ, Bamdad MC, Cowles RA (2017) Distribution of muscarinic acetylcholine receptor subtypes in the murine small intestine. Life sciences 169:6-10.

Perrin-Terrin A, Jeton F, Pichon A, Frugiere A, Richalet J, Bodineau L, Voituron N (2016) The c-FOS Protein Immunohistological Detection: A Useful Tool As a Marker of Central Pathways Involved in Specific Physiological Responses In Vivo and Ex Vivo. Jove-Journal of Visualized Experiments.

Peter JC, Tugler J, Eftekhari P, Maurice D, Hoebeke J, Roegel JC (2005) Effects on heart rate of an anti-M2 acetylcholine receptor immune response in mice. FASEB J 19:943-949.

Piomelli D, Astarita G, Rapaka R (2007) A neuroscientist's guide to lipidomics. Nature reviews 8:743-754.

Pradhan SN, Roth T (1968) Comparative behavioral effects of several anticholinergic agents in rats. Psychopharmacologia 12:358-366.

Rinaldo L, Hansel C (2013) Muscarinic acetylcholine receptor activation blocks long-term potentiation at cerebellar parallel fiber-Purkinje cell synapses via cannabinoid signaling. Proceedings of the National Academy of Sciences of the United States of America 110:11181-11186.

Rogers R, Hermann G, Travagli R, Johnson L (2006) Brainstem Control of Gastric Function. Physiology of the Gastrointestinal Tract, Vols 1 and 2, 4th Edition:851-875.

Schindelin J, Arganda-Carreras I, Frise E, Kaynig V, Longair M, Pietzsch T, Preibisch S, Rueden C, Saalfeld S, Schmid B, Tinevez J, White D, Hartenstein V, Eliceiri K, Tomancak P, Cardona A (2012) Fiji: an open-source platform for biological-image analysis. Nature Methods 9:676-682.

Schubert M, Peura D (2008) Control of gastric acid secretion in health and disease. Gastroenterology 134:1842-1860.

Sclafani A (2018) From appetite setpoint to appetition: 50years of ingestive behavior research. Physiol Behav 192:210-217.

Sohn JW, Harris LE, Berglund ED, Liu T, Vong L, Lowell BB, Balthasar N, Williams KW, Elmquist JK (2013) Melanocortin 4 receptors reciprocally regulate sympathetic and parasympathetic preganglionic neurons. Cell 152:612-619.

Stella N, Schweitzer P, Piomelli D (1997) A second endogenous cannabinoid that modulates long-term potentiation. Nature 388:773-778.

Straiker A, Mackie K (2007) Metabotropic suppression of excitation in murine autaptic hippocampal neurons. The Journal of physiology 578:773-785.

Sykaras AG, Demenis C, Case RM, McLaughlin JT, Smith CP (2012) Duodenal enteroendocrine I-cells contain mRNA transcripts encoding key endocannabinoid and fatty acid receptors. PLoS One 7:e42373.

Tao J, Campbell J, Tsai L, Wu C, Liberles S, Lowell B (2021) Highly selective brain-to-gut communication via genetically defined vagus neurons. Neuron 109:2106-+.

Wiley M, Perez P, Argueta D, Avalos B, Wood C, DiPatrizio N (2021) UPLC-MS/MS Method for Analysis of Endocannabinoid and Related Lipid Metabolism in Mouse Mucosal Tissue. Frontiers in Physiology 12.

Wiley MB, DiPatrizio NV (2022) Diet-Induced Gut Barrier Dysfunction Is Exacerbated in Mice Lacking Cannabinoid 1 Receptors in the Intestinal Epithelium. Int J Mol Sci 23.

Williams KW, Elmquist JK (2012) From neuroanatomy to behavior: central integration of peripheral signals regulating feeding behavior. Nature neuroscience 15:1350-1355.

Zhang C, Barkholt P, Nielsen J, Thorbek D, Rigbolt K, Vrang N, Woldbye D, Jelsing J (2020) The dorsomedial hypothalamus and nucleus of the solitary tract as key regulators in a rat model of chronic obesity. Brain Research 1727.

Zhao Y, Tzounopoulos T (2011) Physiological activation of cholinergic inputs controls associative synaptic plasticity via modulation of endocannabinoid signaling. J Neurosci 31:3158-3168.

Figures & Tables

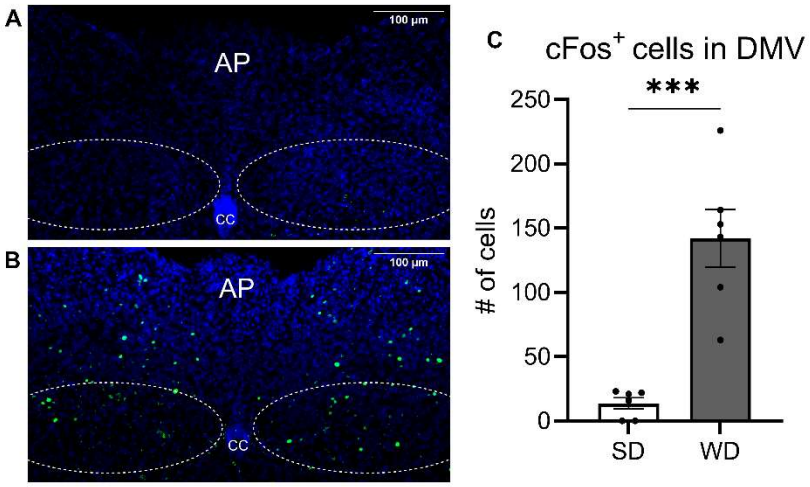

Figure 1.1 Increased cFos immunoreactivity in the DMV of DIO mice. cFos immunoreactivity was quantified in the DMV of mice fed, ***A***, standard diet (SD) and mice fed , ***B,*** western diet (WD) 45-75 minutes following the onset of the dark period. ***C***, The number of cFos^{+} cells was significantly increased in WD mice when compared to SD mice ($t_{(10)} = 5.575$; $p = 0.0002$; unpaired Student's *t* test). All data are presented as mean ± SEM, n = 6 mice per diet, ***$p < 0.001$. AP = Area Postrema, CC = Central Canal.

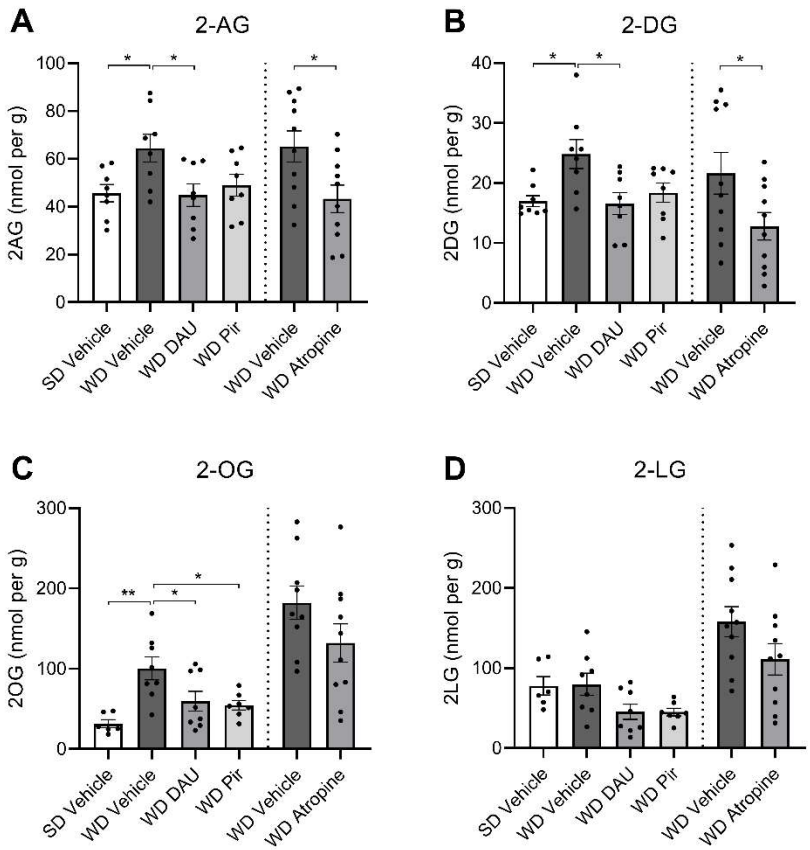
A
2-AG
2AG (nmol per g)
100
80
60
40
20
0
*
*
*
SD Vehicle
WD Vehicle
WD DAU
WD Pir
WD Vehicle
WD Atropine
B
2-DG
2DG (nmol per g)
40
30
20
10
0
*
*
*
SD Vehicle
WD Vehicle
WD DAU
WD Pir
WD Vehicle
WD Atropine
C
2-OG
2OG (nmol per g)
300
200
100
0
**
*
*
SD Vehicle
WD Vehicle
WD DAU
WD Pir
WD Vehicle
WD Atropine
D
2-LG
2LG (nmol per g)
300
200
100
0
SD Vehicle
WD Vehicle
WD DAU
WD Pir
WD Vehicle
WD Atropine

Figure 1.2 mAChR antagonists block MAG formation in the jejunum epithelium of DIO mice. Mice fed standard diet (SD) or western diet (WD) were treated with a single IP injection of vehicle, DAU5884 (2 mg/kg) or PIR (2 mg/kg) 30 minutes prior to tissue harvest (cohort 1). A second group (cohort 2) of WD mice was treated with vehicle or ATR (2 mg/kg), and otherwise processed identically to cohort 1. ***A***, 2-AG and other MAGs in upper small-intestinal epithelium tissue were isolated via lipid extraction and quantitated using UPLC-MS/MS. 2-AG was significantly elevated in vehicle-treated WD mice when compared to vehicle-treated SD mice. Treatment with DAU or ATR in WD mice restored levels of 2-AG to levels in SD control mice (cohort 1: $F_{(3,28)} = 3.721$, $P = 0.0227$; SD vehicle vs. WD vehicle $p = 0.0448$; WD vehicle vs WD DAU $p = 0.0402$; 1-way ANOVA followed by Holm Sidak's multiple comparisons test; cohort 2: $t_{(18)} = 2.510$; $p = 0.0218$; unpaired Student's *t* test). ***B***, 2-DG was significantly elevated in vehicle-treated WD mice compared to vehicle-treated SD mice. Treatment with DAU or ATR in WD mice restored levels of 2-AG to that of SD mice (cohort 1: $F_{(3,28)} = 4.691$, $P = 0.0089$; SD vehicle vs. WD vehicle $p = 0.0200$; WD vehicle vs WD DAU $p = 0.0159$; 1-way ANOVA followed by Holm Sidak's multiple comparisons test; cohort 2: $t_{(18)} = 2.115$; $p = 0.0486$; unpaired Student's *t* test). ***C,*** 2-OG was significantly elevated in vehicle-treated WD mice when compared to vehicle-treated SD mice. Treatment with DAU or PIR restored levels of 2-AG in WD mice to those in SD mice (cohort 1: $F_{(3,25)} = 6.657$, $P = 0.0019$; SD vehicle vs. WD vehicle $p = 0.0014$; WD vehicle vs WD DAU $p = 0.0439$; WD vehicle vs WD PIR $p = 0.0315$; 1-way ANOVA followed by Holm Sidak's multiple comparisons test; cohort 2: $t_{(17)} = 1.565$; $p = 0.1361$; unpaired Student's *t* test). ***D,*** 2-LG levels were not significantly different between any treatment or diet groups (cohort 1: $F_{(3,25)} = 3.346$, $P = 0.0351$; SD vehicle vs. WD vehicle $p = 0.0014$; WD vehicle vs WD DAU $p = 0.0439$; WD vehicle vs WD PIR $p = 0.0315$; 1-way ANOVA followed by Holm Sidak's multiple comparisons test; cohort 2: $t_{(18)} = 1.720$; $p = 0.1026$; unpaired Student's *t* test). All data are presented as mean ± SEM, n = 8-10 per group; $*p < 0.05$, $**p < 0.01$.

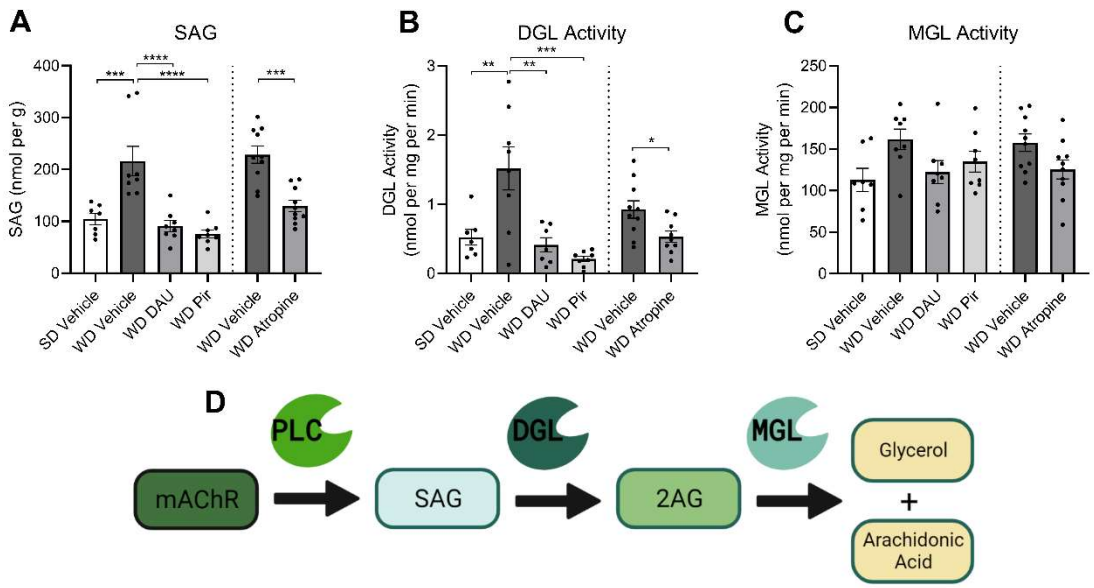
A
SAG
SAG (nmol per g)
400
300
200
100
0
***
****
****
***
SD Vehicle
WD Vehicle
WD DAU
WD Pir
WD Vehicle
WD Atropine
B
DGL Activity
DGL Activity (nmol per mg per min)
3
2
1
0
**
**
***
*
SD Vehicle
WD Vehicle
WD DAU
WD Pir
WD Vehicle
WD Atropine
C
MGL Activity
MGL Activity (nmol per mg per min)
250
200
150
100
50
0
SD Vehicle
WD Vehicle
WD DAU
WD Pir
WD Vehicle
WD Atropine
D
PLC
DGL
MGL
mAChR
SAG
2AG
Glycerol
+
Arachidonic Acid

Figure 1.3 SAG formation and DGL Activity in upper intestinal epithelium are inhibited by mAChR antagonism in DIO mice. Levels of SAG in the upper small-intestinal epithelium tissue were isolated and quantitated using UPLC-MS/MS. The same tissue was analyzed for DGL and MGL activity using an enzymatic assay; enzyme reaction products were isolated and quantitated via UPLC-MS/MS. Enzyme activity was calculated using the nmols of reaction product generated per mg of tissue per minute of the reaction. ***A,*** SAG was significantly elevated in vehicle-treated mice fed western diet (WD) compared to vehicle-treated mice fed standard diet (SD). Treatment with DAU, PIR, or ATR in WD mice restored levels of SAG to that of lean controls (cohort 1: $F_{(3,27)} = 14.76$, $P < 0.0001$; SD Veh vs. WD Veh $p = 0.0004$; WD Veh vs WD DAU $p < 0.0001$; WD Veh vs WD PIR $p < 0.0001$; 1-way ANOVA followed by Holm Sidak's multiple comparisons test; cohort 2: $t_{(18)} = 5.010$; $p = 0<0.0001$; unpaired Student's *t* test). ***B,*** DGL activity was significantly elevated in vehicle-treated WD mice compared to vehicle-treated SD mice. Treatment with DAU, PIR, or ATR in WD mice restored DGL activity to that of lean controls (cohort 1: $F_{(3,26)} = 10.57$, $P = 0.0001$; SD Veh vs. WD Veh $p = 0.0030$; WD Veh vs WD DAU $p = 0.0013$; WD Veh vs WD PIR $p = 0.0001$; 1-way ANOVA followed by Holm Sidak's multiple comparisons test; cohort 2: $t_{(17)} = 2.546$; $p = 0.0209$; unpaired Student's *t* test). ***C,*** MGL activity was not different between any diet or treatment group (cohort 1: $F_{(3,27)} = 2.537$, $P = 0.0777$; 1-way ANOVA; cohort 2: $t_{(18)} = 2.081$; $p = 0.0520$; unpaired Student's *t* test). All data are presented as mean ± SEM, n = 8-10 per group; $*p < 0.05$, $**p < 0.01$, $***p < 0.001$, $****p < 0.0001$. ***D,*** Schematic illustrating that activation of G_q-coupled mAChRs initiates the PLC-dependent generation of SAG, which is subsequently converted to 2-AG by DGL. 2-AG is further hydrolyzed by MGL into glycerol and arachidonic acid. Illustration created with BioRender.com

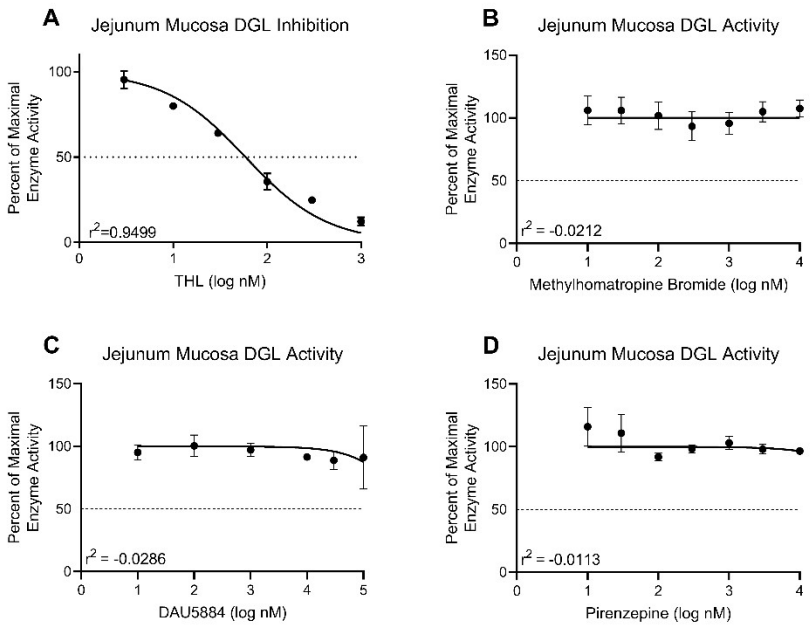

Figure 1.4 Anticholinergics do not affect 2-AG metabolic enzyme activity *ex vivo.* Activity of DGL in the upper small-intestinal epithelium from mice fed western diet (WD) was assayed in the presence increasing concentrations of a DGL-specific inhibitor and various mAChR antagonists. ***A,*** DGL activity was inhibited in a concentration-dependent manner when incubated with THL at concentrations ranging from 3-1,000 nM (IC_{50} = 58.52 nM, R^2 = 0.9499). ***B,*** DGL activity was not directly inhibited by ATR at concentrations ranging from 10-10,000 nM (R^2 = -0.0212). ***C,*** DGL activity was not directly inhibited by DAU at concentrations ranging from 10-10,000 nM (R^2 = -0.0286). ***D,*** DGL activity was not directly inhibited by PIR at concentrations ranging from 10-10,000 nM (R^2 = -0.0113). All data are presented as mean ± SEM, n = 3 animals per drug. All graphs are least squares fit of log[inhibitor] vs. normalized response.

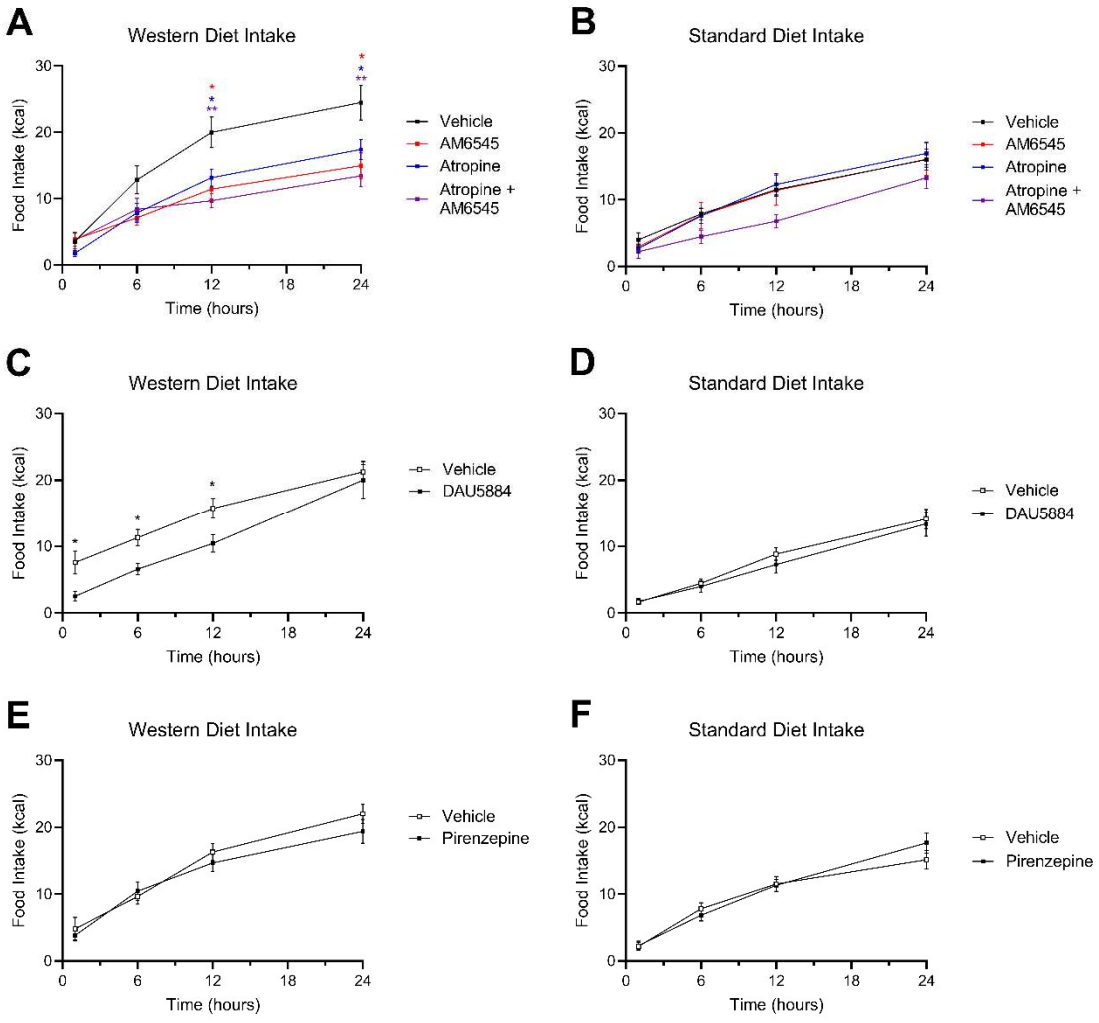
A
Western Diet Intake
Food Intake (kcal)
Time (hours)
Vehicle
AM6545
Atropine
Atropine + AM6545
B
Standard Diet Intake
Food Intake (kcal)
Time (hours)
Vehicle
AM6545
Atropine
Atropine + AM6545
C
Western Diet Intake
Food Intake (kcal)
Time (hours)
Vehicle
DAU5884
D
Standard Diet Intake
Food Intake (kcal)
Time (hours)
Vehicle
DAU5884
E
Western Diet Intake
Food Intake (kcal)
Time (hours)
Vehicle
Pirenzepine
F
Standard Diet Intake
Food Intake (kcal)
Time (hours)
Vehicle
Pirenzepine

Figure 1.5 Anticholinergics inhibit food intake in DIO mice. ***A,*** AM6545 (10 mg/kg), ATR (2 mg/kg), or a combination of AM6545 + ATR reduced caloric intake for up to 24 hours in western diet-fed (WD) mice (time x drug interaction: $F_{(9,158)} = 4.639$; $p < 0.0001$; drug main effect $F_{(3,54)} = 4.560$; $p = 0.0064$; 12 hour vehicle vs. 12 hour ATR $p = 0.0175$, 12 hour vehicle vs. 12 hour AM6545 $p = 0.0143$, 12 hour vehicle vs. 12 hour combination $p = 0.0020$, 24 hour vehicle vs. 24 hour ATR $p = 0.0301$, 24 hour vehicle vs. 24 hour AM6545 $p = 0.0145$, 24 hour vehicle vs. 24 hour combination $p = 0.0049$; 2-way ANOVA followed by Holm Sidak's multiple comparisons test). ***B,*** AM6545, ATR, or both drugs in combination did not affect caloric intake in standard diet-fed (SD) mice (time x drug interaction: $F_{(9,164)} = 0.9117$; $p = 0.5165$; time main effect $F_{(2.103,115.0)} = 142.4$; $p < 0.0001$; drug main effect $F_{(3,56)} = 1.69$; $p = 0.1799$; 2-way ANOVA). ***C,*** DAU5884 (2 mg/kg) reduced caloric intake for up to 12 hours in WD mice (time x drug interaction: $F_{(3,84)} = 1.239$; $p = 0.3009$; drug main effect $F_{(1,28)} = 6.750$; $p = 0.0148$; 1 hour vehicle vs. 1 hour DAU $p = 0.0358$, 6 hour vehicle vs. 6 hour DAU $p = 0.0168$, 12 hour vehicle vs. 12 hour DAU $p = 0.0358$; 2-way ANOVA followed by Holm Sidak's multiple comparisons test). ***D,*** DAU5884 did not affect caloric intake in SD mice for 24 hours (time x drug interaction: $F_{(3,70)} = 0.5839$; $p = 0.6276$; drug main effect $F_{(1,24)} = 0.2090$; $p = 0.6517$; 2-way ANOVA). ***E,*** PIR (2 mg/kg) did not affect caloric intake in WD mice (time x drug interaction: $F_{(3,80)} = 1.526$; $p = 0.2140$; drug main effect $F_{(1,28)} = 0.1463$; $p = 0.7050$; 2-way ANOVA)***. F,*** PIR did not affect caloric intake in standard diet-fed mice (time x drug interaction: $F_{(3,79)} = 1.781$; $p = 0.1576$; drug main effect $F_{(1,28)} = 0.07073$; $p = 0.7922$; 2-way ANOVA). All data are presented as mean ± SEM, n = 15 – 16; $*p < 0.05$, $**p < 0.01$.

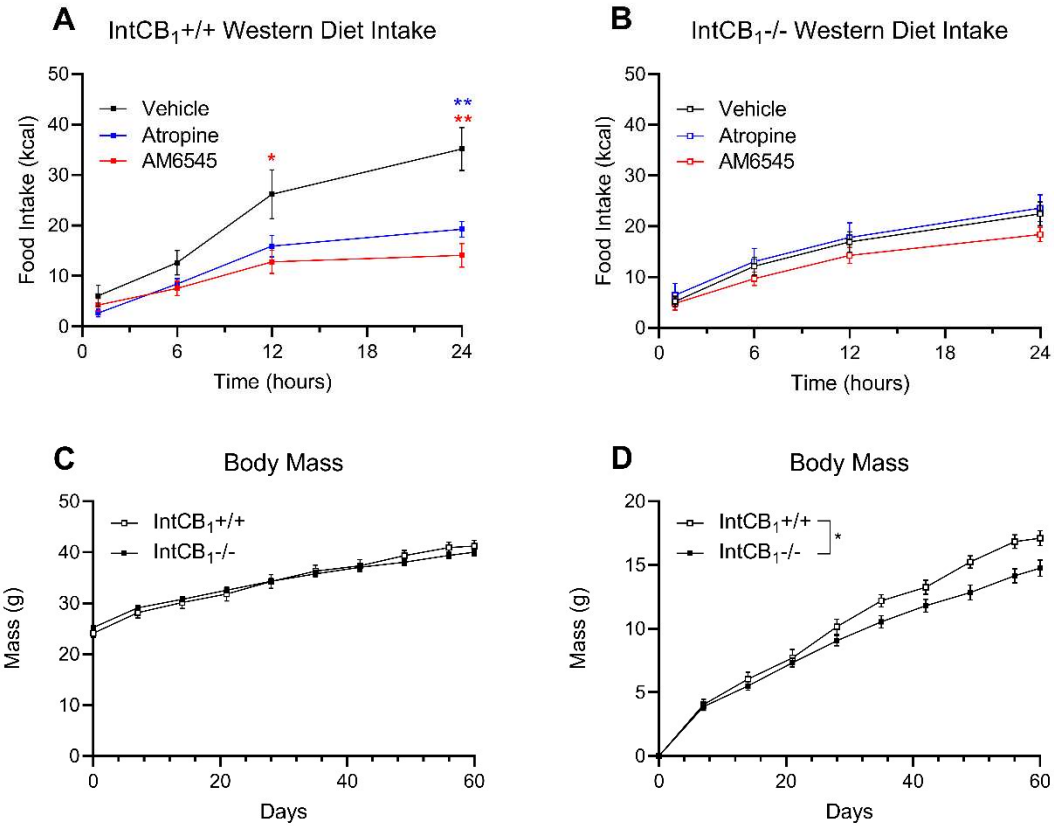
A
IntCB1+/+ Western Diet Intake
Food Intake (kcal)
Time (hours)
Vehicle
Atropine
AM6545
B
IntCB1-/- Western Diet Intake
Food Intake (kcal)
Time (hours)
Vehicle
Atropine
AM6545
C
Body Mass
Mass (g)
Days
IntCB1+/+
IntCB1-/-
D
Body Mass
Mass (g)
Days
IntCB1+/+
IntCB1-/-

Figure 1.6 Inhibiting peripheral CB_1Rs or mAChRs failed to affect food intake in mice conditionally lacking CB_1Rs in the intestinal epithelium. ***A,*** AM6545 (10 mg/kg) or ATR (2 mg/kg) reduced caloric intake for up to 24 hours in control intCB_1+/+ mice (time x drug interaction: $F_{(6,79)} = 5.099$; $p = 0.0002$; drug main effect $F_{(2,30)} = 6.024$; $p = 0.0063$; 12 hour vehicle vs. 12 hour AM6545 $p = 0.0498$, 24 hour vehicle vs. 24 hour AM6545 $p = 0.0012$, 24 hour vehicle vs. 24 hour ATR $p = 0.0043$, 2-way ANOVA followed by Holm Sidak's multiple comparisons test). ***B,*** AM6545 or ATR did not affect caloric intake in intCB_1-/- mice (time x drug interaction: $F_{(6,135)} = 0.7700$; $p = 0.5948$; drug main effect $F_{(2,45)} = 0.9273$; $p = 0.4030$; 2-way ANOVA). ***C,*** Body weights were similar between intCB_1-/- when compared to intCB_1+/+ mice control mice fed western diet (WD; time x genotype interaction: $F_{(9,225)} = 5.327$; $p < 0.0001$; genotype main effect $F_{(1,25)} = 0.01602$; $p = 0.9003$; 2-way ANOVA followed by Holm Sidak's multiple comparisons test). ***D,*** Change in body weight was lower in intCB_1-/- when compared to intCB_1+/+ control mice (time x genotype interaction: $F_{(9,225)} = 5.327$; $p < 0.0001$; genotype main effect $F_{(1,25)} = 5.077$; $p = 0.0333$; 2-way ANOVA followed by Holm Sidak's multiple comparisons test). All data are presented as mean ± SEM, n = 16, 11 (intCB_1-/-, intCB_1+/+ respectively), $p < 0.05$, $^{**}p < 0.01$.

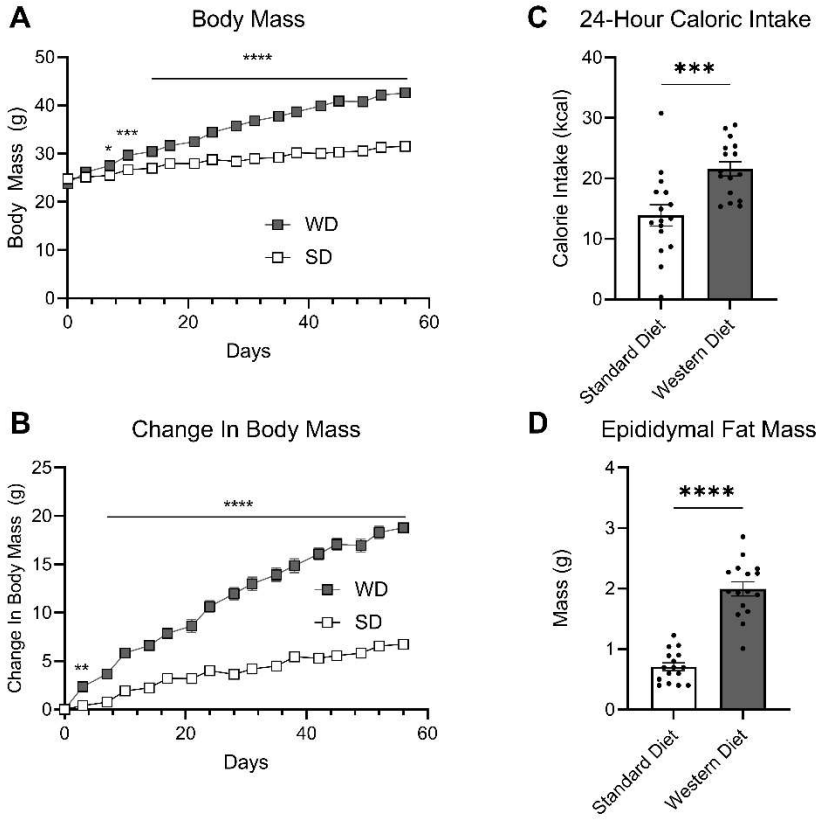
A
Body Mass
Body Mass (g)
Days
WD
SD
****
***
*
B
Change In Body Mass
Change In Body Mass (g)
Days
WD
SD
****
**
C
24-Hour Caloric Intake
Calorie Intake (kcal)
***
Standard Diet
Western Diet
D
Epididymal Fat Mass
Mass (g)
****
Standard Diet
Western Diet

Supplemental Figure 1.1 Mice fed western diet (WD) become obese and hyperphagic. ***A***, Body weight was recorded bi-weekly between 0900h and 1000h (time x diet interaction: $F_{(16,480)} = 121.8$; $p < 0.0001$; diet main effect $F_{(1,30)} = 79.56$; $p < 0.0001$; 2-way ANOVA followed by Holm Sidak's multiple comparisons test). ***B***, Change in body mass (time x diet interaction: $F_{(16,480)} = 121.8$; $p < 0.0001$; diet main effect $F_{(1,30)} = 195.4$; $p < 0.0001$; 2-way ANOVA followed by Holm Sidak's multiple comparisons test). ***C***, Total caloric intake during a 24 h test period ($t_{(30)} = 3.666$; $p = 0.0009$; unpaired Student's *t* test). ***D***, At the end of the 60-day diet exposure period to western diet (WD), epididymal fat pads were weighed ($t_{(30)} = 9.686$; $p > 0.0001$; unpaired Student's *t* test). All data are presented as mean ± SEM, n = 16 per diet; *$p < 0.05$, **$p < 0.01$, ***$p < 0.001$, ****$p < 0.0001$.

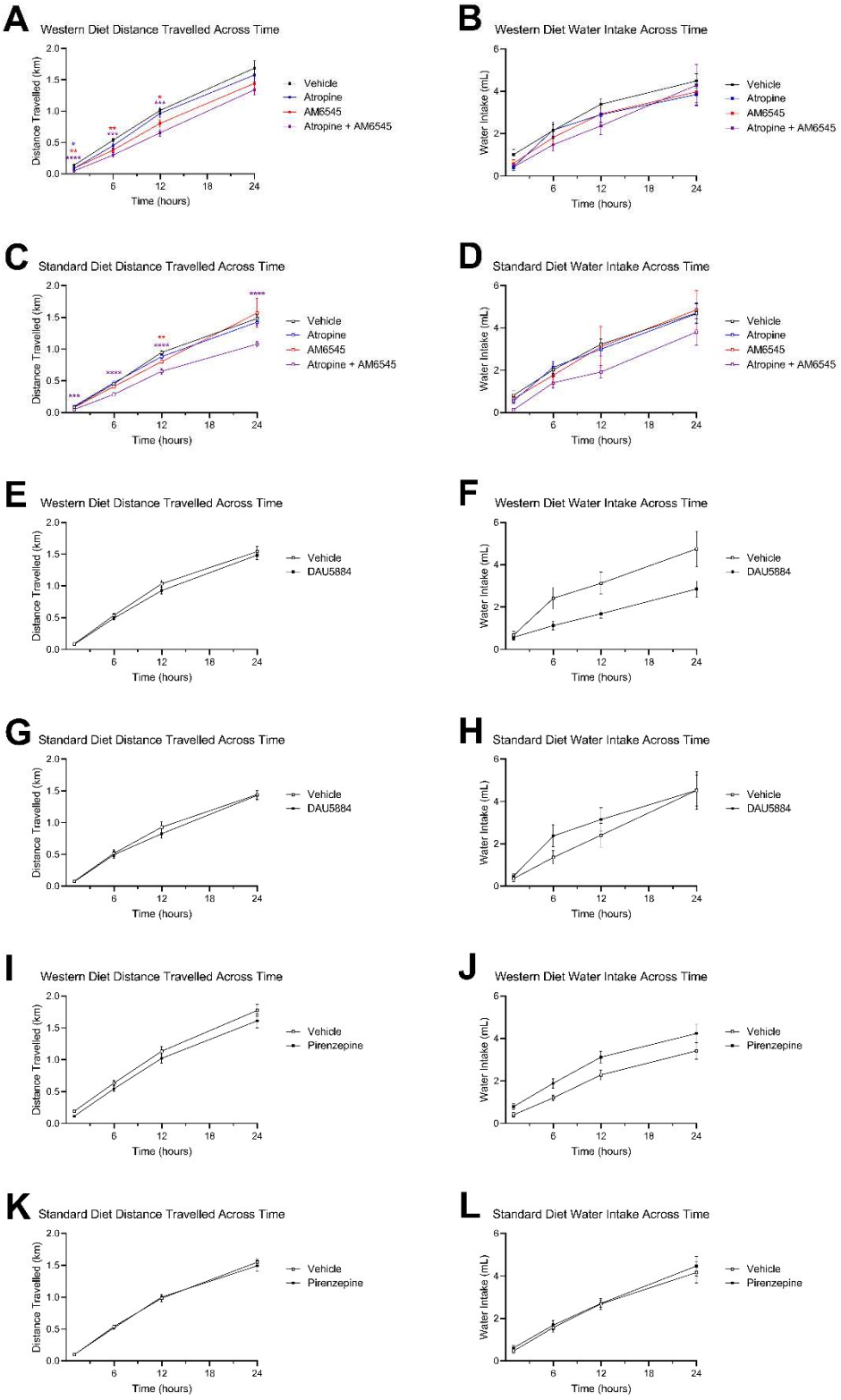
A
Western Diet Distance Travelled Across Time
Distance Travelled (km)
Time (hours)
Vehicle
Atropine
AM6545
Atropine + AM6545
B
Western Diet Water Intake Across Time
Water Intake (mL)
Time (hours)
Vehicle
Atropine
AM6545
Atropine + AM6545
C
Standard Diet Distance Travelled Across Time
Distance Travelled (km)
Time (hours)
Vehicle
Atropine
AM6545
Atropine + AM6545
D
Standard Diet Water Intake Across Time
Water Intake (mL)
Time (hours)
Vehicle
Atropine
AM6545
Atropine + AM6545
E
Western Diet Distance Travelled Across Time
Distance Travelled (km)
Time (hours)
Vehicle
DAU5884
F
Western Diet Water Intake Across Time
Water Intake (mL)
Time (hours)
Vehicle
DAU5884
G
Standard Diet Distance Travelled Across Time
Distance Travelled (km)
Time (hours)
Vehicle
DAU5884
H
Standard Diet Water Intake Across Time
Water Intake (mL)
Time (hours)
Vehicle
DAU5884
I
Western Diet Distance Travelled Across Time
Distance Travelled (km)
Time (hours)
Vehicle
Pirenzepine
J
Western Diet Water Intake Across Time
Water Intake (mL)
Time (hours)
Vehicle
Pirenzepine
K
Standard Diet Distance Travelled Across Time
Distance Travelled (km)
Time (hours)
Vehicle
Pirenzepine
L
Standard Diet Water Intake Across Time
Water Intake (mL)
Time (hours)
Vehicle
Pirenzepine

Supplemental Figure 1.2 Effects of drug treatments on ambulation and water intake. Total distance travelled and cumulative water intake was measured by automated feeding chambers for a 24-hour period starting at the onset of the dark cycle (1800h) following a single IP injection of AM6545 (10 mg/kg), ATR (2 mg/kg), DAU (2 mg/kg), and PIR (2 mg/kg). ***A,*** A single dose of AM6545 in mice fed standard diet (SD) resulted in decreased cumulative distance travelled at the 12 h timepoint. AM6545 and ATR combined reduced ambulation across the 24 h test. ***B,*** In mice fed western diet (WD), ATR and AM6545 alone or in combination reduced distance travelled for up to 12 h. ***C & D,*** AM6545 and ATR alone combined had no significant effects on water intake across the 24 h test in mice fed SD or WD. ***E & F,*** A single IP injection of DAU yielded no significant effects on distance travelled in mice fed SD or WD. ***G,*** DAU did not significantly affect water intake for the 24 h test in mice fed SD. ***H,*** In mice fed WD and treated with DAU, water intake was affected by drug alone, as well as a time x drug interaction, although there were no significant differences at individual time points as revealed by the Holm-Sidak multiple comparisons test. ***I & J,*** A single IP injection of PIR yielded no significant effects on distance travelled in mice fed SD or WD for the 24 h test. ***K & L,*** Treatment with PIR also had no effect on water intake in mice fed with SD or WD for the 24 h test. 2-Way ANOVA followed by Holm-Sidak's multiple comparisons test when appropriate, see **Supplemental Table 1** for detailed statistics. All data are presented as mean ± SEM, n = 15 – 16; *p < 0.05, **$p < 0.01$, ***$p < 0.001$, ****$p < 0.0001$.

Supplemental Table 1, 2-Way ANOVA table				
Figure	**Factor**	**F (DFn, DFd)**	**P value**	**Mulitple Comparisons**
A	Time	F (1.119, 61.57) = 344.2	P<0.0001	n/a
	Drug	F (3, 56) = 7.496	P=0.0003	1 hr: Vehicle vs. AM6545 p = 0.0002, 6 hr: Vehicle vs. Both p < 0.0001, 12 hr: Vehicle vs. AM6545 p = 0.0061, Vehicle vs. Both p < 0.0001, 24 hr: Vehicle vs. both p < 0.0001
	Time x Drug	F (9, 165) = 2.268	P=0.0202	n/a
B	Time	F (1.617, 86.79) = 131.9	P<0.0001	n/a
	Drug	F (3, 56) = 0.9653	P=0.4156	n/a
	Time x Drug	F (9, 161) = 0.5702	P=0.8201	n/a
C	Time	F (1.370, 75.35) = 756.4	P<0.0001	n/a
	Drug	F (3, 55) = 5.875	P=0.0015	1 hr: Vehicle vs. ATR p = 0.0107, Vehicle vs. AM6545 p = 0.0020, Vehicle vs. Both p < 0.0001, 6 hr: Vehicle vs. AM6545 p = 0.0020, Vehicle vs. Both p = 0.0002, 12 hr: Vehicle vs. AM6545 p = 0.0392, Vehicle vs. Both p = 0.0002
	Time x Drug	F (9, 165) = 1.851	P=0.0628	n/a
D	Time	F (1.576, 83.01) = 95.51	P<0.0001	n/a
	Drug	F (3, 54) = 0.6320	P=0.5975	n/a
	Time x Drug	F (9, 158) = 0.6299	P=0.7703	n/a
E	Time	F (2.070, 46.91) = 443.1	P<0.0001	n/a
	Drug	F (1, 24) = 0.3746	P=0.5462	n/a
	Time x Drug	F (3, 68) = 0.5729	P=0.6347	n/a
F	Time	F (1.455, 33.47) = 46.34	P<0.0001	n/a
	Drug	F (1, 24) = 0.4416	P=0.5127	n/a
	Time x Drug	F (3, 69) = 0.5618	P=0.642	n/a
G	Time	F (1.435, 39.70) = 568.4	P<0.0001	n/a
	Drug	F (1, 28) = 1.086	P=0.3063	n/a
	Time x Drug	F (3, 83) = 0.5128	P=0.6746	n/a
H	Time	F (1.632, 42.97) = 44.24	P<0.0001	n/a
	Drug	F (1, 28) = 5.920	P=0.0216	n/a
	Time x Drug	F (3, 79) = 3.963	P=0.011	n/a
I	Time	F (1.643, 43.27) = 576.4	P<0.0001	n/a
	Drug	F (1, 28) = 0.2601	P=0.6141	n/a
	Time x Drug	F (3, 79) = 0.2981	P=0.8267	n/a
J	Time	F (1.421, 36.94) = 108.9	P<0.0001	n/a
	Drug	F (1, 27) = 0.2764	P=0.6033	n/a
	Time x Drug	F (3, 78) = 0.1415	P=0.9348	n/a
K	Time	F (1.377, 38.10) = 456.1	P<0.0001	n/a
	Drug	F (1, 28) = 2.280	P=0.1423	n/a
	Time x Drug	F (3, 83) = 0.4852	P=0.6935	n/a
L	Time	F (1.587, 40.73) = 147.1	P<0.0001	n/a
	Drug	F (1, 27) = 1.323	P=0.2601	n/a
	Time x Drug	F (3, 77) = 0.4454	P=0.7212	n/a

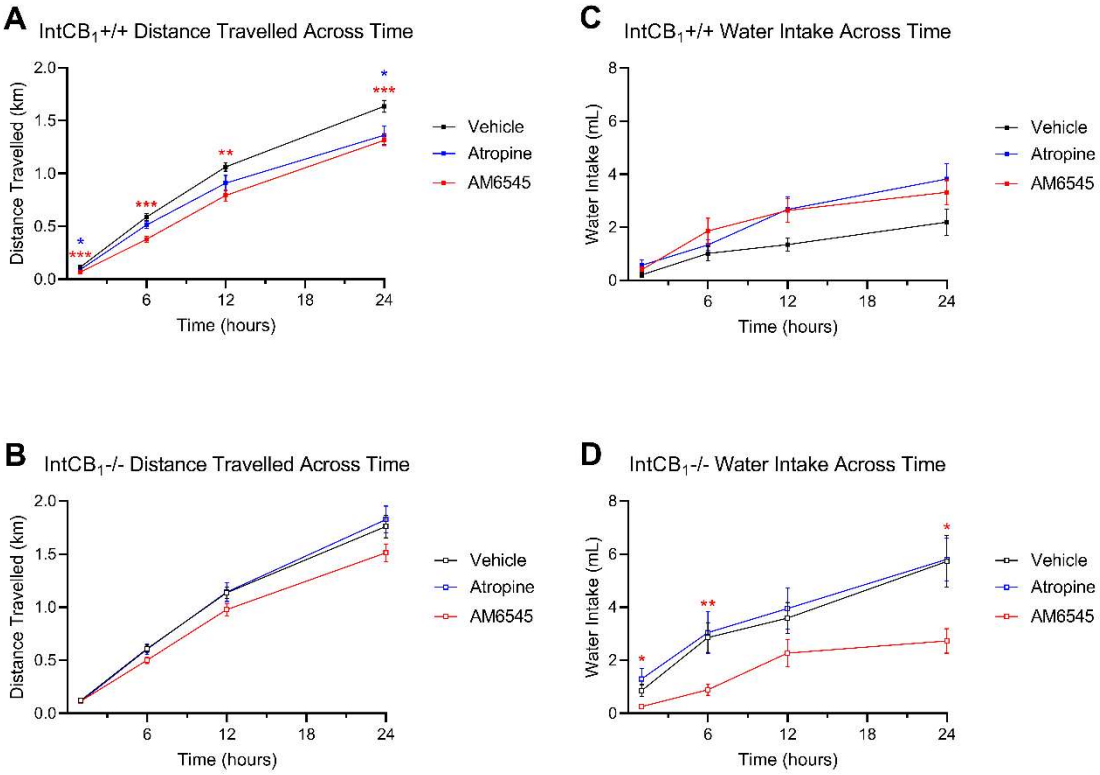
A
IntCB1+/+ Distance Travelled Across Time
Distance Travelled (km)
Time (hours)
Vehicle
Atropine
AM6545
B
IntCB1-/- Distance Travelled Across Time
Distance Travelled (km)
Time (hours)
Vehicle
Atropine
AM6545
C
IntCB1+/+ Water Intake Across Time
Water Intake (mL)
Time (hours)
Vehicle
Atropine
AM6545
D
IntCB1-/- Water Intake Across Time
Water Intake (mL)
Time (hours)
Vehicle
Atropine
AM6545

Supplemental Figure 3. Effects of drug treatments on ambulation and water intake in mice with conditional deletion of CB_1Rs in the intestinal epithelium fed western diet (WD). ***A-B,*** Total distance travelled and, ***C-D,*** cumulative water intake was measured by automated feeding chambers for a 24-hour period starting at the onset of the dark cycle (1800h) following a single IP injection of AM6545 (10 mg/kg) or ATR (2 mg/kg) in intCB_1+/+ and intCB_1-/- fed WD. ***A,*** A single dose of AM6545 in IntCB_1+/+ controls affected distance travelled across the entire 24-hour testing period. ATR also reduced distance travelled in the same mice at the 1- and 24-hour timepoints. ***B,*** There was a significant effect of drug and drug x time interaction in IntCB_1-/- mice on distance travelled, but the Holm-Sidak multiple comparisons *post hoc* analysis did not reveal any significant differences at individual time points. ***C,*** Water intake of intCB_1+/+ mice was not significantly affected by either drug treatment for the 24 h test. ***D,*** There was a significant effect of drug, as well as a drug x time interaction on water intake inintCB_1-/- animals. Specifically, AM6545 treatment significantly reduced cumulative water intake at the 1-, 6-, and 24-h timepoints. 2-way ANOVA followed by Holm-Sidak's multiple comparisons test when appropriate, see **Supplemental Table 2** for detailed statistics. All data are presented as mean ± SEM, n = 11 or 16 (intCB_1+/+ and intCB_1-/-, respectively); *p < 0.05, **p < 0.01, ***p < 0.001, ****p < 0.0001.

Supplemental Table 2, 2-Way ANOVA table				
Figure	**Factor**	**F (DFn, DFd)**	**P value**	**Mulitple Comparisons**
A	Time	F (1.702, 48.23) = 1085	P<0.0001	n/a
	Drug	F (2, 30) = 6.958	P=0.0033	1 hr: Vehicle vs. AM6545 p = 0.0002, Vehicle vs. ATR p = 0.0455, 6 hr: Vehicle vs. AM6545 p = 0.0002, 12 hr: Vehicle vs. AM6545 p = 0.0025, 24 hr: Vehicle vs. AM6545 p = 0.0008, Vehicle vs. ATR p = 0.0195
	Time x Drug	F (6, 85) = 4.619	P=0.0004	n/a
B	Time	F (1.292, 56.85) = 616.7	P<0.0001	n/a
	Drug	F (2, 45) = 2.272	P=0.1148	n/a
	Time x Drug	F (6, 132) = 2.082	P=0.0595	n/a
C	Time	F (2.130, 58.94) = 74.59	P<0.0001	n/a
	Drug	F (2, 29) = 2.217	P=0.1271	n/a
	Time x Drug	F (6, 83) = 1.707	P=0.1296	n/a
D	Time	F (1.849, 80.75) = 68.67	P<0.0001	n/a
	Drug	F (2, 45) = 3.398	P=0.0422	1 hr: Vehicle vs. AM6545 p = 0.0493, 6 hr: Vehicle vs. AM6545 p = 0.0081, 24 hr: Vehicle vs. AM6545 p = 0.0230
	Time x Drug	F (6, 131) = 2.619	P=0.0197	n/a

Chapter 2: A Sexually Dimorphic Role for Intestinal Cannabinoid Receptor Subtype-1 in the Behavioral Expression of Anxiety

Authors: Courtney P. Wood[1], Bryant Avalos[1], Camila Alvarez[1], Nicholas V. DiPatrizio[1]

[1]Division of Biomedical Sciences, School of Medicine, University of California, Riverside, Riverside, CA, 92521, USA; University of California Riverside Center for Cannabinoid Research, Riverside, CA, 92521, USA

Acknowledgements: Research is funded by the National Institutes of Health (R01 DK119498 and L30 DK1149978) and the Tobacco-Related Disease Research Program (T29KT0232). The authors thank Jose Luis Martin for his contribution to chemical analyses.

Abstract

Increasing evidence suggests that the endocannabinoid system (ECS) in the brain controls anxiety and may be a therapeutic target for the treatment of anxiety disorders. For example, both pharmacological and genetic disruption of cannabinoid receptor subtype-1 (CB_1R) signaling in the central nervous system is associated with increased anxiety-like behaviors in rodents, while activating the system is anxiolytic. Sex is also a critical factor that controls the behavioral expression of anxiety; however, roles for the ECS in the gut in these processes and possible differences between sexes are largely unknown. In the current study, we aimed to determine if CB_1Rs in the intestinal epithelium exert control over anxiety-like behaviors in a sex-dependent manner. We subjected male and female mice with conditional deletion of CB_1Rs in the intestinal epithelium ($intCB_1$-/-) and controls ($intCB_1$+/+) to the elevated plus maze (EPM), light/dark box, and open field test. Corticosterone (CORT) levels in plasma were measured at baseline and immediately following EPM exposure. When compared to $intCB_1$+/+ male mice, $intCB_1$-/- male mice exhibited reduced levels of anxiety-like behaviors in the EPM and light/dark box. In contrast to male mice, no differences were found for female $intCB_1$+/+ and $intCB_1$-/- mice during these tests. Circulating CORT was higher in female versus male mice for both genotype groups at baseline and following EPM exposure; however, there was no effect of genotype on CORT levels. Collectively, these results indicate that genetic deletion of CB_1Rs in the intestinal epithelium is associated with an anxiolytic phenotype in a sex-dependent manner.

Graphical Abstract

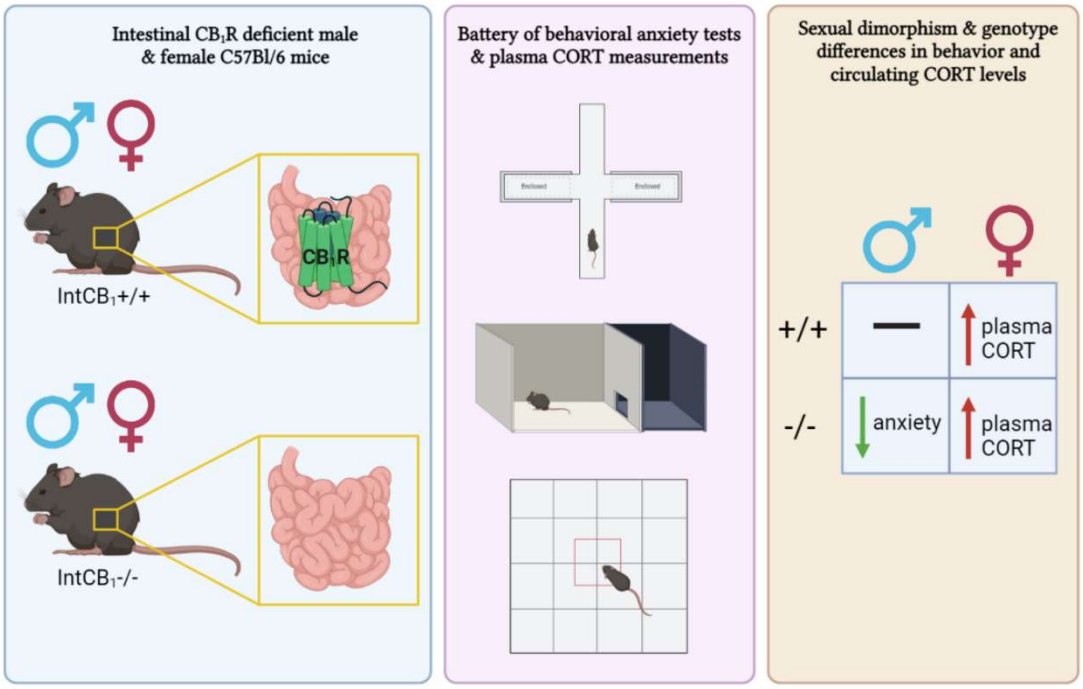

A sexually dimorphic role for intestinal cannabinoid receptor subtype-1 in the behavioral expression of anxiety; Wood, C.P.; Avalos, B.; Alvarez, C.; *DiPatrizio, N.V.; Male and female mice conditionally lacking intestinal CB_1Rs were tested for anxiety-like behaviors in the elevated plus maze, light dark box, and open field test. Circulating plasma CORT levels were quantified prior to and immediately following behavioral testing. Male IntCB_1-/- mice exhibited anxiolytic behavior compared to controls. Females did not display any genotype differences in behavior but did have significantly elevated plasma CORT levels compared to males at all time points. Illustration created with BioRender.com.

Introduction

The endocannabinoid system (ECS) plays a critical role in the behavioral expression of anxiety (Ruehle et al., 2012; Lutz et al., 2015a; Jenniches et al., 2016; Patel et al., 2017; Petrie et al., 2021). Indeed, mice treated with a low dose of the cannabinoid receptor subtype-1 (CB_1R) agonist, WIN 55212-2, exhibited increased open-arm exploration in the elevated plus maze (EPM) (Patel and Hillard, 2006), which suggests that activating the ECS is associated with an anxiolytic phenotype. In contrast, mice lacking CB_1Rs throughout the body spend less time exploring the open arms of the EPM when compared to wild-type mice (Haller et al., 2002), which suggests an anxiogenic effect for global CB_1R deletion. Similarly, mice lacking functional diacylglycerol lipase α, a key enzyme responsible for biosynthesis of the endocannabinoid, 2-arachidonoyl-*sn*-glycerol, in the brain, demonstrated reduced exploration of the central area of an open field test and increased anxiety-like behaviors in the light/dark box (Jenniches et al., 2016). These studies demonstrate the importance for the ECS in the central nervous system (CNS) in controlling anxiety-like behaviors in rodents; however, roles for the ECS in the gastrointestinal (GI) tract in these processes are unclear.

The ECS is found throughout the GI tract and controls food intake (Quarta et al., 2011; Argueta and DiPatrizio, 2017; Argueta et al., 2019; Avalos et al., 2020), gastric emptying and intestinal motility (Aviello et al., 2008; Camilleri et al., 2008; Di Marzo et al., 2008), and gut-barrier function (Kimball et al., 2006; Storr et al., 2009; Wiley and DiPatrizio, 2022). Moreover, recent studies suggest interactions between gut microbiota

and local endocannabinoid formation, which may contribute to anxiety-like behaviors (Markey et al., 2020). In this study, mice colonized with *C. albicans* in the gut had increased basal corticosterone (CORT) production and alterations in the gut endocannabinoidome. These findings reveal a possible mechanism by which the gut-brain axis enables peripheral ECS control over CNS mediated anxiety-like behaviors.

Vagal afferent fibers enable direct communication between the gut and the CNS (Berthoud and Neuhuber, 2000; Mayer, 2011; Critchley and Harrison, 2013). Vagal afferent neurons terminate in the brainstem at the nucleus of the solitary tract (NTS), which communicates with other brain structures that regulate fear and anxiety-like responses including the prefrontal cortex, hippocampus, and amygdala (Berthoud and Neuhuber, 2000). Accordingly, it is possible that alterations in gut function may affect gut-brain signaling and ultimately the behavioral expression of anxiety. For example, Krieger et al. demonstrated that activation of vagal afferent neurons by both food intake and chemogenetic approaches increased anxiety-like behavior, while chemogenetic inhibition of vagal afferent neurons attenuated these responses (Krieger et al., 2022). Importantly, this same study revealed sex differences in anxiety-like behaviors following chronic disruption of vagal afferent signaling from fibers originating in the gut. Notably, human females are more than twice as likely to be affected by mood disorders such as generalized anxiety disorder (GAD) (Kessler et al., 2005; Bekker and van Mens-Verhulst, 2007; Seedat et al., 2009), so it is unsurprising that many rodent studies find similar sex-

dependent outcomes when examining anxiety (Caldarone et al., 2008; An et al., 2011; Nyuyki et al., 2018; Leussis et al., 2021).

Sex dictates many aspects of gut-brain signaling (Holingue et al., 2020), ECS function (Morena et al., 2021; Salemme et al., 2023), and physiology (Rubino and Parolaro, 2011). Therefore, it is essential to understand how sex may differentially impact ECS function in the GI tract and the behavioral expression of anxiety. In the current study, we tested whether CB_1Rs located in the intestinal epithelium exert control over anxiety-like behaviors in male and female mice.

Materials & Methods

Animals

Male and female transgenic mice (described below in *Transgenic Mouse Generation*) 8-10 weeks of age were group-housed with *ad-libitum* access to standard rodent laboratory diet (SD; Teklad 2020x, Envigo, Huntingdon, UK; 16% kcal from fat, 24% kcal from protein, 60% kcal from carbohydrates) and water throughout all experiments unless otherwise stated. Mice were maintained on a 12-h dark/light cycle beginning at 1800 h. All procedures met the U.S. National Institute of Health guidelines for care and use of laboratory animals and were approved by the Institutional Animal Care and Use Committee (IACUC) of the University of California, Riverside.

Transgenic Mouse Generation

Conditional intestinal epithelium-specific CB_1R-deficient mice (IntCB_1-/-, Cnr1$^{tm1.1\ mrl}$/vil-cre ERT2) were generated by crossing Cnr1-floxed mice (IntCB_1+/+, Cnr1$^{tm1.1\ mrl}$; Taconic, Oxnard, CA, USA; Model #7599) with Vil-CRE ERT2 mice donated by Dr. Randy Seeley (University of Michigan, Ann Arbor, MI, USA) with permission from Dr. Sylvie Robin (Curie Institute, Paris, France). Cre recombinase expression in the intestinal epithelium is driven by the villin promotor, which allows for conditional tamoxifen-dependent Cre recombinase action to remove the *Cnr1* gene from these cells, as described by el Marjou et al. (el Marjou et al., 2004). Cnr1$^{tm1.1\ mrl}$/vil-cre ERT2 mice used in these experiments are referred to as IntCB_1-/-, and Cnr1$^{tm1.1\ mrl}$ control mice (lacking Cre recombinase) are referred to as IntCB_1+/+. Tail snips were collected from pups at weaning and DNA was extracted and analyzed by conventional PCR using the following primers (5'-3'): GCAGGGATTATGTCCCTAGC (CNR1-ALT), CTGTTACCAGGAGTCTTAGC (1415-35), GGCTCAAGGAATACACTTATACC (1415-37), GAACCTGATGGACATGTTCAGG (vilcre, AA), AGTGCGTTCGAACGCTAGAGCCTGT (vilcre, SS), TTACGTCCATCGTGG-ACAGC (vilcre, MYO F), TGGGCTGGGTGTTAGCCTTA (vilcre, MYO R). Intestinal epithelial CB_1R knockdown was verified by RT-qPCR immediately following experiments. Expression of the Cnr1 mRNA in the intestinal epithelium of intCB_1-/- mice (0.1563 ± 0.04848) is strongly reduced compared to intCB_1+/+ controls (1.000 ± 0.2223), $t_{(19)} = 3.543$, $p = 0.0022$.

Gene Expression

Total RNA from intestinal epithelium tissue was extracted using an RNeasy kit (Qiagen, Valencia, CA, USA) and first-strand cDNA was generated using M-MLV reverse transcriptase (Invitrogen, Carlsbad, CA, USA). Areas used for tissue collection and processing were sanitized with 70% ethanol solution then treated with RNAse inhibitor (RNAse Out, G-Biosciences, St. Louis, MO, USA). Reverse transcription of total RNA was performed as previously described (Argueta et al., 2019). Quantitative RT-PCR was performed using PrimePCR Assays (Biorad, Irvine, CA, USA) with primers for CB_1R (Cnr1) gene transcripts under preconfigured SYBR green assays (Biorad, Irvine, CA, USA). Hprt was used as a housekeeping gene. Reactions were run in duplicates and values expressed as relative mRNA expression.

Drug Preparation and Administration

IntCB_1-/- and intCB_1+/+ mice were administered tamoxifen (IP, 40 mg per kg) every 24 h for five consecutive days. Tamoxifen (Sigma-Aldrich, St. Louis, MO, USA) was dissolved in corn oil using bath sonication at a concentration of 10 mg per mL then stored at 37°C protected from light until administration. Mice were group housed in disposable cages throughout the injection period and for a 3-day post-injection period.

Elevated Plus Maze

On the day of the experiment, animals were allowed to acclimate to the testing room for 3-4 hours prior to testing. The EPM is a white plexiglass apparatus consisting of four equal-length arms (30 cm x 5 cm). The maze is elevated 39 cm off the ground. The

"closed" arms of the EPM are enclosed by 15 cm tall walls on all sides, while the "open" arms have a 1 mm border around the edges of the arm to prevent animals from falling off. Light intensity on the open arms was approximately 150 lux during testing. At the time of the test, animals were placed in the center of the maze facing one of the open arms and were allowed to freely explore the maze for a 5-minute period. The entire test was recorded by a stationary camera fixed on the ceiling above the maze which allowed simultaneous tracking of the center-point and nose-point of the mouse by EthoVision 13 XT software (Noldus Information Technology, Wageningen, Netherlands). The mouse was only considered to be in a zone if both the nose-point and the center-point were in that zone at the same time for at least 0.1 second. Between tests, the maze was thoroughly cleaned with a 70% EtOH solution followed by DIUF and allowed to completely dry before the next mouse entered the maze.

Light/Dark Box Test

On the day of the experiment, animals were allowed to acclimate to the testing room for 3-4 hours prior to testing. The Light/Dark box consists of two acrylic chambers. The "dark" box is an enclosed gray plexiglass chamber (8 cm x 20 cm x 30 cm) with a solid roof. The "light" box is an open gray plexiglass chamber (18 cm x 20 cm x 30 cm) without a roof. The entire apparatus was placed on a table during recording. Light intensity in the light box was approximately 150-200 lux during testing. At the time of the test, animals were placed in the corner of the light box furthest from the entry to the dark box and were allowed to freely explore the apparatus for a 10-minute period. The entire test was

recorded by a stationary camera fixed on the ceiling above the box which allowed simultaneous tracking of the center-point and nose-point of the mouse by EthoVision 13 XT software (Noldus Information Technology, Wageningen, Netherlands). The mouse was only considered to be in a zone if both the nose-point and the center-point were in that zone at the same time for at least 0.1 second. Between tests, the maze was thoroughly cleaned with a 70% EtOH solution followed by DIUF and allowed to completely dry before the next mouse entered the apparatus.

Open Field Test

On the day of testing, animals were allowed to acclimate to the testing room for 3-4 hours prior to testing. The open field is an open white plexiglass square (50 cm x 50 cm x 40 cm) without a roof. The open field apparatus was placed on a table during recording. Light intensity in the center of the open field was approximately 150-200 lux during testing. At the time of the test, animals were placed in the bottom left corner of the open field apparatus and were allowed to freely explore the apparatus for a 10-minute period. The entire test was recorded by a stationary camera fixed on the ceiling above the apparatus which allowed simultaneous tracking of the center-point and nose-point of the mouse by EthoVision 13 XT software (Noldus Information Technology, Wageningen, Netherlands). The mouse was only considered to be in a zone if both the nose-point and the center-point were in that zone at the same time for at least 0.1 second. Between tests, the open field was thoroughly cleaned with a 70% EtOH solution

followed by DIUF and allowed to completely dry before the next mouse entered the apparatus.

CORT ELISA

On the day of the experiment, mice were allowed to freely explore the EPM for 5 minutes. 30 minutes following EPM exposure, mice were anesthetized by isoflurane and blood was collected via retroorbital bleed using non-heparinized capillary tubes and stored on ice. Blood samples were spun at 4,900 RPM for 10 minutes at 4°C to isolate serum. Serum was collected and stored at -80°C until analysis. Serum corticosterone (CORT) levels were quantified using the DetectX Corticosterone ELISA kit (Arbor Assays, Ann Arbor, MI, USA). Samples were diluted at 1:100 and plated in duplicate. The assay was completed as described by the kit insert. Average OD values were calculated for each sample, and the mean OD for the NSB was subtracted from each average sample OD value. Sample concentrations interpolated on a 4PL $\%B/B_0$ standard curve and multiplied by the dilution factor of 100 to obtain neat sample concentrations.

Experimental Design & Statistical Analysis

Details regarding the experimental design of individual experiments are provided in the figure legends. Data were analyzed by GraphPad Prism version 9.5.0 (GraphPad Software, La Jolla, CA, USA) using unpaired Student's *t*-tests (two-tailed), two-way ANOVA, or three-way ANOVA with Holm-Sidak's multiple comparisons *post-hoc* test when appropriate.

Results

Male, but Not Female, IntCB$_1$-/- Mice Exhibit Anxiolytic Behaviors in the Elevated Plus Maze (EPM)

We tested the hypothesis that CB$_1$Rs in the intestinal epithelium play a role in anxiety-like behaviors in the EPM. Male intCB$_1$-/- mice entered the open arms of the EPM more often (**Fig. 2.1*B*,*C***) and spent more time exploring the open arms (**Fig. 2.1*E***) when compared to male intCB$_1$+/+ control mice (**Fig. 2.1*A*,*E***) during the five-minute test. There were no genotype differences in closed arm entries or cumulative exploration time of the closed arm (**Fig. 2.1*D, F***). Male intCB$_1$-/- mice had an increased number of head dips (**Fig. 2.1*G***) and spent more time performing the head dipping behavior (**Fig. 1*H***) when compared to male intCB$_1$+/+ mice. In contrast to male mice, female intCB$_1$-/- mice did not exhibit any differences in number of open (**Fig. 2.2*B*, *C***) or closed (**Fig. 2.2*B*, *D***) arm entries when compared to female intCB$_1$+/+ mice (**Fig. *2.2A, C, D***). Furthermore, female intCB$_1$-/- and female intCB$_1$+/+ mice spent a similar amount of time exploring the open arms (**Fig. 2.2*E***) and closed arms (**Fig. 2.2*F***). There were no genotype differences in the frequency of head dips (**Fig. 2.2G**) or cumulative duration of head dipping behavior in female mice (**Fig. 2.2H**). We also evaluated general movement parameters in male and female intCB$_1$-/- and intCB$_1$+/+ mice. There were no significant differences in average velocity (**Fig. 2.3*A, B***), total distance traveled (**Fig. 2.3*E, F***), cumulative duration of movement (**Fig. 2.3*C, D***), or cumulative duration of non-movement (**Fig. 2.3*G, H***) between genotypes of male or female mice.

Male, but Not Female, IntCB$_1$-/- Mice Exhibit Anxiolytic Behaviors in the Light/Dark Box

We next asked if CB$_1$Rs in the intestinal epithelium play a role in anxiety-like behaviors in the light/dark box. Male intCB$_1$-/- mice entered the light zone more frequently (**Fig. 2.4*A* top right, *B***) and spent more time in the light box (**Fig. 2.4*A* top right, *C***) than male intCB$_1$+/+ control mice (**Fig. 2.4*A* top left, *B, C***) during the 10-minute test. In contrast to male mice, female mice did not exhibit any differences in light box exploration, irrespective of genotype (**Fig. 2.4*A* bottom left and right, *C, D***).

IntCB$_1$-/- Mice do Not Exhibit Anxiolytic Behaviors in the Open Field Test

Exploratory behaviors of intCB$_1$-/- mice were also evaluated in the open field test. Neither male or female intCB$_1$-/- mice exhibited a difference in center zone entries (**Fig. 2.5*B***) or cumulative duration in center zone (**Fig. 2.5*C***) when compared to intCB$_1$+/+ control mice during the 10-minute test. There were also no genotype differences observed in latency to first center zone entry (**Fig. 2.5*D***) for male or female mice. Furthermore, female intCB$_1$-/- mice exhibited a significant decrease in ambulation (**Fig. 2.5*E***, total number of zones entered) when compared to female intCB$_1$+/+ mice; however, no genotype differences in ambulation were found for male mice. Both male and female intCB$_1$-/- mice exhibited a decrease in the total distance traveled (**Fig. 2.5*F***) and average velocity (**Fig. 2.5*G***) when compared to respective control mice. In addition, male and female intCB$_1$-/- animals demonstrated a decrease in the cumulative duration of

movement (**Fig. 2.5*H***) and a corresponding increase in the cumulative duration of non-movement (**Fig. 2.5*G***) when compared to control mice.

Circulating CORT Levels are Sex-Dependent

We next quantified circulating corticosterone (CORT) levels in male and female intCB_1-/- and intCB_1+/+ control mice at baseline and 30 minutes after EPM exposure. There was a strong effect of sex and timepoint on plasma CORT levels (**Fig. 2.6*A***). CORT was significantly higher in females than males, regardless of genotype, both at baseline and following EPM exposure. CORT levels were also significantly elevated in all groups following EPM exposure when compared to their respective baseline levels. There was no effect of genotype on circulating CORT in either male or female mice at baseline or post-EPM. Although there were strong effects of sex and timepoint on plasma CORT, no significant differences were observed in % change of CORT when comparing baseline and post-EPM levels (**Fig. 2.6*B***).

Discussion

We report that *(i)* male mice lacking CB_1Rs in the intestinal epithelium exhibit anxiolytic behavior during the EPM and light/dark box tests, but not in the open field test, *(ii)* female mice lacking CB_1Rs in the intestinal epithelium do not display an anxiolytic phenotype during any of the three tests, and *(iii)* sex differences in behaviors are associated with elevated levels of circulating corticosterone (CORT) in female mice at

baseline and immediately following behavioral testing. The findings reveal an important and sexually dimorphic role for CB_1Rs in the intestinal epithelium in the behavioral expression of anxiety.

To better understand how peripheral components of the ECS contribute to the expression of anxiety-like behaviors, we utilized our transgenic mouse line that conditionally lacks CB_1Rs selectively in the intestinal epithelium. Male intCB_1-/- mice spent significantly more exploring the open arms of the EPM when compared to corresponding controls, as shown by total entries into open arms and cumulative time spent in open arms. IntCB_1-/- males also participated in head dipping behaviors more than corresponding controls. These anxiolytic behaviors observed in mice were not due to changes in mobility as evidenced by no differences detected versus control mice for mean velocity, total distance moved, and cumulative duration of movement or non-movement. A similar anxiolytic phenotype was observed in the light/dark box: intCB_1-/- male mice exhibited in increase in light box entries and cumulative duration in the light box when compared to control mice. Since mice cannot be recorded in the dark box due to the opaque lid, measures of mobility in the dark compartment were not analyzed. Notably, intCB_1-/- males did not display an anxiolytic phenotype on any measurable outcomes in the open field test when compared to corresponding controls. It is possible, however, that the 10-minute testing period was not long enough for mice to display behavioral differences in the open field test. Although many groups utilize a 5-10 minute range for this test (Prut and Belzung, 2003; Gould et al., 2009; Kraeuter et al., 2019), others allow

up to 30 minutes of exploration (Choleris et al., 2001; McIlwain et al., 2001; Dulawa et al., 2004). Nonetheless, differential effects observed among genotypes in male mice on the three tests highlight the importance of utilizing a battery of behavioral tests to assess anxiety-like behaviors in rodents (Ramos, 2008).

In contrast to male mice, female intCB_1-/- mice did not exhibit anxiolytic phenotypes on any of the three tests versus corresponding control mice. Female mice, however, displayed an increase in baseline EPM exploration when compared to male mice. This is particularly apparent when comparing the heat maps for intCB_1+/+ control male and female mice (**Fig. 2.1*A* and 2.2*A*,** respectively). Specifically, female intCB_1+/+ control mice exhibited a higher number of open-arm entries and cumulative duration in open arms when compared to those displayed by male control mice. This observation may explain the lack of genotype differences observed in female anxiety-like behaviors. Accordingly, it is possible that there is a "ceiling effect" for exploration of open arms in the EPM in female mice, thus preventing any further increases in open-arm exploration irrespective of genotype. To confirm this hypothesis, future experiments could be conducted in combination with administration of anxiety-reducing drugs (e.g., benzodiazepines) or stimuli in female intCB_1-/- and control mice to evaluate if exploration can be increased above the baseline.

Both male and female intCB_1-/- mice demonstrated a significant reduction in several locomotor parameters in the open field test when compared to corresponding control mice. The relationship between locomotor activity and rodent emotionality,

however, is unclear (Archer, 1973; Walsh and Cummins, 1976; Gray, 1979; Ramos, 2008; Seibenhener and Wooten, 2015). Indeed, inconsistencies have been widely noted in open field test protocols across labs, which suggest that measures of emotionality may confound analyses of locomotor activity, and vice-versa (Stanford, 2007). Therefore, genotype differences in ambulation, total distance traveled, average velocity, and cumulative duration of movement and non-movement may reflect anxiety-related changes in behavior of mice, including intCB_1-/- mice, or they may be a result of the other changes in behaviors. Nonetheless, the current results indicate that CB_1Rs in the intestinal epithelium contribute to the expression of several behaviors that are widely used to analyze an "anxiety" phenotype in mice.

Global and cell type-specific deletion of CB_1R in the brain of rodents yields pronounced anxious-like phenotypes (Urigüen et al., 2004; Lutz et al., 2015b; Lutz et al., 2015a; Soriano et al., 2021). To the best of our knowledge, we are the first group to test the effect of intestinal epithelium-specific CB_1R deletion on anxiety-like behaviors. Unexpectedly, our findings indicate that male mice lacking CB_1Rs in the intestinal epithelium exhibit an anxiolytic phenotype when compared to corresponding controls. We also show that female mice lacking CB_1Rs in the intestinal epithelium perform similarly to controls on the EPM, light/dark box, and open field test. It is important to note that deletion is specific to CB_1 cannabinoid receptors. Some reports indicate a role for CB_2Rs in the brain (García-Gutiérrez and Manzanares, 2011; Almeida-Santos et al., 2013; Ishiguro et al., 2018; Li et al., 2023) in the control of anxiety-like behaviors; however, roles

for intestinal CB_2Rs in anxiety are unknown and their investigation in this context remains for future studies. These should include use of mice with conditional deletion of CB_2Rs in the intestinal epithelium in combination with pharmacological interventions to fully characterize the contribution of intestinal CB_1- versus CB_2-cannabinoid receptors in the behavioral expression of anxiety.

Sex differences related to ECS control of behavior have been described by other groups as well. For example, female rats displayed both anxiolytic and anxiogenic effects in response to treatment with the fatty acid amide inhibitor, URB587, and the monoacylglycerol lipase inhibitor, MJN110, that were dependent on estrous cycles, while male rats responded to the same treatments with only anxiolytic or anxiogenic behaviors, respectively (Salemme et al., 2023). In a different study, inhibition of anandamide (AEA) or 2-AG hydrolysis had no effect in males, but did alter fear-memory extinction in females (Morena et al., 2021). These differences may be attributed, in part, to sexual dimorphism and function of the amygdala, hippocampus, and medial prefrontal cortices (Goldstein et al., 1999; Lebron-Milad and Milad, 2012), all of which densely express ECS components (Marsicano and Kuner, 2008; Katona and Freund, 2012) and estrogen receptors (Walf and Frye, 2006; Montague et al., 2008; Spencer et al., 2008). Moreover, significant elevations in circulating levels of CORT were observed in female mice in the current study, regardless of genotype, both at baseline and immediately following EPM exposure. Therefore, is it also possible that elevated CORT levels in female mice may prevent the deletion of CB_1Rs

in the intestinal epithelium from having anxiolytic effects. Differential levels of circulating CORT, however, is insufficient to explain the genotype differences observed in male mice.

CB_1Rs are expressed on a variety of cells expressed in the intestinal epithelium, including enteroendocrine I cells (Sykaras et al., 2012; Argueta et al., 2019). Nutrient-induced CCK release by I cells enables gut-brain satiation communication via CCK_A receptors located on vagal afferent fibers (Clemmensen et al., 2017). Indeed, vagal afferent fibers may play a critical role in the transmission of affective signals from the gut to the brain (Forsythe et al., 2010; Mayer, 2011). Accordingly, it is possible that the absence of CB_1Rs in I cells in intCB_1-/- mice leads to alterations in gut-brain signaling that impacts anxiety-like behaviors. Moreover, several studies report that vagal afferent signaling has a direct impact on anxiety-like behaviors. For example, subdiaphragmatic vagal deafferentation in rats caused a reduction in anxiety-like behaviors on the EPM, open field test, and food neophobia test (Klarer et al., 2014). Another group demonstrated that both feeding and chemogenetic activation of gut-innervating vagal afferents increased anxiety-like behaviors, while fasting and chemogenetic inhibition of the same fibers blocked increases in anxiety-like behaviors (Krieger et al., 2022). Similarly, Maniscalco et al. found that an overnight fast attenuated anxious behavior in rats tested on the EPM and acoustic startle test (Maniscalco et al., 2015). It is unclear whether the anxiolysis observed in intCB_1-/- males in the current study is the direct result of changes in vagal afferent neuronal signaling, but future studies should evaluate roles for gut-brain signaling in these processes.

Collectively these results suggest that genetic deletion of CB_1Rs in the intestinal epithelium is associated with an anxiolytic phenotype in a sex-dependent manner, with a robust phenotype found for male mice. Future studies will investigate the mechanism(s) by which intestinal CB_1Rs control anxiety-like behaviors.

References

Almeida-Santos AF, Gobira PH, Rosa LC, Guimaraes FS, Moreira FA, Aguiar DC (2013) Modulation of anxiety-like behavior by the endocannabinoid 2-arachidonoylglycerol (2-AG) in the dorsolateral periaqueductal gray. Behav Brain Res 252:10-17.

An XL, Zou JX, Wu RY, Yang Y, Tai FD, Zeng SY, Jia R, Zhang X, Liu EQ, Broders H (2011) Strain and sex differences in anxiety-like and social behaviors in C57BL/6J and BALB/cJ mice. Exp Anim 60:111-123.

Archer J (1973) Tests for emotionality in rats and mice: a review. Anim Behav 21:205-235.

Argueta D, DiPatrizio N (2017) Peripheral endocannabinoid signaling controls hyperphagia in western diet-induced obesity. Physiology & Behavior 171:32-39.

Argueta D, Perez P, Makriyannis A, DiPatrizio N (2019) Cannabinoid CB1 Receptors Inhibit Gut-Brain Satiation Signaling in Diet-Induced Obesity. Frontiers in Physiology 10.

Avalos B, Argueta D, Perez P, Wiley M, Wood C, DiPatrizio N (2020) Cannabinoid CB1 Receptors in the Intestinal Epithelium Are Required for Acute Western-Diet Preferences in Mice. Nutrients 12.

Aviello G, Romano B, Izzo AA (2008) Cannabinoids and gastrointestinal motility: animal and human studies. European review for medical and pharmacological sciences 12 Suppl 1:81-93.

Bekker MH, van Mens-Verhulst J (2007) Anxiety disorders: sex differences in prevalence, degree, and background, but gender-neutral treatment. Gend Med 4 Suppl B:S178-193.

Berthoud HR, Neuhuber WL (2000) Functional and chemical anatomy of the afferent vagal system. Auton Neurosci 85:1-17.

Caldarone BJ, King SL, Picciotto MR (2008) Sex differences in anxiety-like behavior and locomotor activity following chronic nicotine exposure in mice. Neurosci Lett 439:187-191.

Camilleri M, Carlson P, McKinzie S, Grudell A, Busciglio I, Burton D, Baxter K, Ryks M, Zinsmeister AR (2008) Genetic variation in endocannabinoid metabolism, gastrointestinal motility, and sensation. Am J Physiol Gastrointest Liver Physiol 294:G13-19.

Choleris E, Thomas AW, Kavaliers M, Prato FS (2001) A detailed ethological analysis of the mouse open field test: Effects of diazepam, chlordiazepoxide, and an extremely low frequency pulsed magnetic field. Neuroscience and Biobehavioral Reviews 25:235-260.

Clemmensen C, Muller TD, Woods SC, Berthoud HR, Seeley RJ, Tschop MH (2017) Gut-Brain Cross-Talk in Metabolic Control. Cell 168:758-774.

Critchley HD, Harrison NA (2013) Visceral influences on brain and behavior. Neuron 77:624-638.

Di Marzo V, Capasso R, Matias I, Aviello G, Petrosino S, Borrelli F, Romano B, Orlando P, Capasso F, Izzo AA (2008) The Role of Endocannabinoids in the Regulation of Gastric Emptying: Alterations in Mice Fed a High-Fat Diet. Br J Pharmacol 153:1272-7280.

Dulawa SC, Holick KA, Gundersen B, Hen R (2004) Effects of chronic fluoxetine in animal models of anxiety and depression. Neuropsychopharmacology 29:1321-1330.

el Marjou F, Janssen KP, Chang BH, Li M, Hindie V, Chan L, Louvard D, Chambon P, Metzger D, Robine S (2004) Tissue-specific and inducible Cre-mediated recombination in the gut epithelium. Genesis 39:186-193.

Forsythe P, Sudo N, Dinan T, Taylor VH, Bienenstock J (2010) Mood and gut feelings. Brain Behav Immun 24:9-16.

García-Gutiérrez MS, Manzanares J (2011) Overexpression of CB2 cannabinoid receptors decreased vulnerability to anxiety and impaired anxiolytic action of alprazolam in mice. J Psychopharmacol 25:111-120.

Goldstein JM, Kennedy DN, Caviness VS (1999) Images in neuroscience. Brain development, XI: sexual dimorphism. Am J Psychiatry 156:352.

Gould TD, Dao DT, Kovacsics CE (2009) The open field test. In: Mood and anxiety related phenotypes in mice: Characterization using behavioral tests, pp (2009), p 2001-2332.

Gray JA (1979) Emotionality in male and female rodents: a reply to Archer. Br J Psychol 70:425-440.

Haller J, Bakos N, Szirmay M, Ledent C, Freund TF (2002) The effects of genetic and pharmacological blockade of the CB1 cannabinoid receptor on anxiety. Eur J Neurosci 16:1395-1398.

Holingue C, Budavari AC, Rodriguez KM, Zisman CR, Windheim G, Fallin MD (2020) Sex Differences in the Gut-Brain Axis: Implications for Mental Health. Current Psychiatry Reports 22.

Ishiguro H, Horiuchi Y, Tabata K, Liu QR, Arinami T, Onaivi ES (2018) Cannabinoid CB2 Receptor Gene and Environmental Interaction in the Development of Psychiatric Disorders. Molecules 23.

Jenniches I, Ternes S, Albayram O, Otte DM, Bach K, Bindila L, Michel K, Lutz B, Bilkei-Gorzo A, Zimmer A (2016) Anxiety, Stress, and Fear Response in Mice With Reduced Endocannabinoid Levels. Biol Psychiatry 79:858-868.

Katona I, Freund TF (2012) Multiple functions of endocannabinoid signaling in the brain. Annu Rev Neurosci 35:529-558.

Kessler RC, Berglund P, Demler O, Jin R, Merikangas KR, Walters EE (2005) Lifetime prevalence and age-of-onset distributions of DSM-IV disorders in the National Comorbidity Survey Replication. Arch Gen Psychiatry 62:593-602.

Kimball ES, Schneider CR, Wallace NH, Hornby PJ (2006) Agonists of cannabinoid receptor 1 and 2 inhibit experimental colitis induced by oil of mustard and by dextran sulfate sodium. Am J Physiol Gastrointest Liver Physiol 291:G364-371.

Klarer M, Arnold M, Günther L, Winter C, Langhans W, Meyer U (2014) Gut vagal afferents differentially modulate innate anxiety and learned fear. J Neurosci 34:7067-7076.

Kraeuter AK, Guest PC, Sarnyai Z (2019) The Open Field Test for Measuring Locomotor Activity and Anxiety-Like Behavior. Methods Mol Biol 1916:99-103.

Krieger JP, Asker M, van der Velden P, Börchers S, Richard JE, Maric I, Longo F, Singh A, de Lartigue G, Skibicka KP (2022) Neural Pathway for Gut Feelings: Vagal

Interoceptive Feedback From the Gastrointestinal Tract Is a Critical Modulator of Anxiety-like Behavior. Biol Psychiatry 92:709-721.

Lebron-Milad K, Milad MR (2012) Sex differences, gonadal hormones and the fear extinction network: implications for anxiety disorders. Biol Mood Anxiety Disord 2:3.

Leussis MP, Thanos JM, Powers A, Peterson E, Head JP, McGovern NJ, Malarkey FJ, Drake A (2021) Sex differences in long-term behavioral alterations, especially anxiety, following prenatal fluoxetine exposure in C57BL/6 mice. Pharmacol Biochem Behav 211:173293.

Li J, Wang H, Liu D, Li X, He L, Pan J, Shen Q, Peng Y (2023) CB2R activation ameliorates late adolescent chronic alcohol exposure-induced anxiety-like behaviors during withdrawal by preventing morphological changes and suppressing NLRP3 inflammasome activation in prefrontal cortex microglia in mice. Brain Behav Immun 110:60-79.

Lutz B, Marsicano G, Maldonado R, Hillard CJ (2015a) The endocannabinoid system in guarding against fear, anxiety and stress. Nat Rev Neurosci 16:705-718.

Lutz B, Häring M, Enk V, Aparisi Rey A, Loch S, Ruiz De Azua I, Monory K, Weber T, Bartsch D (2015b) Cannabinoid type-1 receptor signaling in central serotonergic neurons regulates anxiety-like behavior and sociability. Frontiers in Behavioral Neuroscience.

Maniscalco JW, Zheng H, Gordon PJ, Rinaman L (2015) Negative Energy Balance Blocks Neural and Behavioral Responses to Acute Stress by "Silencing" Central Glucagon-Like Peptide 1 Signaling in Rats. J Neurosci 35:10701-10714.

Markey L, Hooper A, Melon LC, Baglot S, Hill MN, Maguire J, Kumamoto CA (2020) Colonization with the commensal fungus Candida albicans perturbs the gut-brain axis through dysregulation of endocannabinoid signaling. Psychoneuroendocrinology 121:104808.

Marsicano G, Kuner R (2008) Anatomical distribution of receptors, ligands and enzymes in the brain and in the spinal cord: Circuitries and neurochemistry. In: Cannabinoids and the brain, pp (2008), p 2161-2743.

Mayer EA (2011) Gut feelings: the emerging biology of gut-brain communication. Nat Rev Neurosci 12:453-466.

McIlwain KL, Merriweather MY, Yuva-Paylor LA, Paylor R (2001) The use of behavioral test batteries: effects of training history. Physiol Behav 73:705-717.

Montague D, Weickert CS, Tomaskovic-Crook E, Rothmond DA, Kleinman JE, Rubinow DR (2008) Oestrogen receptor alpha localisation in the prefrontal cortex of three mammalian species. J Neuroendocrinol 20:893-903.

Morena M, Nastase AS, Santori A, Cravatt BF, Shansky RM, Hill MN (2021) Sex-dependent effects of endocannabinoid modulation of conditioned fear extinction in rats. British Journal of Pharmacology 178:983-996.

Nyuyki KD, Cluny NL, Swain MG, Sharkey KA, Pittman QJ (2018) Altered Brain Excitability and Increased Anxiety in Mice With Experimental Colitis: Consideration of Hyperalgesia and Sex Differences. Front Behav Neurosci 12:58.

Patel S, Hillard CJ (2006) Pharmacological evaluation of cannabinoid receptor ligands in a mouse model of anxiety: further evidence for an anxiolytic role for endogenous cannabinoid signaling. J Pharmacol Exp Ther 318:304-311.

Patel S, Hill MN, Cheer JF, Wotjak CT, Holmes A (2017) The endocannabinoid system as a target for novel anxiolytic drugs. Neurosci Biobehav Rev 76:56-66.

Petrie GN, Nastase AS, Aukema RJ, Hill MN (2021) Endocannabinoids, cannabinoids and the regulation of anxiety. Neuropharmacology 195:108626.

Prut L, Belzung C (2003) The open field as a paradigm to measure the effects of drugs on anxiety-like behaviors: a review. Eur J Pharmacol 463:3-33.

Quarta C, Mazza R, Obici S, Pasquali R, Pagotto U (2011) Energy balance regulation by endocannabinoids at central and peripheral levels. Trends Mol Med 17:518-526.

Ramos A (2008) Animal models of anxiety: do I need multiple tests? Trends Pharmacol Sci 29:493-498.

Rubino T, Parolaro D (2011) Sexually dimorphic effects of cannabinoid compounds on emotion and cognition. Front Behav Neurosci 5:64.

Ruehle S, Rey AA, Remmers F, Lutz B (2012) The endocannabinoid system in anxiety, fear memory and habituation. J Psychopharmacol 26:23-39.

Salemme BW, Raymundi AM, Sohn JMB, Stern CA (2023) The Estrous Cycle Influences the Effects of Fatty Acid Amide Hydrolase and Monoacylglycerol Lipase Inhibition in the Anxiety-Like Behavior in Rats. Cannabis Cannabinoid Res.

Seedat S et al. (2009) Cross-national associations between gender and mental disorders in the World Health Organization World Mental Health Surveys. Arch Gen Psychiatry 66:785-795.

Seibenhener ML, Wooten MC (2015) Use of the Open Field Maze to measure locomotor and anxiety-like behavior in mice. J Vis Exp:e52434.

Soriano D, Brusco A, Caltana L (2021) Further evidence of anxiety- and depression-like behavior for total genetic ablation of cannabinoid receptor type 1. Behav Brain Res 400:113007.

Spencer JL, Waters EM, Romeo RD, Wood GE, Milner TA, McEwen BS (2008) Uncovering the mechanisms of estrogen effects on hippocampal function. Front Neuroendocrinol 29:219-237.

Stanford SC (2007) The Open Field Test: reinventing the wheel. J Psychopharmacol 21:134-135.

Storr MA, Keenan CM, Zhang H, Patel KD, Makriyannis A, Sharkey KA (2009) Activation of the cannabinoid 2 receptor (CB2) protects against experimental colitis. Inflamm Bowel Dis 15:1678-1685.

Sykaras AG, Demenis C, Case RM, McLaughlin JT, Smith CP (2012) Duodenal enteroendocrine I-cells contain mRNA transcripts encoding key endocannabinoid and fatty acid receptors. PLoS ONE 7:e42373.

Urigüen L, Pérez-Rial S, Ledent C, Palomo T, Manzanares J (2004) Impaired action of anxiolytic drugs in mice deficient in cannabinoid CB1 receptors. Neuropharmacology 46:966-973.

Walf AA, Frye CA (2006) A review and update of mechanisms of estrogen in the hippocampus and amygdala for anxiety and depression behavior. Neuropsychopharmacology 31:1097-1111.

Walsh RN, Cummins RA (1976) The Open-Field Test: a critical review. Psychol Bull 83:482-504.

Wiley MB, DiPatrizio NV (2022) Diet-Induced Gut Barrier Dysfunction Is Exacerbated in Mice Lacking Cannabinoid 1 Receptors in the Intestinal Epithelium. Int J Mol Sci 23.

Figures

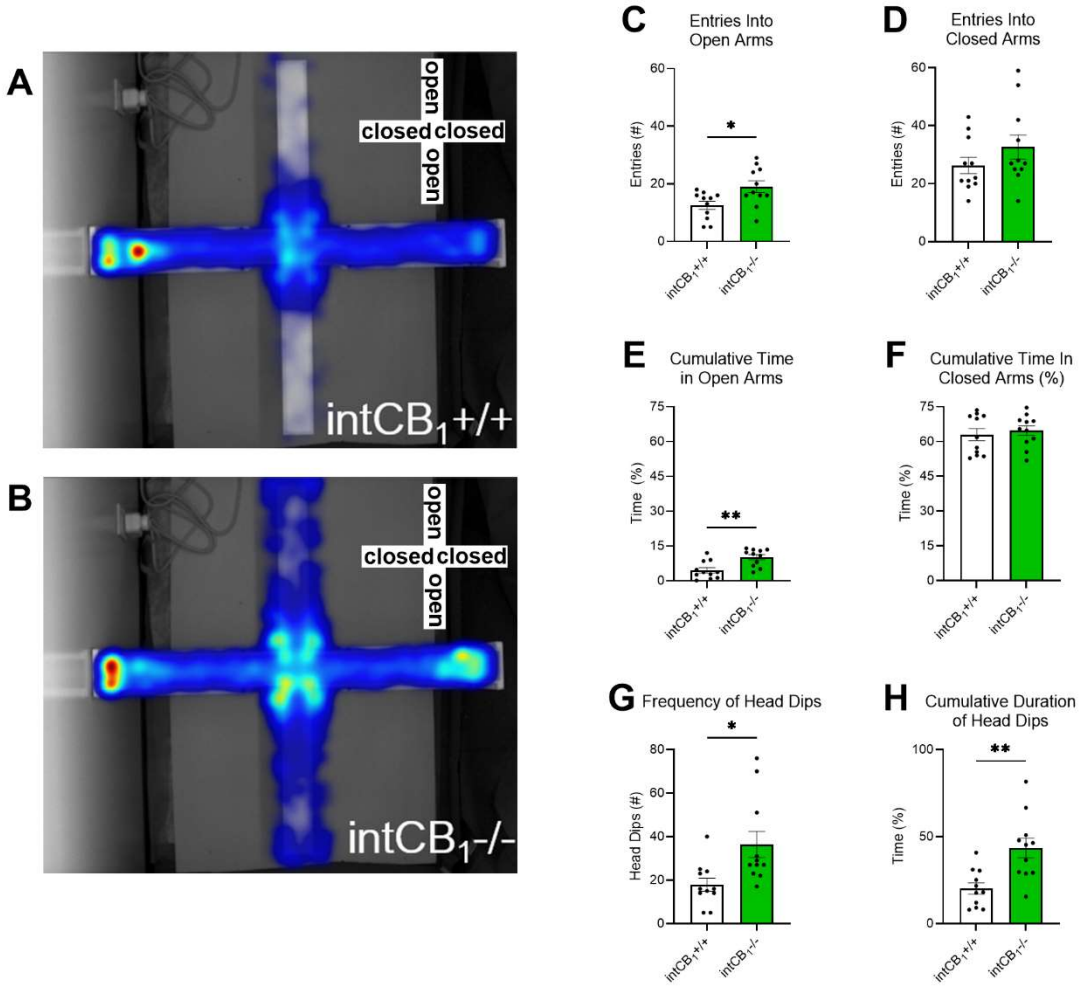
A
open
closed closed
open
intCB1+/+
B
open
closed closed
open
intCB1-/-
C
Entries Into Open Arms
Entries (#)
D
Entries Into Closed Arms
Entries (#)
E
Cumulative Time in Open Arms
Time (%)
F
Cumulative Time In Closed Arms (%)
Time (%)
G
Frequency of Head Dips
Head Dips (#)
H
Cumulative Duration of Head Dips
Time (%)
intCB1+/+
intCB1-/-

Figure 2.1 Male intCB$_1$-/- mice exhibit anxiolytic behaviors in the EPM. Male intCB$_1$-/- mice and intCB$_1$+/+ controls were allowed to freely explore the EPM for 5 minutes. Merged heatmaps of all trials for **(A)** intCB$_1$+/+ and **(B)** intCB$_1$-/- mice show general exploration patterns of the open (vertical) and closed (horizontal) arms. Increasing time spent in area designated from blue to red, with red being most time. **(C)** IntCB$_1$-/- male mice entered the open arms significantly more than controls ($t_{(20)} = 2.602$, $p = 0.0170$). **(D)** There were no differences in closed arm entries between genotypes ($t_{(20)} = 1.275$, $p = 0.2170$). **(E)** IntCB$_1$-/- male mice spent more time exploring the open arms when compared to controls ($t_{(20)} = 3.570$, $p = 0.0019$), but there were no differences in **(F)** cumulative time of closed arm exploration ($t_{(20)} = 0.5128$, $p = 0.6137$). **(G)** IntCB$_1$-/- male mice exhibited an increased number of head dips compared to controls ($t_{(20)} = 2.736$, $p = 0.0127$) and **(H)** spent more time performing the head dipping behavior than controls ($t_{(20)} = 3.566$, $p = 0.0019$). All analyses are unpaired Student's *t* tests. Data presented as ± SEM, n = 11 mice per genotype. *$p < 0.05$, **$p < 0.01$.

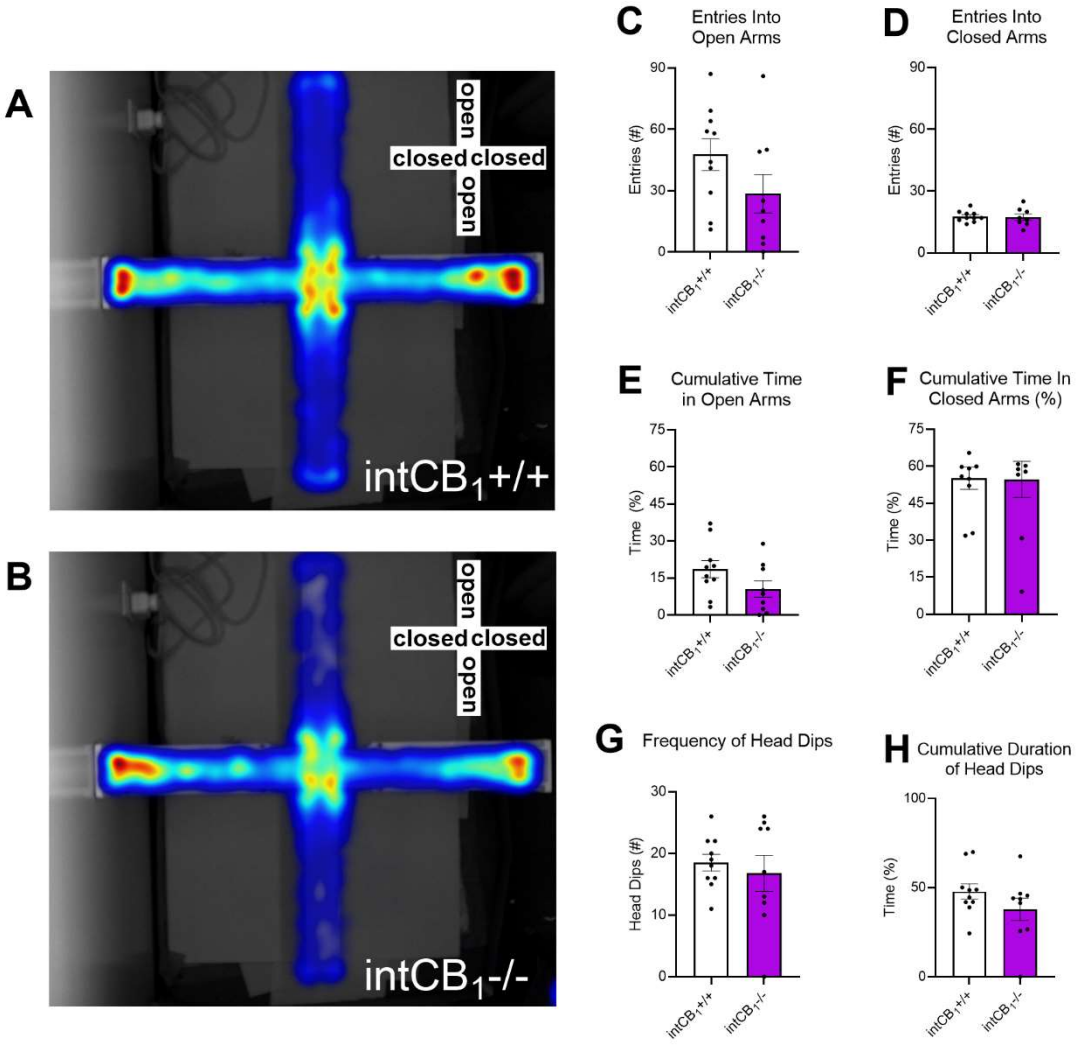
A
open
closed closed
open
intCB1+/+
B
open
closed closed
open
intCB1-/-
C
Entries Into Open Arms
Entries (#)
90
60
30
0
intCB1+/+
intCB1-/-
D
Entries Into Closed Arms
Entries (#)
90
60
30
0
intCB1+/+
intCB1-/-
E
Cumulative Time in Open Arms
Time (%)
75
60
45
30
15
0
intCB1+/+
intCB1-/-
F
Cumulative Time In Closed Arms (%)
Time (%)
75
60
45
30
15
0
intCB1+/+
intCB1-/-
G
Frequency of Head Dips
Head Dips (#)
30
20
10
0
intCB1+/+
intCB1-/-
H
Cumulative Duration of Head Dips
Time (%)
100
50
0
intCB1+/+
intCB1-/-

Figure 2.2 Female intCB$_1$-/- mice do not perform differently from controls in the EPM. Female intCB$_1$-/- mice and intCB$_1$+/+ controls were allowed to freely explore the EPM for 5 minutes. Merged heatmaps of all trials for **(A)** intCB$_1$+/+ and **(B)** intCB$_1$-/- mice show general exploration patterns of the open (vertical) and closed (horizontal) arms. Increasing time spent in area designated from blue to red, with red being most time. **(C)** IntCB$_1$-/- female mice did not exhibit any differences in open arm entries compared to controls ($t_{(17)}$ = 1.588, p = 0.1307). **(D)** There were no differences in closed arm entries between genotypes ($t_{(16)}$ = 0.1938, p = 0.8488). **(E)** IntCB$_1$-/- female mice and controls spent a similar amount of time exploring the open arms ($t_{(17)}$ = 1.665, p = 0.1142) and **(F)** closed arms of the EPM ($t_{(17)}$ = 0.05312, p = 0.9853). There were no genotype differences in the **(G)** total number of head dips ($t_{(17)}$ = 0.5512, p = 0.5886) or the **(H)** cumulative time spent performing head dip behavior ($t_{(17)}$ = 1.334, p = 0.1999) in female mice. All analyses are unpaired Student's *t* tests. Data presented as ± SEM, n = 9-10 mice per genotype.

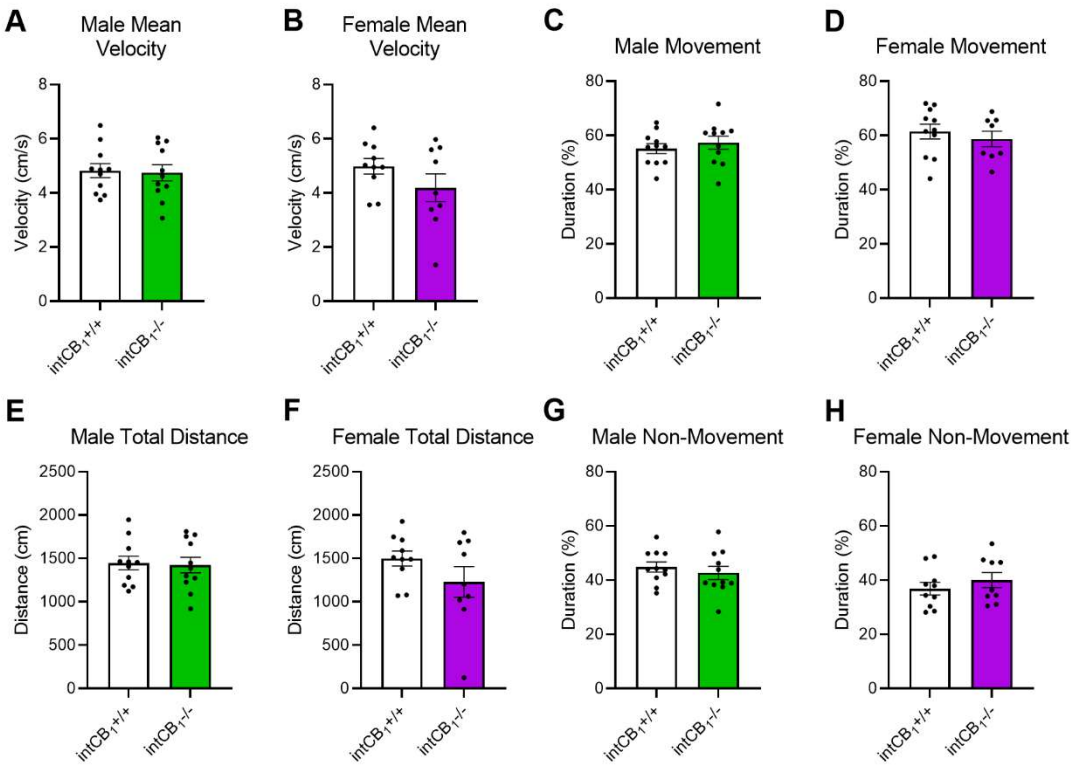
A
Male Mean Velocity
Velocity (cm/s)
0
2
4
6
8
intCB1+/+
intCB1-/-
B
Female Mean Velocity
Velocity (cm/s)
0
2
4
6
8
intCB1+/+
intCB1-/-
C
Male Movement
Duration (%)
0
20
40
60
80
intCB1+/+
intCB1-/-
D
Female Movement
Duration (%)
0
20
40
60
80
intCB1+/+
intCB1-/-
E
Male Total Distance
Distance (cm)
0
500
1000
1500
2000
2500
intCB1+/+
intCB1-/-
F
Female Total Distance
Distance (cm)
0
500
1000
1500
2000
2500
intCB1+/+
intCB1-/-
G
Male Non-Movement
Duration (%)
0
20
40
60
80
intCB1+/+
intCB1-/-
H
Female Non-Movement
Duration (%)
0
20
40
60
80
intCB1+/+
intCB1-/-

Figure 2.3 Genotype differences in EPM exploration are not due to changes in movement. General movement parameters were quantified for both male and female mice on the EPM. **(A)** There were no differences in average velocity between male intCB_1-/- mice and controls ($t_{(20)}$ = 0.1997, p = 0.8437) or **(B)** female intCB_1-/- mice and controls ($t_{(17)}$ = 1.394, p = 0.1813). **(C)** There were no differences in cumulative duration of movement between male intCB_1-/- mice and controls ($t_{(20)}$ = 0.7119, p = 0.4847) or **(D)** female intCB_1-/- mice and controls ($t_{(17)}$ = 0.6774, p = 0.5072). **(E)** There were no differences in total distance traveled between male intCB_1-/- mice and controls ($t_{(20)}$ = 0.1986, p = 0.8446) or **(F)** female intCB_1-/- mice and controls ($t_{(17)}$ = 1.427, p = 0.1718). **(G)** There were no differences in cumulative duration of non-movement between male intCB_1-/- mice and controls ($t_{(20)}$ = 0.7119, p = 0.4847) or **(H)** female intCB_1-/- mice and controls ($t_{(17)}$ = 0.8910, p = 0.3854). All analyses are unpaired Student's t tests. Data presented as ± SEM, n = 9-11 mice per sex & genotype.

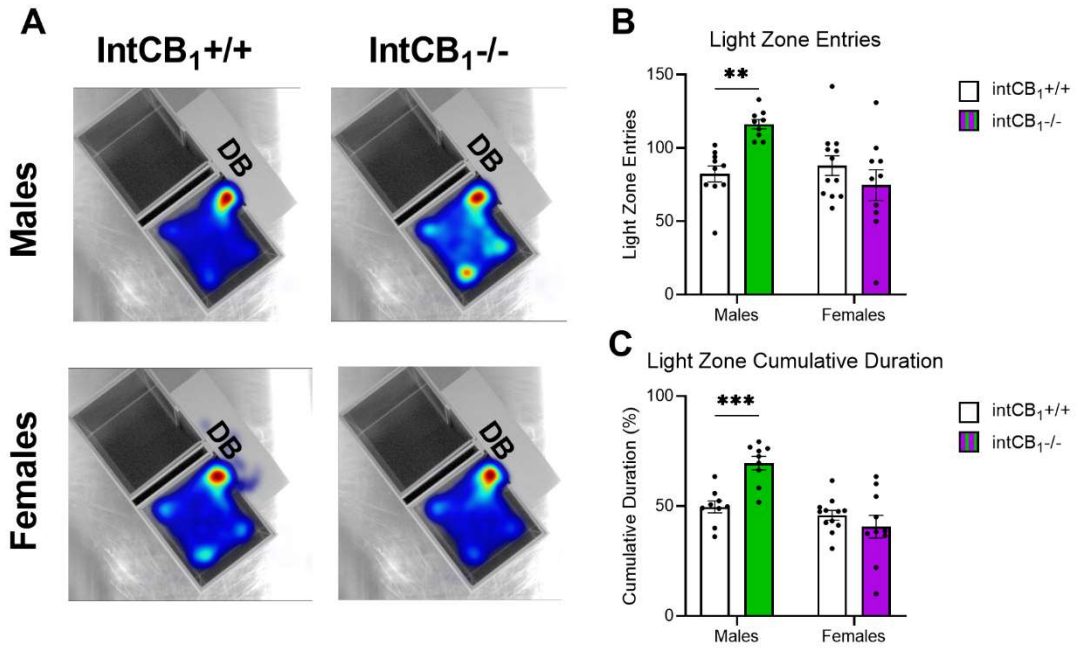
A
IntCB1+/+
IntCB1-/-
Males
Females
DB
DB
DB
DB
B
Light Zone Entries
**
Light Zone Entries
150
100
50
0
Males
Females
intCB1+/+
intCB1-/-
C
Light Zone Cumulative Duration
***
Cumulative Duration (%)
100
50
0
Males
Females
intCB1+/+
intCB1-/-

Figure 2.4 Male intCB$_1$-/- mice, but not female, exhibit anxiolytic behaviors in the light/dark box. Male and female intCB$_1$-/- mice and intCB$_1$+/+ controls were allowed to freely explore the light/dark box for 10 minutes. **(A)** Merged heatmaps of all trials for male intCB$_1$+/+, male intCB$_1$-/- mice, female intCB$_1$+/+, female intCB$_1$-/- mice show general exploration patterns of the light box. Mice were unable to be recorded in the dark box (DB) due to the opaque roof. Increasing time spent in area designated from blue to red, with red being most time. **(B)** Male intCB$_1$-/- mice exhibited an increase in total light zone entries compared to controls, but there were no differences observed in light zone entries for female intCB$_1$-/- mice and controls (sex x genotype interaction: $F_{(1,37)} = 10.75$; $p = 0.0023$; sex main effect $F_{(1,37)} = 6.236$; $p = 0.0171$; male intCB$_1$-/- vs. male intCB$_1$+/+ $p = 0.0053$; 2-way ANOVA followed by Holm Sidak's multiple comparisons test). **(C)** Male intCB$_1$-/- mice exhibited an increase in light zone cumulative duration compared to controls, but there were no differences observed in light zone cumulative duration for female intCB$_1$-/- mice and controls (sex x genotype interaction: $F_{(1,36)} = 13.18$; $p = 0.0009$; sex main effect $F_{(1,36)} = 22.21$; $p < 0.0001$; genotype main effect $F_{(1,36)} = 4.521$; $p = 0.0404$; male intCB$_1$-/- vs. male intCB$_1$+/+ $p = 0.0008$; 2-way ANOVA followed by Holm Sidak's multiple comparisons test). Data presented as ± SEM, n = 9-12 mice per sex & genotype, $^{**}p < 0.01$, $^{***}p < 0.001$.

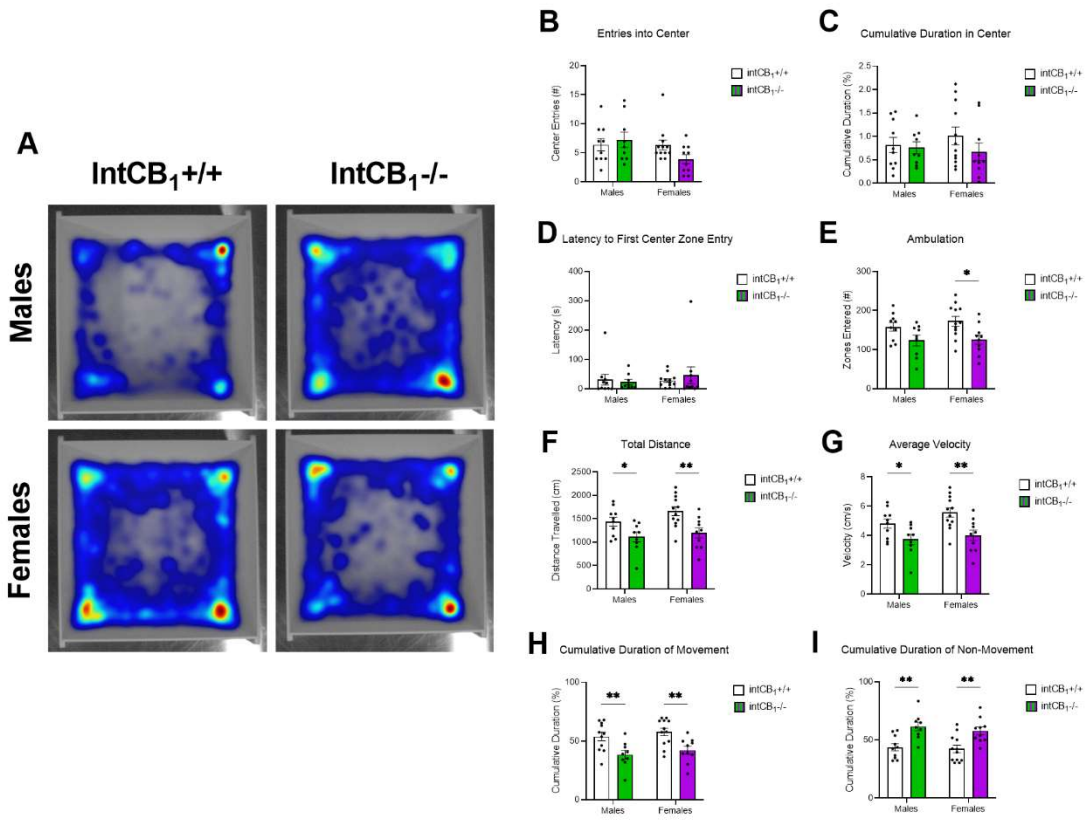
A
IntCB1+/+
IntCB1-/-
Males
Females
B
Entries into Center
Center Entries (#)
C
Cumulative Duration in Center
Cumulative Duration (%)
D
Latency to First Center Zone Entry
Latency (s)
E
Ambulation
Zones Entered (#)
F
Total Distance
Distance Travelled (cm)
G
Average Velocity
Velocity (cm/s)
H
Cumulative Duration of Movement
Cumulative Duration (%)
I
Cumulative Duration of Non-Movement
Cumulative Duration (%)
Males
Females
intCB1+/+
intCB1-/-

Figure 2.5 IntCB$_1$-/- mice do not exhibit anxiolytic behaviors in the open field test. Male and female intCB$_1$-/- mice and int CB$_1$+/+ controls were allowed to freely explore the open field apparatus for 10 minutes. **(A)** Merged heatmaps of all trials for male intCB$_1$+/+, male intCB$_1$-/- mice, female intCB$_1$+/+, female int CB$_1$-/- mice show general exploration patterns of the open field. Increasing time spent in area designated from blue to red, with red being most time. There were no sex or genotype differences observed in **(B)** number of center zone entries, **(C)** cumulative duration in center zone, or **(D)** latency to first center zone entry. **(E)** IntCB$_1$-/- female mice displayed a significant reduction in ambulation (total number of zones entered) compared to controls. There were no differences in ambulation between IntCB$_1$-/- males and controls (genotype main effect $F_{(1,37)} = 10.85$; $p = 0.0022$; female intCB$_1$-/- vs. female intCB$_1$+/+ $p = 0.0168$). **(F)** IntCB$_1$-/- male and female mice demonstrated a reduction in total distance traveled compared to controls (genotype main effect $F_{(1,37)} = 14.93$; $p = 0.0004$; male intCB$_1$-/- vs. male int CB$_1$+/+ $p = 0.0378$; female intCB$_1$-/- vs. female intCB$_1$+/+ $p = 0.0037$). **(G)** IntCB$_1$-/- male and female mice demonstrated a reduction in average velocity to controls (genotype main effect $F_{(1,37)} = 14.96$; $p = 0.0004$; male intCB$_1$-/- vs. male int CB$_1$+/+ $p = 0.0379$; female intCB$_1$-/- vs. female intCB$_1$+/+ $p = 0.0036$). **(H)** IntCB$_1$-/- male and female mice demonstrated a reduction in the cumulative duration of movement to controls (genotype main effect $F_{(1,38)} = 19.15$; $p < 0.0001$; male intCB$_1$-/- vs. male int CB$_1$+/+ $p = 0.0057$; female intCB$_1$-/- vs. female intCB$_1$+/+ $p = 0.0057$). **(G)** IntCB$_1$-/- male and female mice demonstrated an increase in the cumulative duration of movement compared to controls (genotype main effect $F_{(1,37)} = 24.04$; $p < 0.0001$; male intCB$_1$-/- vs. male int CB$_1$+/+ $p = 0.0020$; female intCB$_1$-/- vs. female intCB$_1$+/+ $p = 0.0020$). All analyses are 2-way ANOVA followed by Holm Sidak's multiple comparisons test. Data presented as ± SEM, n = 9-12 mice per sex & genotype. *$p < 0.05$, **$p < 0.01$.

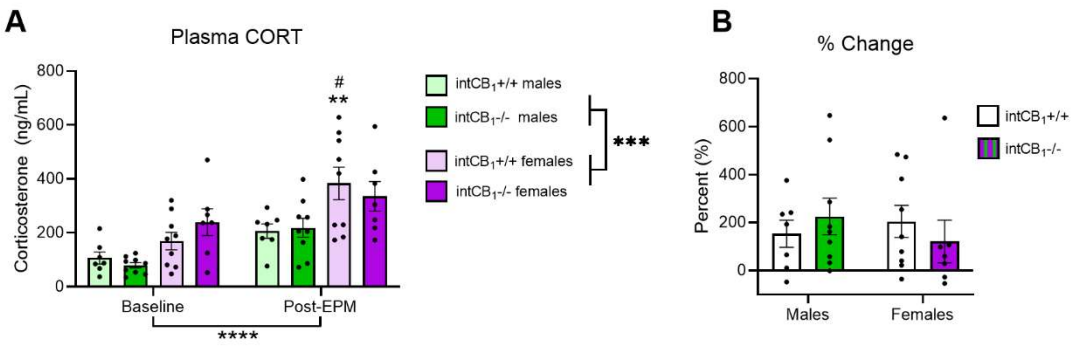

Figure 2.6 Circulating CORT levels are sex dependent. Circulating CORT levels were quantified in male and female intCB$_1$-/- mice and intCB$_1$+/+ controls at baseline and following a 5-minute EPM exposure. **(A)** There was a significant effect of timepoint and sex on plasma CORT levels. IntCB$_1$+/+ female mice exhibited significantly higher CORT following EPM exposure when compared to IntCB$_1$+/+ female mice at baseline. IntCB$_1$+/+ females post-EPM also exhibited a significant increase in CORT when compared to IntCB$_1$+/+ males post-EPM (timepoint main effect $F_{(1,28)}$ = 24.44; p < 0.0001; sex main effect $F_{(1,28)}$ = 19.76; p = 0.0001; ** = baseline female intCB$_1$+/+ vs. post-EPM female int CB$_1$+/+ p = 0.0036; # = post-EPM female int CB$_1$+/+ vs. post-EPM male intCB$_1$+/+ p = 0.0311; 3-way ANOVA followed by Holm Sidak's multiple comparisons test). **(B)** There were no significant differences in % Change of plasma CORT. % Change = ((Post-EPM CORT – Baseline CORT)/Baseline CORT) x 100. Data presented as ± SEM, n = 7-9 mice group. *** p < 0.001, ****p < 0.0001

Conclusion

This work examines how the endocannabinoid system (ECS) participates in gut-brain signaling to mediate control over obesity and anxiety. The ECS is densely expressed in the brain and GI tract, and thus plays a prominent role in gut-brain signaling. As a homeostatic regulator of various aspects of physiology and behavior, dysregulation of ECS function often results in pathophysiological outcomes. For example, obesity is associated with elevated endocannabinoid (eCB) tone both in the brain (Di Marzo et al., 2001; Bourdy et al., 2021) and in the GI tract (Artmann et al., 2008; Izzo et al., 2009; Argueta and DiPatrizio, 2017; Argueta et al., 2019). Here, we showed that diet-induced obesity (DIO) in mice is associated with increased neuronal activation in the dorsal motor nucleus (DMV) of the vagus which may contribute to elevated eCB content within the intestinal epithelium and drive hyperphagia. We further demonstrated that this elevated eCB content and caloric intake could be attenuated by treatment with muscarinic acetylcholine receptor (mAChR) antagonists via a mechanism which requires functional intestinal cannabinoid receptor subtype-1 (intCB_1R). Mounting evidence also suggests that dysregulation of the ECS is associated with mood disorders such as generalized anxiety disorder (Viveros et al., 2005; Witkin et al., 2005; Hill and Gorzalka, 2009; Lutz et al., 2015). We sought to investigate the role of intCB_1Rs in expression of anxiety-like behaviors in both male and female mice. Our study revealed a strong reduction in anxiety-like behaviors for male mice lacking intCB_1Rs, but not females. We also showed a significant increase in the circulating stress hormone, corticosterone (CORT), for female mice

regardless of genotype at baseline and immediately following behavioral testing. Taken together, these findings highlight the importance of the intestinal ECS in the regulation of gut-brain signaling and should be considered when investigating possible treatments for obesity, anxiety, and other conditions that may be regulated by the gut-brain axis.

To further understand the mechanism by which DMV signaling becomes dysregulated in DIO, upstream circuitry of the brainstem and other connected structures should be considered. Melanocortin 4 receptors (MC4Rs) within the central nervous system (CNS) regulate food intake (Shah et al., 2014), energy expenditure, and glucose homeostasis (Rossi et al., 2011). MC4R mutations are associated with obesity and diabetes in both rodents and humans (Fan et al., 1997; Huszar et al., 1997; Yeo et al., 1998; Ho and MacKenzie, 1999; Tallam et al., 2005), so it follows that MC4R may exert some control over gut-brain signaling which participates in the regulation of food intake and metabolic homeostasis. Indeed, MC4Rs are present on preganglionic parasympathetic neurons within the DMV and MC4R agonism was found to directly inhibit DMV neuronal activity (Sohn et al., 2013). It is possible that MC4R activity is dysfunctional in our DIO mouse model, leading to the elevated DMV activity that drives intestinal eCB formation. The direct relationship between MC4R signaling and DMV activation should be further investigated.

In 2019, our lab showed that activation of CB_1Rs on enteroendocrine I-cells was able to inhibit CCK release (Argueta et al., 2019), thereby uncovering a mechanism by

which elevated intestinal eCBs in DIO mice could drive hyperphagia. In the current body of work, it is unclear whether treatment with the mAChR antagonist, atropine, reduced food intake in DIO mice via the same CCK-dependent mechanism. Preliminary data revealed a minor restoration of CCK release in DIO mice treated with atropine 30 minutes prior to a corn oil gavage, but not to the extent of AM6545 in the 2019 study (Argueta et al., 2019). It is possible that the *in vivo* pharmacodynamics of atropine differ from those of AM6545. A timecourse study should be conducted to determine at which timepoint, if any, atropine treatment is able to restore CCK release to lean control levels.

The dorsal vagal complex (DVC) is an important structure for the regulation of GI function and food intake (Clyburn and Browning, 2021). It is comprised of the nucleus of the solitary tract (NTS), the DMV, and area postrema (AP). Information from the GI tract is relayed directly to the DVC via second order neurons of the NTS, which extend glutamatergic, GABAergic, and catecholaminergic inputs to the DMV (Travagli et al., 1991; Davis et al., 2004; Babic et al., 2011). These signals are then integrated, along with other signals from descending brainstem regions, and relayed back to peripheral targets in the GI tract by way of the efferent motor neurons of the DMV (Sivarao et al., 1998; Sivarao et al., 1999). Under normal conditions DMV neurons act as pacemaker neurons, firing spontaneously at a rate of approximately 1 Hz (Travagli et al., 1991). However, their activity has been shown to be altered by inputs from the NTS (Davis et al., 2004; Babic et al., 2011). Given the findings of the present study that DMV neurons are hyperactive in DIO, and previous discussions regarding dysregulation of afferent signaling in obesity (de

Lartigue et al., 2011; de Lartigue et al., 2014; McDougle et al., 2021; Chrobok et al., 2022), it would be valuable to assess the temporal properties governing DVC and vago-vagal complex dysregulation in obesity. It is difficult to say which structure is the first to be affected by obesity and how exactly that disruption impacts the rest of the circuit. Studying the precise timing of vago-vagal signaling dynamics during obesity development would offer crucial insights into how the gut-brain connection regulates obesogenic mechanisms.

While the vagus nerve plays a critical role in orchestrating gut-brain control over ingestive behaviors and metabolic functions, it has also been identified for its contribution to modulation of mood and affective behaviors. Indeed, vagal deafferentation has been shown to reduce anxiety-like behaviors in rats (Klarer et al., 2014). In humans Vagal Nerve Stimulation (VNS) is under investigation as a possible treatment for anxiety disorders (George et al., 2008; Shivaswamy et al., 2022), mood improvement (Elger et al., 2000; Harden et al., 2000; Klinkenberg et al., 2012), and clinical depression (Rush et al., 2005; Carreno and Frazer, 2017). The findings that male intCB_1-/- mice exhibited reduced anxiety-like behaviors may be indicative of a vagally-mediated mechanism. Previous studies from the lab indicate that CB_1Rs are co-expressed on CCK-containing I-cells within the upper small-intestinal epithelium. Activation of these CB_1Rs by endocannabinoids in the GI tract inhibits CCK release (Argueta et al., 2019), thereby reducing signaling at CCK_ARs located on vagal afferent fibers which enable rapid gut-brain signal transmission (Moran et al., 1997; Ritter et al., 1999; Moran and Kinzig, 2004; Peters et al., 2006). It is

possible that the conditional elimination of CB_1Rs from the intestinal epithelium influences anxiety-like behaviors by modulation of vagal afferent activity. To test this hypothesis, experiments should be conducted to examine differences in afferent vagus nerve electrical properties in intCB_1-/- mice. Activity levels within the NTS could be assessed by quantifying immunoreactivity for the cFos protein at baseline and immediately following behavioral testing. This would elucidate how gut-brain neurotransmission is altered in the intCB_1-/- animals compared to controls.

In addition to a potential vagally-mediated mechanism, circulating factors that govern mood and behavior should also be assessed in the IntCB_1-/- mice. Circulating concentrations of the endocannabinoid, anandamide (AEA), are inversely correlated with measures of anxiety in human subjects (Hill et al., 2008; Dlugos et al., 2012). Stress may also alter circulating endocannabinoid levels (Hillard, 2014). In turn, endocannabinoid signaling at CB_1Rs can reduce stress-induced HPA-axis activation (Hill et al., 2009) and helps to restore homeostasis following onset of the stress response (Hill et al., 2011). Therefore, it is feasible that differences in circulating endocannabinoids contribute to the behavioral changes observed in male intCB_1-/- mice. It is unclear exactly how or why ligand availability would fluctuate in response to changes in receptor expression, but this phenomenon should be investigated, nonetheless.

This body of work provides novel insights on the relationship between the endocannabinoid system and gut-brain communication in the context of obesity and

anxiety. Independently this dissertation serves as a small contribution to the fields of neuroscience, endocannabinoids, and gut-brain signaling; but in combination with the greater ensemble of my graduate school experiences, it has contributed substantially to my development as an independent scientist. At the bench I have refined my technical skills, learned the art critical observation, achieved reproducibility, and mastered a steady hand. As a researcher I have overcome failure and disappointment, improved my hypothesis-driven testing, developed the ability to eloquently present my research, and learned to manage multiple projects amidst a constantly fluctuating timeline and unexpected diversions. As an academic I have recognized where my research fits in to the bigger picture, learned how to question the things I don't understand, and evaluated the importance of reliable and consistent mentorship.

I recognize that my journey as a scientist and an individual is an ongoing process of growth and learning, and my time spent in the DiPatrizio lab has undoubtedly played an invaluable role in shaping my development as an independent scientist. The challenges of graduate school tested the limits of my capabilities, often pushing me beyond what I thought possible and causing moments of (extreme) doubt. In retrospect, I now perceive this experience as the most arduous and transformative endeavor I have ever encountered. Over the past five years, I have undergone profound personal and professional changes, fostering within me a newfound confidence in my ability to overcome even the most daunting obstacles. The attainment of my PhD has instilled in me the mindset to perceive challenges as opportunities for growth and setbacks as invaluable

lessons. As I move into the next chapter of my life, I carry with me the wealth of knowledge accumulated and the wisdom gained through these experiences as a young researcher. I am filled with gratitude for the privilege of receiving training as a PhD scientist, and I humbly acknowledge that this journey would not have been possible without the guidance of my mentor, Dr. DiPatrizio, the unwavering support of my lab mates, and the encouragement of my loving family and friends. It is my intention that this dissertation will serve as a tangible reminder of the tremendous effort that I exerted, the overwhelming support I received, the rich knowledge I acquired, and the indescribable sense of fulfillment that could only be experienced in the pursuit of such a deeply meaningful endeavor.

References

Argueta D, DiPatrizio N (2017) Peripheral endocannabinoid signaling controls hyperphagia in western diet-induced obesity. Physiology & Behavior 171:32-39.

Argueta D, Perez P, Makriyannis A, DiPatrizio N (2019) Cannabinoid CB1 Receptors Inhibit Gut-Brain Satiation Signaling in Diet-Induced Obesity. Frontiers in Physiology 10.

Artmann A, Petersen G, Hellgren LI, Boberg J, Skonberg C, Nellemann C, Hansen SH, Hansen HS (2008) Influence of dietary fatty acids on endocannabinoid and N-acylethanolamine levels in rat brain, liver and small intestine. Biochim Biophys Acta 1781:200-212.

Babic T, Browning KN, Travagli RA (2011) Differential organization of excitatory and inhibitory synapses within the rat dorsal vagal complex. Am J Physiol Gastrointest Liver Physiol 300:G21-32.

Bourdy R, Hertz A, Filliol D, Andry V, Goumon Y, Mendoza J, Olmstead MC, Befort K (2021) The endocannabinoid system is modulated in reward and homeostatic brain regions following diet-induced obesity in rats: a cluster analysis approach. Eur J Nutr 60:4621-4633.

Carreno FR, Frazer A (2017) Vagal Nerve Stimulation for Treatment-Resistant Depression. Neurotherapeutics 14:716-727.

Chrobok L, Klich JD, Sanetra AM, Jeczmien-Lazur JS, Pradel K, Palus-Chramiec K, Kepczynski M, Piggins HD, Lewandowski MH (2022) Rhythmic neuronal activities of the rat nucleus of the solitary tract are impaired by high-fat diet - implications for daily control of satiety. J Physiol 600:751-767.

Clyburn C, Browning KN (2021) Glutamatergic plasticity within neurocircuits of the dorsal vagal complex and the regulation of gastric functions. Am J Physiol Gastrointest Liver Physiol 320:G880-G887.

Davis SF, Derbenev AV, Williams KW, Glatzer NR, Smith BN (2004) Excitatory and inhibitory local circuit input to the rat dorsal motor nucleus of the vagus originating from the nucleus tractus solitarius. Brain Res 1017:208-217.

de Lartigue G, Ronveaux CC, Raybould HE (2014) Deletion of leptin signaling in vagal afferent neurons results in hyperphagia and obesity. Mol Metab 3:595-607.

de Lartigue G, de la Serre C, Espero E, Lee J, Raybould H (2011) Diet-induced obesity leads to the development of leptin resistance in vagal afferent neurons. American Journal of Physiology-Endocrinology and Metabolism 301:E187-E195.

Di Marzo V, Goparaju SK, Wang L, Liu J, Bátkai S, Járai Z, Fezza F, Miura GI, Palmiter RD, Sugiura T, Kunos G (2001) Leptin-regulated endocannabinoids are involved in maintaining food intake. Nature 410:822-825.

Dlugos A, Childs E, Stuhr KL, Hillard CJ, de Wit H (2012) Acute stress increases circulating anandamide and other N-acylethanolamines in healthy humans. Neuropsychopharmacology 37:2416-2427.

Elger G, Hoppe C, Falkai P, Rush AJ, Elger CE (2000) Vagus nerve stimulation is associated with mood improvements in epilepsy patients. Epilepsy Res 42:203-210.

Fan W, Boston BA, Kesterson RA, Hruby VJ, Cone RD (1997) Role of melanocortinergic neurons in feeding and the agouti obesity syndrome. Nature 385:165-168.

George MS, Ward HE, Ninan PT, Pollack M, Nahas Z, Anderson B, Kose S, Howland RH, Goodman WK, Ballenger JC (2008) A pilot study of vagus nerve stimulation (VNS) for treatment-resistant anxiety disorders. Brain Stimul 1:112-121.

Harden CL, Pulver MC, Ravdin LD, Nikolov B, Halper JP, Labar DR (2000) A Pilot Study of Mood in Epilepsy Patients Treated with Vagus Nerve Stimulation. Epilepsy Behav 1:93-99.

Hill MN, Gorzalka BB (2009) The endocannabinoid system and the treatment of mood and anxiety disorders. CNS Neurol Disord Drug Targets 8:451-458.

Hill MN, Miller GE, Ho WS, Gorzalka BB, Hillard CJ (2008) Serum endocannabinoid content is altered in females with depressive disorders: a preliminary report. Pharmacopsychiatry 41:48-53.

Hill MN, McLaughlin RJ, Morrish AC, Viau V, Floresco SB, Hillard CJ, Gorzalka BB (2009) Suppression of amygdalar endocannabinoid signaling by stress contributes to

activation of the hypothalamic-pituitary-adrenal axis. Neuropsychopharmacology 34:2733-2745.

Hill MN, McLaughlin RJ, Pan B, Fitzgerald ML, Roberts CJ, Lee TT, Karatsoreos IN, Mackie K, Viau V, Pickel VM, McEwen BS, Liu QS, Gorzalka BB, Hillard CJ (2011) Recruitment of prefrontal cortical endocannabinoid signaling by glucocorticoids contributes to termination of the stress response. J Neurosci 31:10506-10515.

Hillard CJ (2014) Stress regulates endocannabinoid-CB1 receptor signaling. Semin Immunol 26:380-388.

Ho G, MacKenzie RG (1999) Functional characterization of mutations in melanocortin-4 receptor associated with human obesity. J Biol Chem 274:35816-35822.

Huszar D, Lynch CA, Fairchild-Huntress V, Dunmore JH, Fang Q, Berkemeier LR, Gu W, Kesterson RA, Boston BA, Cone RD, Smith FJ, Campfield LA, Burn P, Lee F (1997) Targeted disruption of the melanocortin-4 receptor results in obesity in mice. Cell 88:131-141.

Izzo A, Piscitelli F, Capasso R, Aviello G, Romano B, Borrelli F, Petrosino S, Di Marzo V (2009) Peripheral endocannabinoid dysregulation in obesity: relation to intestinal motility and energy processing induced by food deprivation and re-feeding. British Journal of Pharmacology 158:451-461.

Klarer M, Arnold M, Günther L, Winter C, Langhans W, Meyer U (2014) Gut vagal afferents differentially modulate innate anxiety and learned fear. J Neurosci 34:7067-7076.

Klinkenberg S, Majoie HJ, van der Heijden MM, Rijkers K, Leenen L, Aldenkamp AP (2012) Vagus nerve stimulation has a positive effect on mood in patients with refractory epilepsy. Clin Neurol Neurosurg 114:336-340.

Lutz B, Marsicano G, Maldonado R, Hillard CJ (2015) The endocannabinoid system in guarding against fear, anxiety and stress. Nat Rev Neurosci 16:705-718.

McDougle M, Quinn D, Diepenbroek C, Singh A, de la Serre C, de Lartigue G (2021) Intact vagal gut-brain signalling prevents hyperphagia and excessive weight gain in response to high-fat high-sugar diet. Acta Physiol (Oxf) 231:e13530.

Moran TH, Kinzig KP (2004) Gastrointestinal satiety signals II. Cholecystokinin. Am J Physiol Gastrointest Liver Physiol 286:G183-188.

Moran TH, Baldessarini AR, Salorio CF, Lowery T, Schwartz GJ (1997) Vagal afferent and efferent contributions to the inhibition of food intake by cholecystokinin. Am J Physiol 272:R1245-1251.

Peters JH, Simasko SM, Ritter RC (2006) Modulation of vagal afferent excitation and reduction of food intake by leptin and cholecystokinin. Physiol Behav 89:477-485.

Ritter RC, Covasa M, Matson CA (1999) Cholecystokinin: proofs and prospects for involvement in control of food intake and body weight. Neuropeptides 33:387-399.

Rossi J, Balthasar N, Olson D, Scott M, Berglund E, Lee CE, Choi MJ, Lauzon D, Lowell BB, Elmquist JK (2011) Melanocortin-4 receptors expressed by cholinergic neurons regulate energy balance and glucose homeostasis. Cell Metab 13:195-204.

Rush AJ, Marangell LB, Sackeim HA, George MS, Brannan SK, Davis SM, Howland R, Kling MA, Rittberg BR, Burke WJ, Rapaport MH, Zajecka J, Nierenberg AA, Husain MM, Ginsberg D, Cooke RG (2005) Vagus nerve stimulation for treatment-resistant depression: a randomized, controlled acute phase trial. Biol Psychiatry 58:347-354.

Shah BP, Vong L, Olson DP, Koda S, Krashes MJ, Ye C, Yang Z, Fuller PM, Elmquist JK, Lowell BB (2014) MC4R-expressing glutamatergic neurons in the paraventricular hypothalamus regulate feeding and are synaptically connected to the parabrachial nucleus. Proc Natl Acad Sci U S A 111:13193-13198.

Shivaswamy T, Souza RR, Engineer CT, McIntyre CK (2022) Vagus Nerve Stimulation as a Treatment for Fear and Anxiety in Individuals with Autism Spectrum Disorder. J Psychiatr Brain Sci 7.

Sivarao DV, Krowicki ZK, Hornby PJ (1998) Role of GABAA receptors in rat hindbrain nuclei controlling gastric motor function. Neurogastroenterol Motil 10:305-313.

Sivarao DV, Krowicki ZK, Abrahams TP, Hornby PJ (1999) Vagally-regulated gastric motor activity: evidence for kainate and NMDA receptor mediation. Eur J Pharmacol 368:173-182.

Sohn JW, Harris LE, Berglund ED, Liu T, Vong L, Lowell BB, Balthasar N, Williams KW, Elmquist JK (2013) Melanocortin 4 receptors reciprocally regulate sympathetic and parasympathetic preganglionic neurons. Cell 152:612-619.

Tallam LS, Stec DE, Willis MA, da Silva AA, Hall JE (2005) Melanocortin-4 receptor-deficient mice are not hypertensive or salt-sensitive despite obesity, hyperinsulinemia, and hyperleptinemia. Hypertension 46:326-332.

Travagli RA, Gillis RA, Rossiter CD, Vicini S (1991) Glutamate and GABA-mediated synaptic currents in neurons of the rat dorsal motor nucleus of the vagus. Am J Physiol 260:G531-536.

Viveros MP, Marco EM, File SE (2005) Endocannabinoid system and stress and anxiety responses. Pharmacol Biochem Behav 81:331-342.

Witkin JM, Tzavara ET, Nomikos GG (2005) A role for cannabinoid CB1 receptors in mood and anxiety disorders. Behav Pharmacol 16:315-331.

Yeo GS, Farooqi IS, Aminian S, Halsall DJ, Stanhope RG, O'Rahilly S (1998) A frameshift mutation in MC4R associated with dominantly inherited human obesity. Nat Genet 20:111-112.